

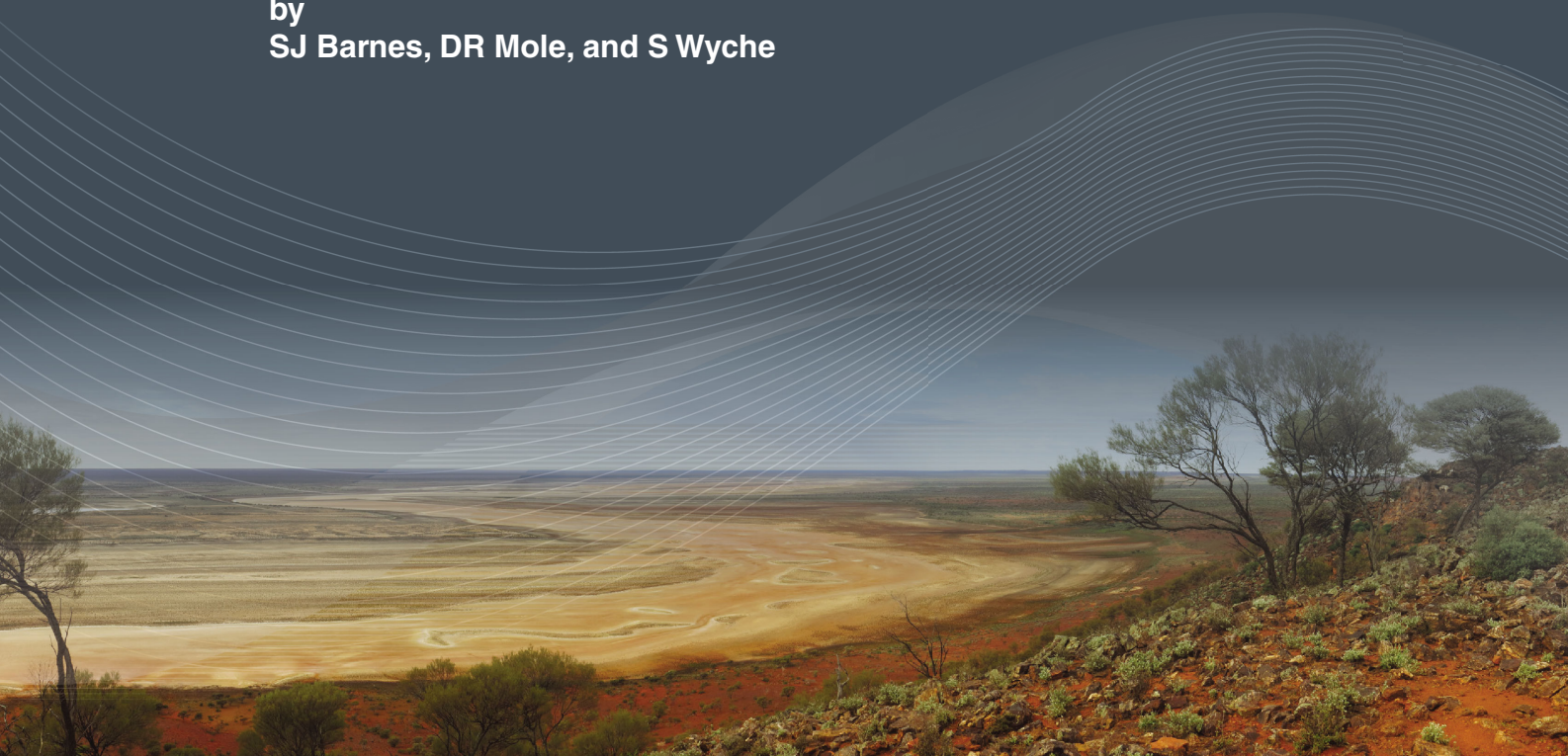


Government of **Western Australia**
Department of **Mines and Petroleum**

RECORD 2016/12

KOMATIITES AND ASSOCIATED ROCKS OF THE KALGOORLIE–LEONORA REGION

by
SJ Barnes, DR Mole, and S Wyche



Geological Survey of
Western Australia



POSEIDON NICKEL
AUSTRALIA'S NEW NICKEL

RNC



Government of **Western Australia**
Department of **Mines and Petroleum**

Record 2016/12

KOMATIITES AND ASSOCIATED ROCKS OF THE KALGOORLIE–LEONORA REGION

by
SJ Barnes¹, DR Mole¹, and S Wyche

¹ CSIRO Mineral Resources, PO Box 1130, Bentley WA 6102

Perth 2016



**Geological Survey of
Western Australia**

MINISTER FOR MINES AND PETROLEUM
Hon. Sean K L'Estrange MLA

DIRECTOR GENERAL, DEPARTMENT OF MINES AND PETROLEUM
Richard Sellers

EXECUTIVE DIRECTOR, GEOLOGICAL SURVEY OF WESTERN AUSTRALIA
Rick Rogerson

REFERENCE

The recommended reference for this publication is:

Barnes, SJ, Mole, D and Wyche, S 2016, Komatiites and associated rocks of the Kalgoorlie–Leonora region: Geological Survey of Western Australia, Record 2016/12, 70p.

National Library of Australia Card Number and ISBN 978-1-74168-702-6

Grid references in this publication refer to the Geocentric Datum of Australia 1994 (GDA94). Locations mentioned in the text are referenced using Map Grid Australia (MGA) coordinates, Zone 51. All locations are quoted to at least the nearest 100 m.



Disclaimer

This product was produced using information from various sources. The Department of Mines and Petroleum (DMP) and the State cannot guarantee the accuracy, currency or completeness of the information. DMP and the State accept no responsibility and disclaim all liability for any loss, damage or costs incurred as a result of any use of or reliance whether wholly or in part upon the information provided in this publication or incorporated into it by reference.

Published 2016 by Geological Survey of Western Australia

This Record is published in digital format (PDF) and is available online at <www.dmp.wa.gov.au/GSWApublications>.

Further details of geological products and maps produced by the Geological Survey of Western Australia are available from:

Information Centre
Department of Mines and Petroleum
100 Plain Street
EAST PERTH WESTERN AUSTRALIA 6004
Telephone: +61 8 9222 3459 Facsimile: +61 8 9222 3444
www.dmp.wa.gov.au/GSWApublications

Cover image: Elongate salt lake on the Yilgarn Craton — part of the Moore–Monger paleovalley — here viewed from the top of Wownaminy Hill, 20 km southeast of Yalgoo, Murchison Goldfields. Photograph taken by I Zibra for the Geological Survey of Western Australia

Contents

Excursion itinerary	1
Abstract	3
Introduction to komatiites	3
What are komatiites?.....	3
Large-scale controls and localization of major komatiite sequences.....	6
The textural diversity of komatiitic rocks	7
Spinifex textures.....	7
Cumulate textures	12
Heteradcumulates.....	12
Harrisites	12
Adcumulates	12
Field relationships in komatiite sequences.....	14
Spinifex-bearing compound flow sequences.....	14
Lenticular dunite bodies	14
Sheeted dunite bodies.....	15
Invasive flows or high-level intrusions in bimodal volcanic terranes	16
Volcanic architecture of komatiite flow fields	16
Origin of adcumulate bodies	17
Contrasting stratigraphic associations.....	17
Komatiite-basalt associations.....	18
Felsic and intermediate volcanic assemblages and relationship to komatiites and basalts.....	20
Excursion stops	21
Mount Hunt (MGA 356815E 6586475N)	21
Hannan Lake and Mount Hunt.....	21
The Hannan Lake – Mount Hunt traverse.....	21
Serpentine Bay	21
Mount Hunt.....	21
Paringa Basalt	23
Black Flag Group.....	26
The Long–Victor Mine and the Moran Shoot, Kambalda (MGA 373976E 6549856N).....	26
Breakaway locality, Kanowna (MGA 367575E 6616985N)	29
Harper Lagoon (MGA 364230E 6623120N).....	30
Gordon Sirdar (Kanowna) (MGA 364100E 6628600N).....	35
Black Swan nickel mine (MGA 369225E 6636965N)	41
Stratigraphy and host rocks	41
The Silver Swan orebody	43
The Cygnet and Black Swan disseminated sulfide orebody	44
Kanowna Town Dam (MGA 367310E 6609870N)	46
Kalgoorlie Terrane stratigraphy at Ghost Rocks (MGA 298330E 6724968N)	46
Comet Vale ultramafic rocks (MGA 319710E 6685732N)	50
Vettors Hill ultramafic rocks (MGA 329397E 6651857N).....	50
Western Mining Corporation SM7 nickel laterite pit (MGA 307372E 6652923N).....	52
The Murrin Murrin komatiite complex in the Kilkenny Syncline (MGA 380772E 6795244N).....	52
Regional geology	54
1. Basal chill zone	54
2. Layered olivine orthocumulates.....	54
3. Contact between ultramafic and gabbroic cumulates.....	54
4. Spinifex-textured komatiitic basalt flow lobe	57
5. Test costean in lateritic clays.....	57
6. Lateral gradation between gabbro and high-Mg basalt lobes	57
Summary and interpretation.....	57
Komatiites in the Mount Clifford – Marshall Pool area (MGA 303100E 6850500N).....	58
Regional geology	58
Mount Clifford area	58
Traverse from the Mount Clifford dunite to Marriotts nickel prospect	63
Marshall Pool area	63
Marshall Pool traverse	64
Melita Formation (MGA 352558E 6784296N).....	64
King of the Hills Dolerite (MGA 324371E 6832069N).....	65
References	67

Figures

1.	Basic geology of the Archean Yilgarn Craton	4
2.	Simplified geological map of the Eastern Goldfields Superterrane	5
3.	Lu–Hf (ϵ_{Hf}) map of the Yilgarn Craton at 3050–2820 Ma	7
4.	Lu–Hf (ϵ_{Hf}) map of the Yilgarn Craton at 2720–2600 Ma	8
5.	Isotopic cross-section and interpreted lithospheric architecture during the emplacement of 2.9 Ga komatiites in the southern Youanmi Terrane	9
6.	Isotopic cross-sections and interpreted lithospheric architecture during the emplacement of the 2.7 Ga komatiites in the Eastern Goldfields (Kalgoorlie Terrane)	10
7.	Spinifex textures	11
8.	Cumulate textures	13
9.	Kambalda facies model	15
10.	Plan view of a hypothetical komatiite lava flow field fed by inflationary pathways	16
11.	Stratigraphic columns for Kambalda and Boorara Domains of the Kalgoorlie Terrane, and for the Kurnalpi Terrane farther east	18
12.	Basalt chemistry summary	19
13.	Geochemistry of Boorara Domain felsic rocks at Black Swan	20
14.	Subdivisions of the Yilgarn Craton	22
15.	Interpreted bedrock geology of the Kalgoorlie area	23
16.	Outcrop sketch of the Mount Hunt – Hannan Lake area	24
17.	Serpentine pseudomorphs after platy olivine-spinifex texture in carbonate-altered, serpentinized komatiite at Serpentine Bay	24
18.	Mount Hunt structures	25
19.	Variolitic Paringa Basalt on Mount Hunt	26
20.	Relict pillow structures in saprolite after Paringa Basalt west of Mount Hunt	26
21.	Relict hyaloclastite breccia in saprolite after Paringa Basalt west of Mount Hunt	26
22.	Folds in graded volcanoclastic beds of weathered Black Flag Group	27
23.	Map of Kambalda Dome showing location of Long–Victor Mine	27
24.	3D geology model showing morphology and relationship of the various ore shoots in the Long and Victor channels	28
25.	Simplified cross-section showing the morphology of the Moran orebody and its containing trough feature	28
26.	Moran underground face	29
27.	Boorara Domain map	30
28.	Breakaway map	31
29.	High-resolution orthophoto mosaic of the southern section of the Breakaway outcrop: geo-rectified photomosaics collected using drone-based photogrammetry	32
30.	Orthophoto of a complete section of epiclastic sediments with enlargements showing details of individual units	33
31.	Komatiite (K) dacite (D) mingling textures in outcrops, Breakaway locality	34
32.	Photographs from Harper Lagoon	34
33.	Gordon Sirdar lake locality map	35
34.	High-resolution orthophotos of dacite–komatiite intercalations in the Gordon Sirdar lake bed outcrops	36
35.	Gordon Sirdar orthophotos showing field relationships between thin komatiite flow lobe ‘fingers’ and intercalated dacite flows	37
36.	High-resolution orthophotos of dacite–komatiite intercalations in the Gordon Sirdar lake bed	38
37.	Photographs of komatiite flow features at Gordon Sirdar	40
38.	Black Swan geology	41
39.	Black Swan komatiite textures	42
40.	Silver Swan orebody plan and massive ore textures	43
41.	Disseminated ore textures, Black Swan deposit	45
42.	Szaibellyite (hydrated magnesium borate) in serpentinite from within the Black Swan orebody	45
43.	High-resolution orthophotos collected using drone-based photogrammetry of a portion of the outcrop of turbidites at the Kanowna Town Dam locality	47
44.	Photographs of sedimentary features at Kanowna Town Dam locality	48
45.	Regional geology of the Walter Williams Formation	49
46.	Stratigraphy of the Walter Williams Formation	50
47.	Ghost Rocks geology map	51
48.	Geological map of the Comet Vale area	52
49.	Geology of the Kilkenny Syncline, showing the Murrin Murrin komatiite complex	53
50.	Detailed outcrop map of the southwestern part of the Kilkenny Syncline area, showing the access track ..	55
51.	Photomicrographs of Murrin Murrin ultramafic rocks	56
52.	Plot of FeO v. MgO (recalculated anhydrous wt%) for samples from the Murrin Murrin Ultramafic–Mafic Complex	57
53.	Regional geology of the Agnew–Wiluna greenstone belt from Mount Clifford to Wiluna	59
54.	Schematic geological sections across the Agnew–Wiluna greenstone belt	60
55.	Regional geology of the Mount Clifford – Marshall Pool area	61
56.	Geological cross-section through the Mount Clifford complex and the Marriotts Prospect	62
57.	Lithological and geochemical profile through the Mount Clifford complex	62
58.	Globular sulfide blebs at the Marriotts Prospect	64
59.	Volcanic, volcanoclastic and epiclastic rocks of the bimodal Melita Formation	65
60.	Photographs of the King of the Hills Dolerite	66

Excursion itinerary

Date	Day	Morning	Page	Afternoon	Page
11/09/2016		Perth–Kalgoorlie drive			
12/09/2016	1	Long–Victor (IGO) and Beta Hunt (RNC) mine visits	26	Mount Hunt regional geology	21
13/09/2016	2	Kanowna Gordon Sirdar lake	35	Black Swan mine visit (Poseidon)	41
14/09/2016	3	Kanowna dam section	46	Kanowna breakaway and Harper Lagoon	29, 30
15/09/2016	4	Melita Formation section	64	Murrin Murrin ultramafic complex	52
16/09/2016	5	King of the Hills Dyke – Mount Clifford	65	Mount Clifford – Marshall Pool	58, 63
17/09/2016	6	Ghost Rocks – Comet Vale – Vettors Hill – Siberia	46	GSWA Core Library	
18/09/2016		Kalgoorlie–Perth drive			

We would like to thank Independence Group NL, Royal Nickel Corporation and Poseidon Nickel Ltd for hosting us at their mining operations.

Day 1

The morning will consist of a mine visit to the Long–Victor komatiite-hosted nickel mine in Kambalda, which is operated by Independence Group NL (appropriate personal protective equipment [PPE] will be required). In the afternoon, we will drive back up to Kalgoorlie and traverse the geology at Mount Hunt, regarded as the type section of Kalgoorlie Terrane stratigraphy.

Day 2

This is the first of two days in the Kanowna area (Boorara Domain). In the morning, we will visit the komatiites exposed in the lake bed at Gordon Sirdar, with a visit to the Black Swan komatiite-hosted nickel mine in the afternoon (appropriate PPE will be required).

Day 3

This morning will focus on the geology at the Kanowna Dam including komatiites and turbidites, with an afternoon at the Kanowna breakaway locality where we will view synchronous komatiite–dacite magmatism.

Day 4

On the drive from Kalgoorlie to Leonora, we will spend the morning at a series of outcrops of the Melita Formation, here consisting primarily of rhyolite–dacite lavas, fragmentals, tuffs and associated volcanogenic sediments. In the afternoon, we will traverse a section through the Murrin Murrin ultramafic complex, finishing the day in Leonora.

Day 5

This day will be taken up almost completely by the visit to the Mount Clifford – Marshall Pool area at the base of Agnew–Wiluna greenstone belt, with a short stop in the morning at the King of the Hills dyke — a dioritic intrusive with unusual breccia and xenolith textures.

Day 6

The final day will consist of a number of stops along the drive from Leonora to Kalgoorlie looking at various occurrences of the Walter Williams Formation. Once back in Kalgoorlie, we will view a number of key drillholes from deposits throughout the Yilgarn at the Geological Survey of Western Australia (GSWA) Joe Lord core library in Kalgoorlie.

Komatiites and associated rocks of the Kalgoorlie–Leonora region

by

SJ Barnes¹, DR Mole¹, and S Wyche

Abstract

This volume was put together to accompany a field trip held in conjunction with the 13th International Nickel–Copper–PGE Symposium, held in Perth and Fremantle in September 2016. The volume is a compilation of a number of previous guidebooks, updated to incorporate ongoing developments in the understanding of the komatiites of the Eastern Goldfields region in the Yilgarn Craton over the last several decades. Over that time, these observations have been synthesized and refined into a volcanological framework for the komatiites and their ore deposits. The most significant recent research direction has been the application of isotopic terrane mapping, integrated with large-scale, deep-imaging geophysics and petrotectonic studies of the volcanic rocks associated with the komatiites. Combined with the volcanology framework, this has led to a ‘mineral system’ multiscale view of the eastern Yilgarn Craton komatiite nickel sulfide province: the third largest in the world after Sudbury and Noril’sk.

A running theme in this field trip and guidebook is the stratigraphic and volcanological framework of the komatiites, seen in relation to the nature and chemical affinity of the rocks with which they are interlayered. There are fundamental differences between the dominantly komatiite–basalt association of the Kalgoorlie–Kambalda – Ora Banda domains and the komatiite–felsic–(basaltic) bimodal and trimodal sequences seen in the Boorara and Agnew–Wiluna domains. This contrast is described here and exemplified by some outstanding field localities.

KEYWORDS: komatiite, nickel, peridotite, serpentinite, ultramafic rocks

Introduction to komatiites

Nickel sulfide deposits of the Yilgarn Craton are almost exclusively associated with komatiites. The nickel laterites of the craton are exclusively developed over komatiitic rocks. The aim of this introduction is to provide an overview of the essential features of komatiites to provide context for the localities described in this field guide.

True komatiites are an economically and scientifically important class of ultramafic lavas, which are relatively common within Archean greenstone belts but extremely rare elsewhere. They have a strongly clustered age distribution with peaks around 3.4 and 2.7 Ga (Arndt, 1994). The majority of Archean komatiites fall within a narrow band of ages within 20 million years of 2.7 Ga (Nelson, 1998), and sequences of this age contain the majority of the known komatiite-associated nickel sulfide

deposits. The Forrestania greenstone belt at 2.9 Ga and the recently recognized belt of mineralized komatiites extending northward from Mount Windarra to Mount Fisher along the Duketon greenstone belt (Fig. 1) contain the only known significantly older economic deposits, between 2.8 and 2.92 Ga.

In this field guide, we summarize the essential features of komatiites as observed in the southern part of the Kalgoorlie Terrane and Kurnalpi Terranes of the Eastern Goldfields Superterrane within the Yilgarn Craton (Figs 1 and 2). The following general introduction to the textures, field characteristics, tectonic associations and volcanology of komatiites is modified from Barnes (2006b).

What are komatiites?

Komatiites made their first appearance in the geological literature in the late 1960s, with the recognition of ultramafic lava flows in the Komati River Valley of the Barberton Greenstone Belt (Viljoen and Viljoen, 1969).

¹ CSIRO Mineral Resources, PO Box 1130 Bentley WA 6102

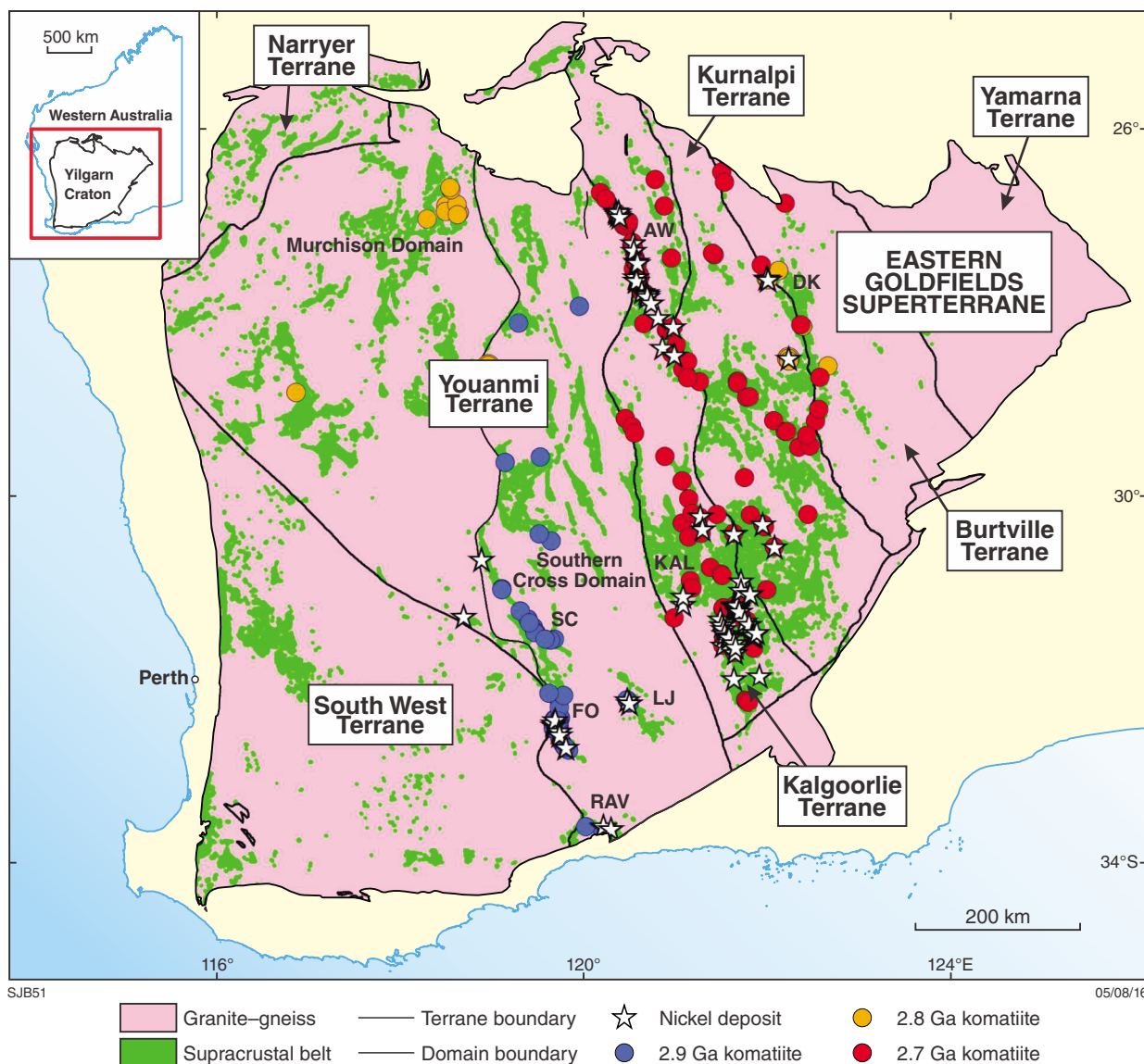
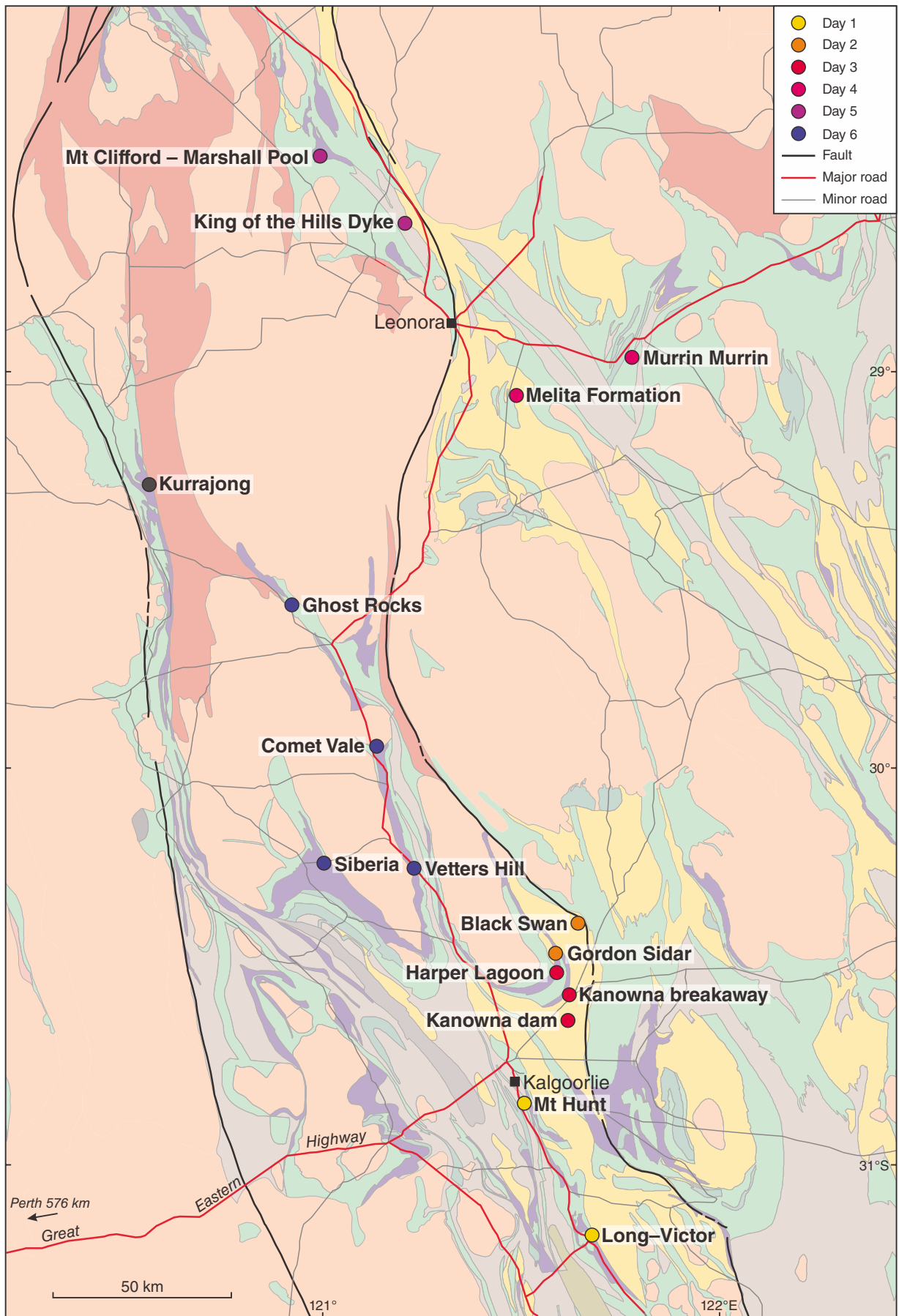


Figure 1. Basic geology of the Archean Yilgarn Craton showing the location of the 2.9, 2.8 and 2.7 Ga komatiite events, and associated nickel deposits. In this simplified diagram, areas of granite-gneiss (2.68 – 2.64 Ga) are shown in pink and volcano-sedimentary rocks (3.0 – 2.6 Ga) are shown in green. Greenstone belt abbreviations are as follows: MD – Marda-Diemals; SC – Southern Cross; FO – Forrestania; LJ – Lake Johnston; RAV – Ravensthorpe; AW – Agnew-Wiluna; DK – Duketon; KAL – Kalgoorlie-Kambalda.

Figure 2. (opposite) Simplified geological map of the Eastern Goldfields Superterrane showing the localities to be visited on the field excursion. Areas to be visited are colour coded by day. Major geological units include: komatiite/ultramafic (purple); mafic volcanic and intrusive (green); felsic-intermediate volcanic/volcaniclastic (yellow); chemical and clastic sedimentary rocks (shades of grey); granite and granitic gneiss (shades of red and pink).



SJB52

05/08/16

Examples of spinifex-textured flows had been recognized at about the same time in Western Australia, and landmark papers on these occurrences appeared shortly after the original Viljoen papers (McCall and Leishman, 1971; Williams, 1971; Hallberg and Williams, 1972; Barnes et al., 1974). These rocks were remarkable in their spectacular and distinctive skeletal olivine textures, which came to be known as ‘spinifex texture’ owing to the superficial resemblance to the widespread Australian grass. Several years of controversy about nomenclature led to a generally accepted definition of komatiite as a volcanic rock, containing at least 18% MgO (on an anhydrous basis) in the erupted liquid (Arndt and Nisbet, 1982). Komatiites are thus distinguished from ‘picrites’, which are lavas with considerably less than 18% MgO in the liquid, but with higher bulk MgO due to entrainment of phenocryst olivine and higher alkali contents.

In this standard usage, ‘komatiite’ is the ultramafic equivalent of the mafic ‘basalt’. However, it is widely recognized that lavas of mafic composition exist, usually intercalated with true komatiites, containing spinifex textures and showing clear evidence of derivation from true komatiite parent magmas. These rocks typically fail the test of having more than 18% MgO in the liquid, and are termed ‘komatiitic basalts’. In this sense, the term ‘komatiitic’ refers to a magma series and corresponds to terms such as ‘tholeiitic’.

Komatiites typically contain abundant cumulus olivine and less commonly pyroxene, in some cases forming 100% of the rock and developing coarse adcumulate textures. Komatiite sequences in some cases also contain gabbros or dolerites. Following current common usage, and the recommendations of Leshner and Keays (2002), standard International Union of Geological Sciences (IUGS) rock names are used for cumulate rocks without any genetic implications. It has also become standard practice to use cumulate terminology as developed for layered intrusions (Irvine, 1982) to denote these rocks, and many publications (including this one) use mixtures of terms such as ‘dunite’ and ‘olivine adcumulate’ more or less interchangeably according to context. In most cases the prefix ‘komatiitic’, in the magma series sense, is omitted but can be assumed.

Archean komatiites are never fresh, and researchers on these rocks have developed a habit of referring to original igneous lithologies and mineralogy even when the rocks being described are clearly metamorphic. Usually this is justified by the preservation of igneous textured through pseudomorphing relations during hydration, but in many cases, as discussed below, recognizing primary features in komatiites is complicated greatly by extensive modification of primary textures during metamorphism, deformation and weathering.

Large-scale controls and localization of major komatiite sequences

In the Yilgarn Craton, major komatiite sequences consisting of thick voluminous flows of high-MgO

magmas, erupted at high flux, and containing Ni–Cu–PGE mineralization, occur in the Norseman–Wiluna belt of the Kalgoorlie Terrane (Cassidy et al., 2006) at 2.7 Ga, and the Forresteria and Lake Johnston greenstone belts in the Southern Cross Domain (Youanmi Terrane) at 2.9 Ga. The occurrence of these events in specific belts, restricted to specific terranes, has been puzzling because mantle plumes, which are the ultimate sources of the komatiites, likely had a diameter of about 1000 km and hence, would have impinged upon the entire craton. So why don’t we find high-MgO komatiite sequences cratonwide?

The current explanation of the spatial and temporal localization of these magmas invokes evolving lithospheric architecture through time (Figs 3 and 4). As has been demonstrated for modern and ancient plume-derived magmas (Thompson and Gibson, 1991; Sleep, 1997; Sleep et al., 2002), thickness variations in the mantle lithosphere can control the localization of volcanism. For example, if a plume impinges upon a piece of heterogeneous lithosphere with thin and thick sections, plume material will ‘flow’ and be localized into the more shallow regions, whereas in thicker regions magmatism will be less voluminous or, depending on the thickness, absent altogether.

This theory is applied to the Yilgarn Craton using Hf isotopes in zircons from crustal rocks, mainly granites and felsic volcanic rocks (Mole et al., 2014). The Hf isotopes represent a proxy for the age and source of the crust–lithosphere system at the time of magmatism, where positive Hf values represent younger, mantle-derived crust, and negative ϵ_{Hf} represent older, reworked crustal material. As mantle addition of juvenile crust commonly involves crustal thinning, and crustal reworking involves anatexis in thickened crust, we can use the ϵ_{Hf} as a proxy for lithospheric thickness, where positive ϵ_{Hf} represents relatively thin lithosphere compared to negative ϵ_{Hf} values.

When we map the time-resolved Hf isotopes across the craton at 2.9 Ga (Fig. 3), the komatiites of the Forresteria and Lake Johnston belts (Fig. 1) and their host nickel mineralization, can be seen to occur within a juvenile (thin?) terrane adjacent to a narrow reworked lithospheric block (Fig. 3). Using the thickness proxy, this suggests that a plume impinged on the thicker reworked block and was diverted into the more juvenile region. In this area, more voluminous decompression melting could occur, and the path to the surface of such melts was much less restricted. Active rifting at the margin of the two blocks may have contributed to the localization of komatiites in the Forresteria belt (Fig. 5).

The map of Hf isotopes 2.7 Ga (Fig. 4) shows the evolution of the western Yilgarn Craton to a more reworked state since 2.9 Ga. Accordingly, when the 2.7 Ga plume event occurs, it is localized into the more juvenile lithosphere in the Kalgoorlie Terrane, which is where we find the most high-MgO, voluminous komatiites and the majority of major nickel deposits (Fig. 6).

As a result, the time–space evolution of the lithosphere appears to control the localization of komatiites in the Yilgarn Craton, and explains the spatial variability in komatiite occurrence, flux and temperature (MgO).

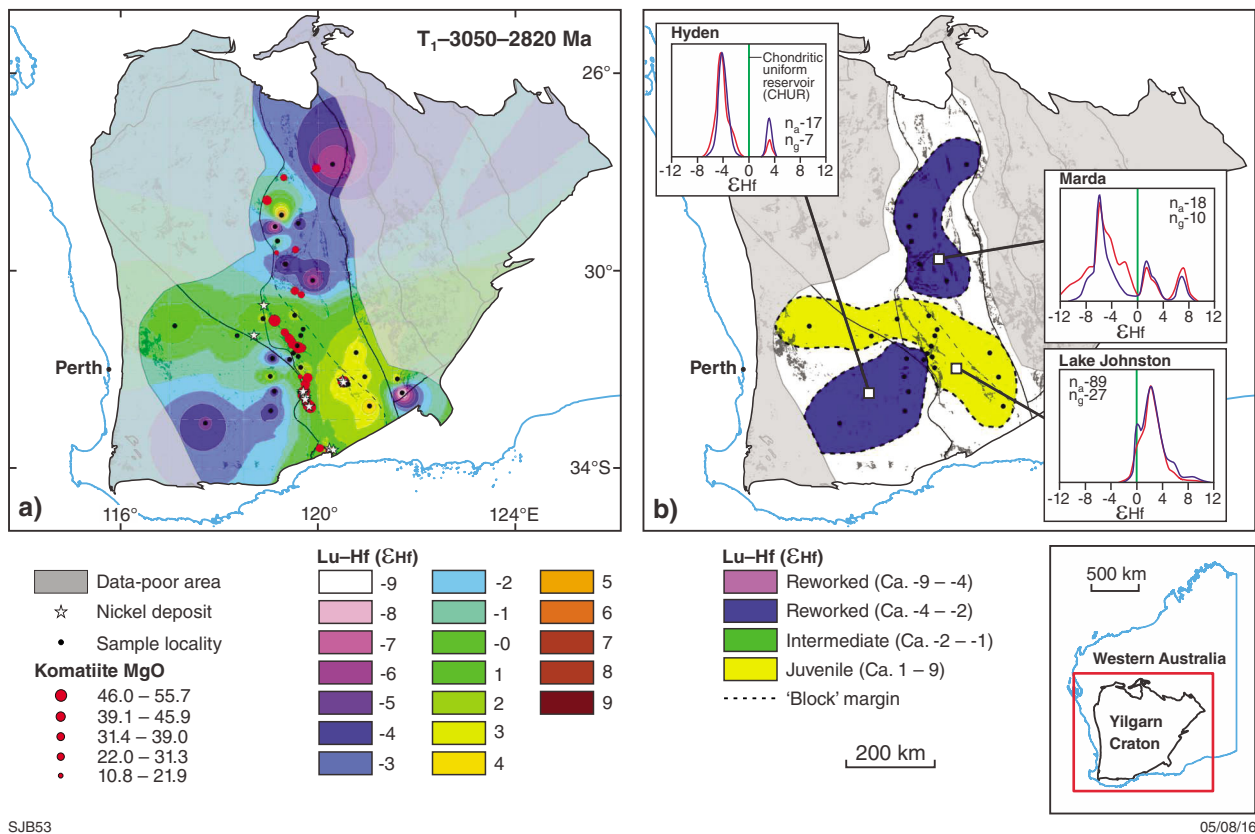


Figure 3. Lu–Hf (ϵ_{Hf}) map of the Yilgarn Craton at 3050–2820 Ma: a) Hf isotope map with the location of sample sites and komatiite localities (graded by MgO content); b) interpretive map of the area, showing the individual crustal blocks identified from the Hf isotope map and corresponding probability density plots. The blue curve represents the median ϵ_{Hf} for discrete temporal groups, i.e. grouped data (n_g), whereas the red curve represents all the individual grain analyses, i.e. all analyses (n_a). All diagrams demonstrate agreement between these methods that indicates grouping the data and producing a median is representative of the individual analyses that comprise each sample and temporal group. The chondritic uniform reservoir (CHUR) is labelled and represented by the green lines.

The textural diversity of komatiitic rocks

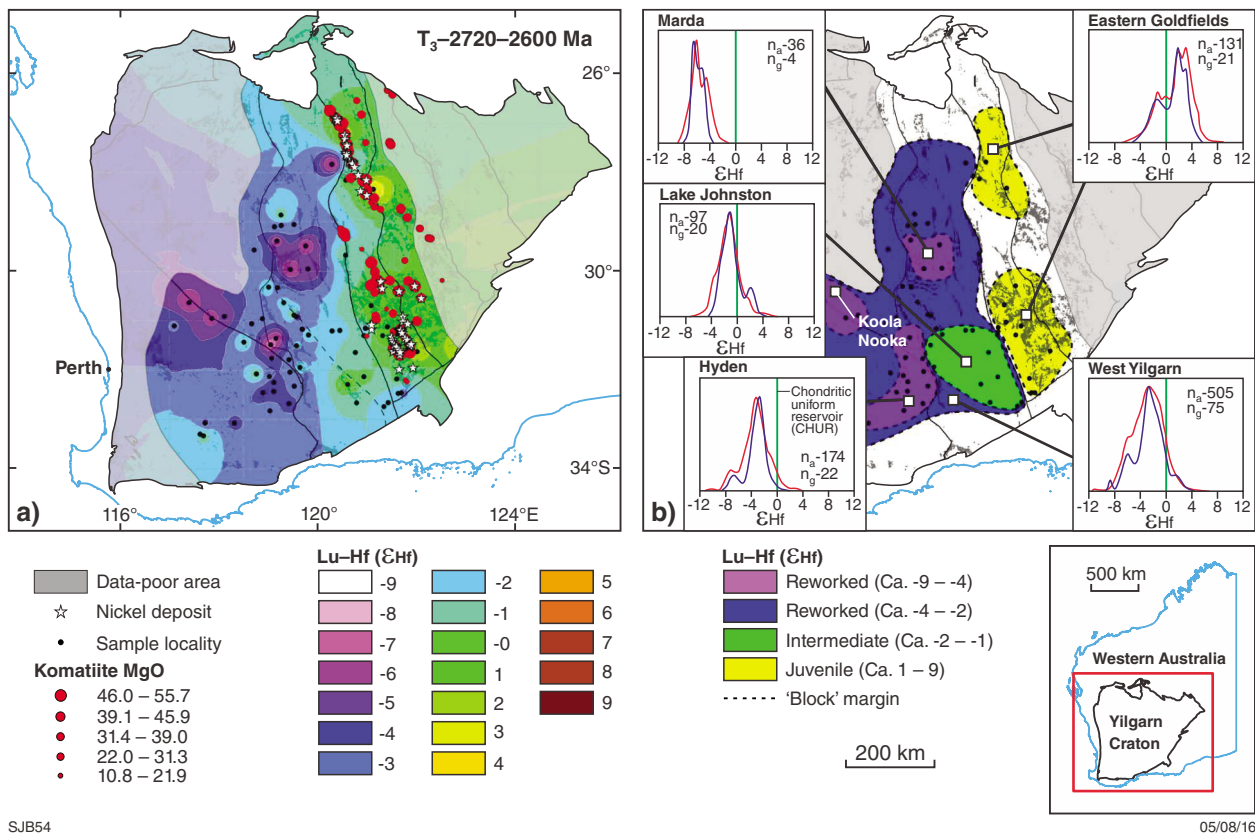
Komatiite sequences are composed of multiple compound cooling units varying greatly in thickness, lateral extent and relative proportions of different lithologies, representing a spectrum from rapidly cooled liquid to cumulates. Much of the diversity arises from varying proportion and morphology of original igneous olivine crystals. The spatial distribution of textural types provides the basis for interpreting the nature and origin of large komatiite flow fields as exposed in the eastern Yilgarn Craton.

Olivine is by far the predominant liquidus phase in komatiite systems, crystallizing over a very wide range of temperatures from possibly as high as 1600°C to below 1200°C (Green, 1975; Arndt, 1976; Thy, 1995; Herzberg and O’Hara, 1998) and occurring in the wide and spectacular array of morphologies which is the definitive characteristic of komatiites.

Spinifex textures

Spinifex textures are the major definitive characteristic of komatiites. The typical textural sequence of Munro-style komatiite flows (Fig. 7) consists of a fine aphanitic flow-top crust, underlain by a zone of downward-coarsening randomly oriented olivine plates, grading downward into parallel plates or radiating sheaves of very coarse skeletal olivine crystals which can, in extreme cases, be more than a metre long and commonly exceed ten centimetres (Pyke et al., 1973; Arndt et al., 1977; Donaldson, 1982a). In the case of flows with lower MgO contents (less than about 15% MgO), spinifex texture is defined by pyroxene: typically, composite, hollow needles comprising augite and pigeonite (Arndt and Fleet, 1979). The needles form conical sheaves, which, in the more spectacular examples, can be several metres long.

Spinifex textures are widely referred to as ‘quench textures’ but, as pointed out by Donaldson (1976), only the most finely grained material within centimetres of flow tops can properly be described as quenched.



SJB54

05/08/16

Figure 4. Lu-Hf (ϵ_{Hf}) map of the Yilgarn Craton at 2720–2600 Ma: a) Hf isotope map with the location of sample sites and komatiite localities (graded by MgO content); b) interpretive map of the area, showing the individual crustal blocks identified from the Hf isotope map and corresponding probability density plots. The blue curve represents the median ϵ_{Hf} for discrete temporal groups, i.e. grouped data (n_g), whereas the red curve represents all the individual grain analyses, i.e. all analyses (n_a). All diagrams demonstrate agreement between these methods that indicates grouping the data and producing a median is representative of the individual analyses that comprise each sample and temporal group. The chondritic uniform reservoir (CHUR) is labelled and represented by the green lines.

Coarse platy spinifex with crystals tens of centimetres in length can be found as much as 20 m below the nearest cooling surface. Coarse spinifex texture appears to form from an unusual combination of circumstances: very low nucleation rates and rapid growth rates corresponding to high degrees of undercooling in an environment where cooling rates are not exceptionally high. Coarse-grained spinifex textures remain very hard to explain. The Donaldson (1976) experiments suggest that they require rates of cooling higher by at least an order of magnitude than would be expected in the interior of a lava flow several metres thick.

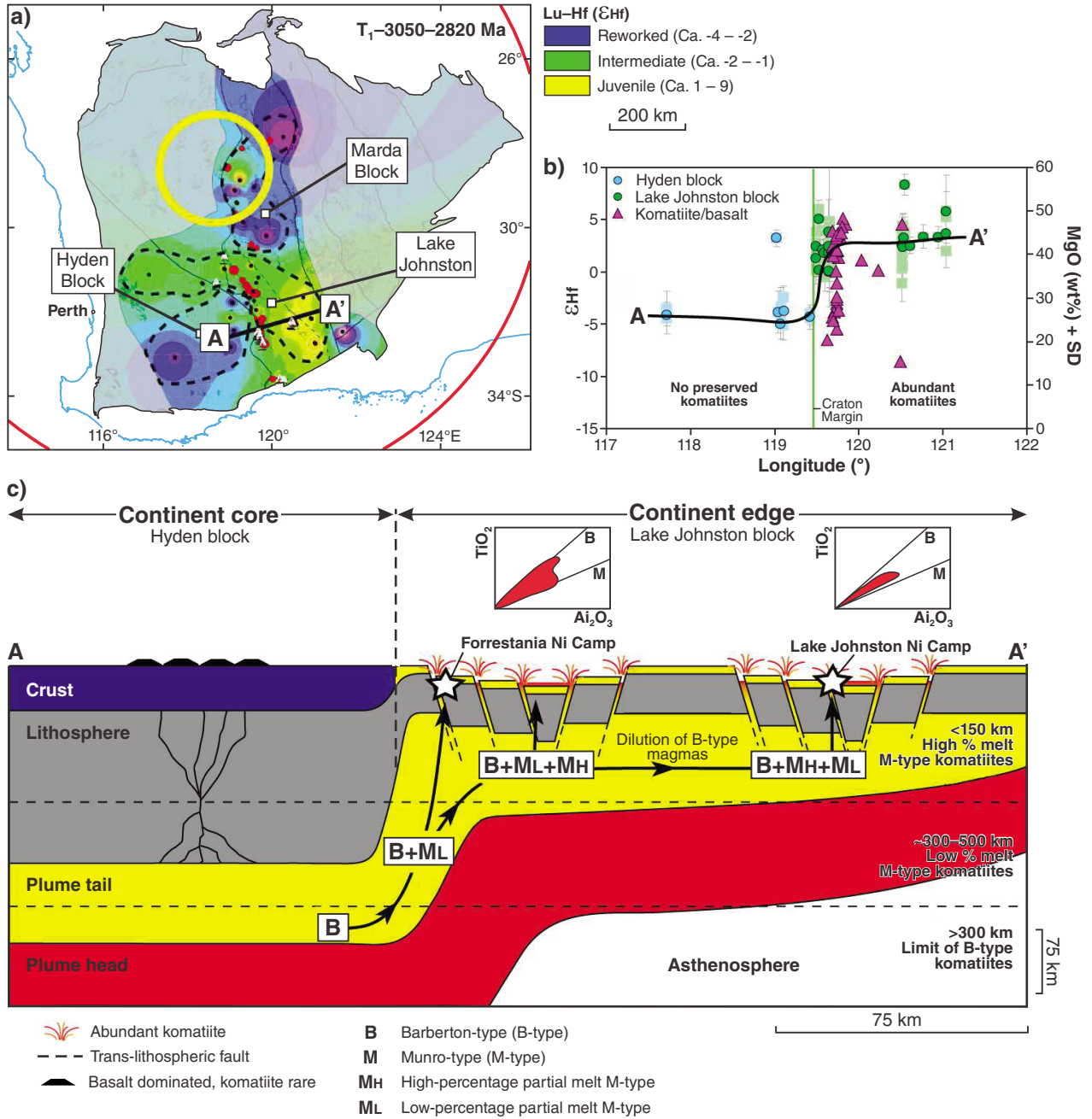
Several hypotheses have been advanced to explain this apparent paradox:

1. The low viscosity of komatiite melts leads to very rapid settling of homogeneously nucleated olivine crystals leaving the upper part of the flow depleted in nuclei
2. The very high content of 'olivine component' in the melt gives rise to high degrees of supercooling for a given temperature drop (Donaldson, 1982a)
3. Density relations cause olivine-depleted liquid to pool within the zone of crystallization at the top of the flow (Turner et al., 1986)

4. The high anisotropic thermal properties of olivine result in rapid heat conduction to the cooling surface along preferentially oriented olivine plates (Shore and Fowler, 1999; Fowler et al., 2002)
5. A pre-emplacment history of prolonged superheating results in destruction of melt structure and proto-nuclei (Arndt, 1994)
6. Crystallization in steep thermal gradients (Faure et al., 2002).

Regardless of the precise mechanism, coarse spinifex textures imply a combination of prolonged directional cooling and olivine supersaturation. Consequently, spinifex textures have been taken as diagnostic evidence of forming in an extrusive environment. This has been called into question with the recognition of spinifex textures in high-level intrusions emplaced into uncompacted sediments at Dundonald Beach in the Abitibi Belt (Davis, 1999; Arndt et al., 2004) and in the Kanowna – Black Swan area in Western Australia (Trofimovs et al., 2004b). Spinifex textures are clearly diagnostic of either extrusive or very shallow subvolcanic emplacement.

Setting of Southern Youanmi komatiites at ~2.9 Ga

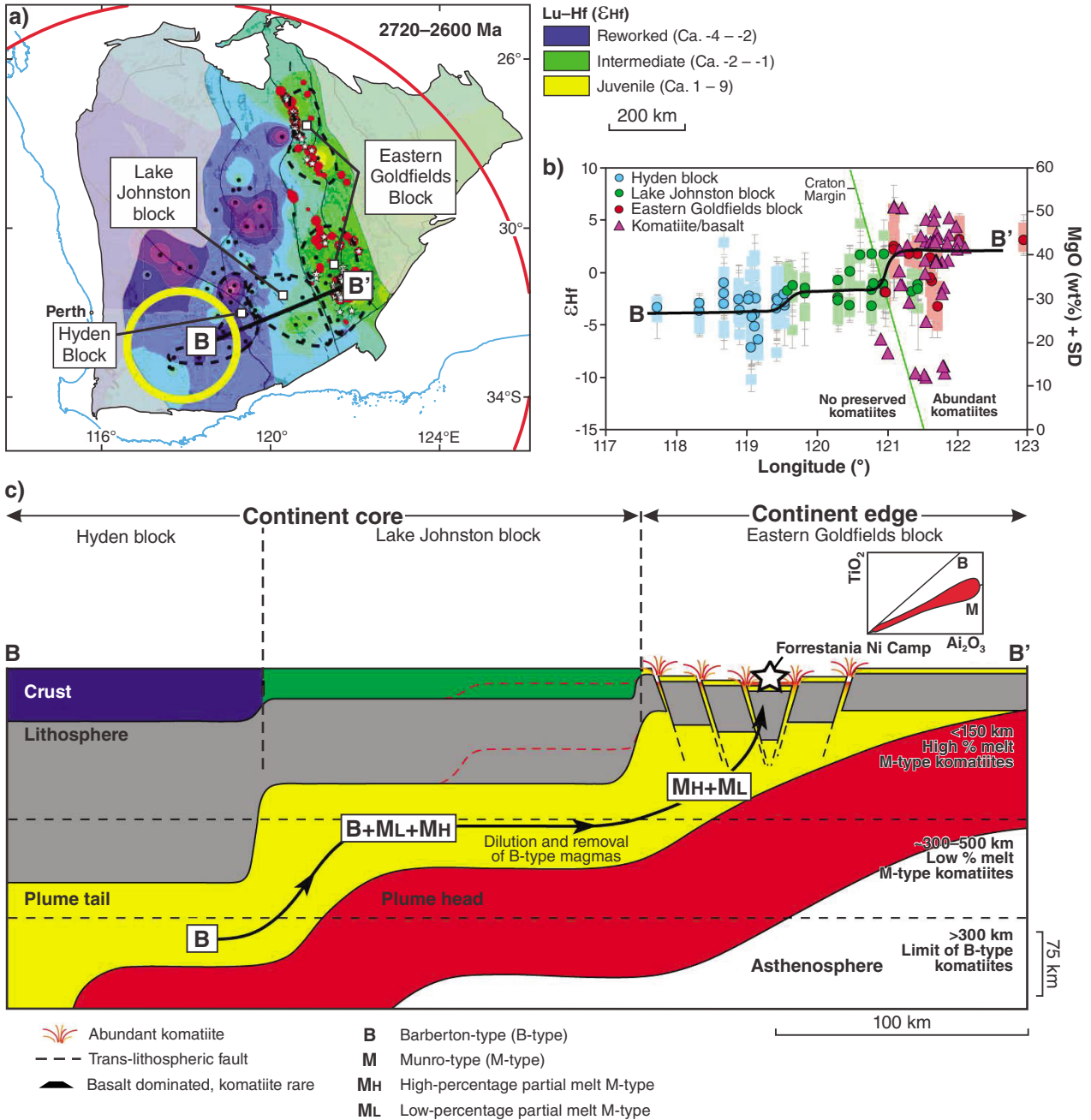


SJB55

05/08/16

Figure 5. Isotopic cross-section and interpreted lithospheric architecture during the emplacement of 2.9 Ga komatiites in the southern Youanmi Terrane: a) ϵ_{Hf} map showing the isotopic architecture at the time of plume emplacement with the approximate extent of the plume head (red) and tail (yellow) shown for scale, including the location of the cross-section; b) isotopic cross-sections documenting the changing crustal source from east to west together with the occurrence of ultramafic–mafic magmatism and corresponding MgO content (green lines show the approximate position of the inferred craton margin); c) interpreted lithospheric architecture based on the changing isotopic properties of the crust. The ‘B’ and ‘M’ markers indicate the approximate generation of Barberton- and Munro-type komatiites, respectively. Approximate thickness values for developed Archean lithosphere were ~250–150 km taken from Boyd et al. (1985) and Begg et al. (2009). The approximate scale of the plume head (~1600 km), tail (200–100 km) and thickness (150–100 km) were taken from Campbell et al. (1989). These values are proxies based on modern analogues and experiments.

Setting of Southern Youanmi komatiites at ~2.7 Ga

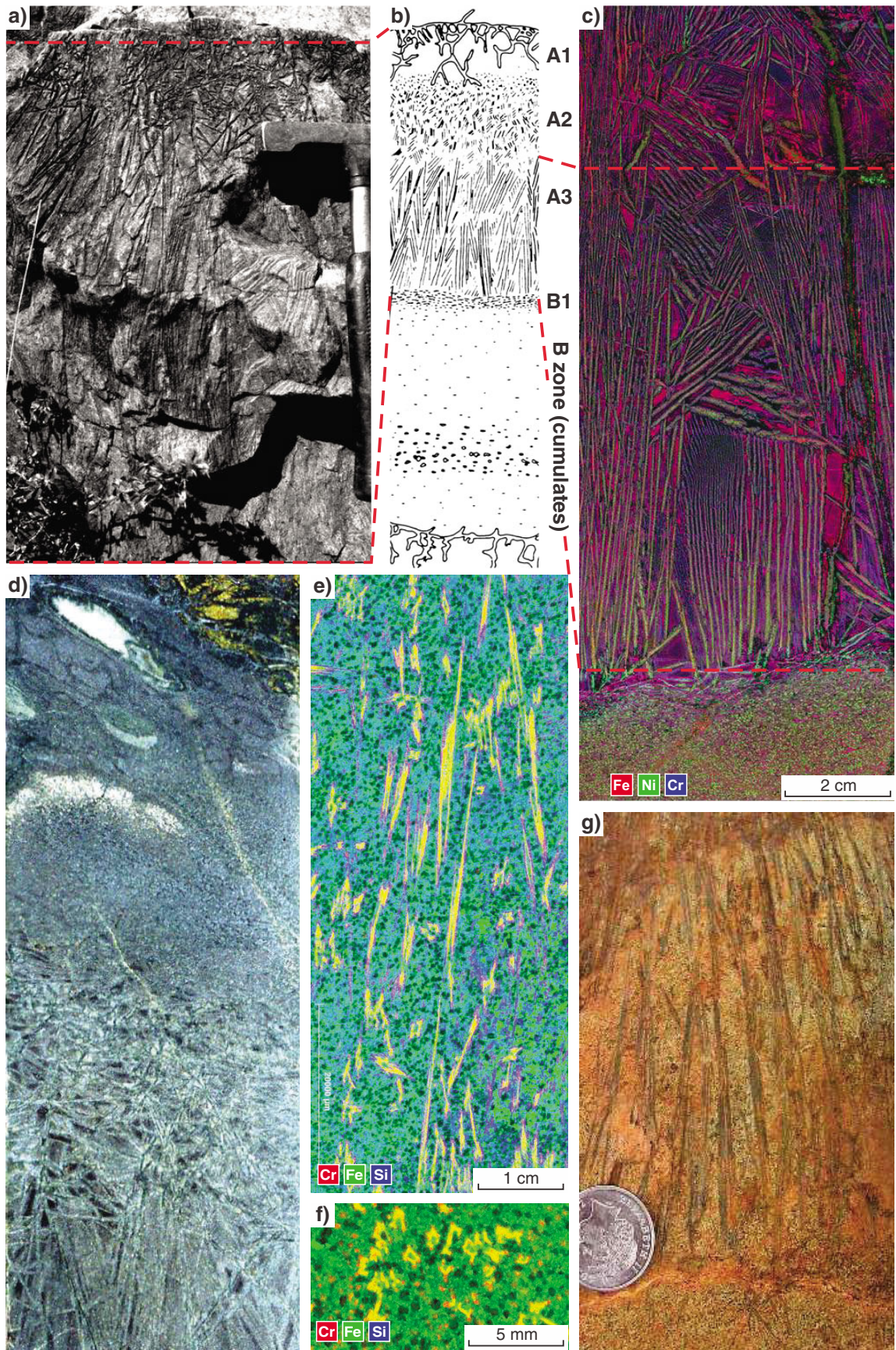


SJB56

05/08/16

Figure 6. Isotopic cross-sections and interpreted lithospheric architecture during the emplacement of the 2.7 Ga komatiites in the Eastern Goldfields (Kalgoorlie Terrane): a) ϵ_{Hf} map showing the isotopic architecture at the time of plume emplacement with the approximate extent of the plume head (red) and tail (yellow) shown for scale, including the location of the cross-section; b) isotopic cross-sections documenting the changing crustal source from east to west together with the occurrence of ultramafic-mafic magmatism and corresponding MgO content (green lines show the approximate position of the inferred craton margin); c) interpreted lithospheric architecture based on the changing isotopic properties of the crust. The ‘M’ markers indicate the approximate generation of Munro-type komatiites. Note that no Barberton-type komatiites occur at this time. The dashed red lines shown in c) account for the potential variation in lithospheric architecture within the Lake Johnston block.

Figure 7. (opposite) Spinifex textures: a,b) outcrop of A-zone of differentiated olivine spinifex-textured flow lobe from the Komati River valley traverse, Barberton Mountainland; c) A2, A3, B1 and B2 zone of a differentiated olivine spinifex flow lobe from Fly Bore, near Wildara, Western Australia. Note layer-parallel alignment of olivine plates in B1 zone at A–B zone contact. Image is a false-colour microbeam XRF element map; d) A1–A3 flow top of olivine spinifex from Scotia, Western Australia; e,f) false-colour element maps of pyroxene spinifex from the top of the Kurrajong sequence, Western Australia; e) is cut parallel to orthopyroxene needles (now replaced by Mg-amphibole); f) is end-on; g) outcrop of pyroxene spinifex from Murrin Murrin South showing downward radiating ‘cones’ of pyroxene needles and top of underlying B zone.



SJB57

06/07/16

Cumulate textures

Cumulate rocks are rocks formed by accumulation of crystals growing at or near the liquidus temperature of the parent magma. Formation of cumulates requires, by definition, some mechanism to separate the crystals from the liquid from which they grew. According to the original cumulus theory, the prime mechanism was gravitational settling of crystals, giving rise to bedding and other sedimentary features (Wager et al., 1960; Wager and Brown, 1968). This view was revised during a major reappraisal of the role of crystal settling in layered intrusions in the late 1970s (Campbell, 1978) and it is now recognized that cumulates can form by a variety of mechanisms ranging from gravitational deposition in density currents to in situ growth on the floors, walls and roofs of magma bodies (Latypov et al., 2015).

Cumulate rocks are classified into three textural types (Fig. 8): orthocumulates, adcumulates and mesocumulates (Wager et al., 1960). Orthocumulates consist of cumulus crystals predominantly in point contact, with interstices occupied by the solidification products of the original trapped interstitial liquid (the ‘intercumulus’ material). Adcumulates consist entirely of cumulus crystals in full face contact, typically with annealed 120° triple point boundaries and less than 10% intercumulus material. Mesocumulates are transitional between the other two, having typically between 10 and 30% intercumulus material and crystals predominantly in face contact.

In addition, there are two other varieties that are found in komatiitic rocks: heteradcumulates and harrisites.

Heteradcumulates

Heteradcumulates consist typically of two phases in a poikilitic texture: one phase shows mesocumulate to orthocumulate texture while the other forms large oikocrysts occupying the interstitial space and enclosing multiple grains of the other phase. According to cumulus theory, the poikilitic phase crystallizes from the trapped liquid but it commonly has a composition that implies that it crystallized in equilibrium with the liquid, simultaneously with the clearly cumulus phase. This would require that the intercumulus liquid convected freely through a permeable crystal pile, continuously maintaining equilibrium with the main mass of supernatant magma (Kerr and Tait, 1985). A simpler interpretation of this texture is that it forms by in situ competitive growth of the two phases, the poikilitic phase growing much more rapidly from dispersed nuclei and overtaking the more slowly growing enclosed (chadacryst) phase (McBirney and Noyes, 1979). The poikilitic phase in komatiitic olivine cumulates is most commonly clinopyroxene and, more rarely, orthopyroxene. Komatiitic dunites are unique in containing olivine-chromite heteradcumulates where chromite is the poikilitic phase (Barnes and Hill, 1995). Three-dimensional textural analysis has shown that these poikilitic chromites have dendritic morphologies (Godel et al., 2013).

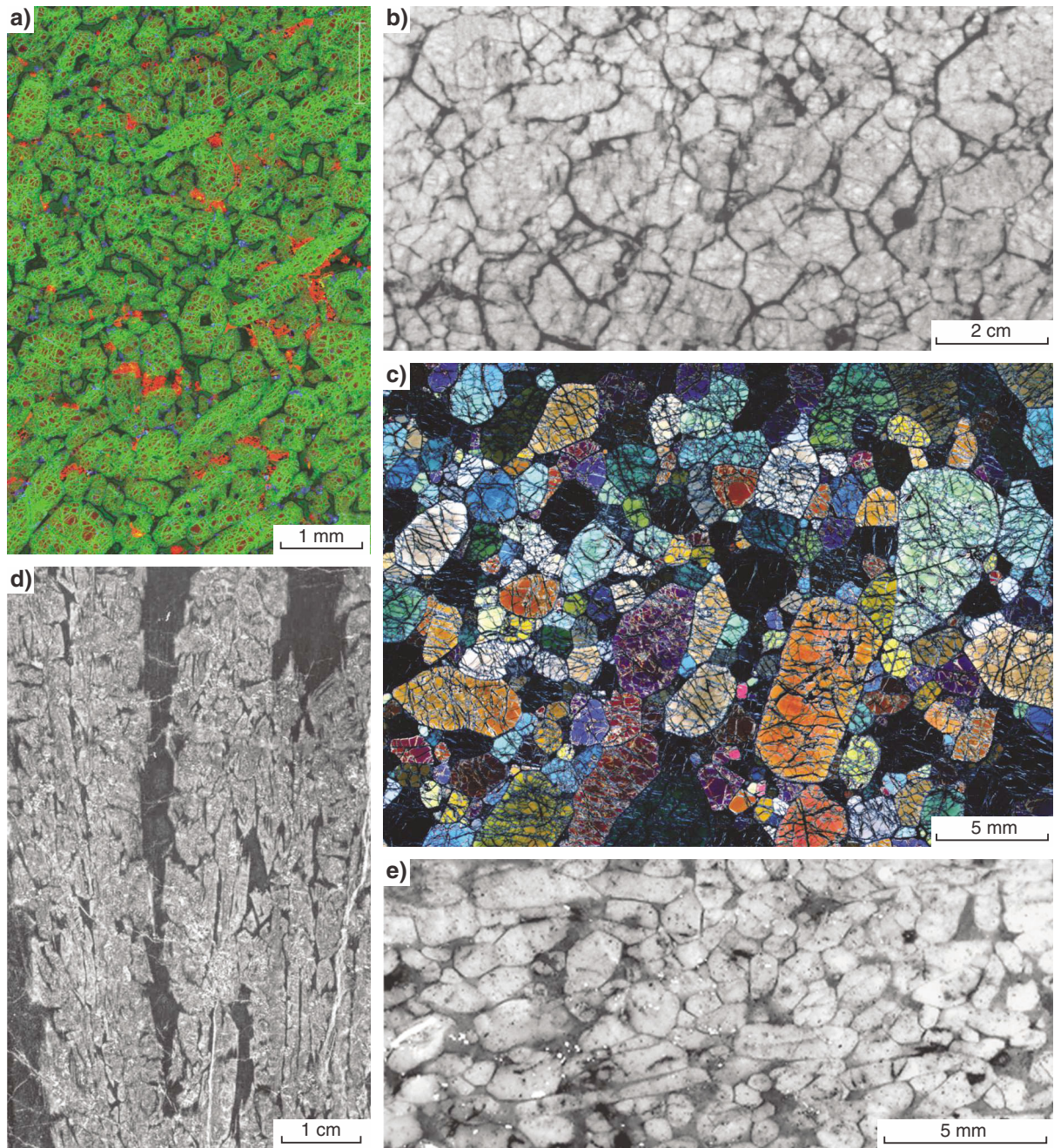
Harrisites

Harrisites consist of very large, branching crystals, decimetres in size, typically developed within thick sequences of conventional cumulates (Fig. 8d). They commonly show evidence of directional growth at right angles to a cooling surface and are transitional into spinifex textures, the major difference being that spinifex textures commonly grow downward from the cooling surface while harrisites grow up from the floor or inward from the wall. Harrisites (named after the type locality of Harris Bay in the Rum layered intrusion) were first recognized in layered intrusions (Donaldson, 1974) and were classified as ‘crescumulates’, indicating that they grew in situ rather than forming by mechanically transported crystals. This term has fallen out of use with the realization that most other textural types can also form in situ.

Most komatiitic harrisites are developed within thick packages of cumulates and are typically in the form of thin, discontinuous and probably slightly discordant layers. This raises the strong possibility that they are in fact analogous to the ‘spinifex veins’ described by Houlié et al. (2009) in cumulate komatiites in the Abitibi Belt. Houlié et al. (2009) interpret them in terms of injection of residual komatiite melt during inflation of compound flows. A further possibility is that they are formed in the manner of segregation veins in basaltic lava flows (Sigmasson et al., 2009; Costa et al., 2006) where high strain rates cause local brittle failure of partially consolidated cumulates and the transient pressure drop causes temporarily supercooled residual melt to flow into the crack.

Adcumulates

A distinctive characteristic of komatiitic sequences in parts of the Yilgarn Craton, particularly those in the Forrestania and Agnew–Wiluna greenstone belts (Fig. 1), is the presence of very coarse-grained olivine adcumulates with very little intercumulus material (Fig. 8b,c). Adcumulate textures have been thought to be unique to large layered intrusions and to have formed as a result of filter pressing and compaction of the crystal pile. Research on layered intrusions has shown that, while it is possible to form mesocumulates from orthocumulates by crystallization from circulating intercumulus liquid, it is impossible to form pure adcumulates in this way (Wilson, 1992), and various lines of evidence support the formation of adcumulates in situ on the floor of magma chambers (Campbell, 1978, 1987). The existence of komatiitic olivine-chromite heteradcumulates supports this view. Chromite is a very minor component, half a percent at most, of the komatiite liquid component. Chromite–olivine heteradcumulate textures can be found in shallow-level or possibly extrusive komatiitic cumulate bodies less than 200 m thick, where compaction, filter pressing and intercumulus liquid circulation are not viable mechanisms. This texture cannot be the result of interstitial crystallization of chromite from trapped liquid, and must have formed in situ at the interface between magma and the crystal pile (Barnes and Hill, 1995; Godel et al., 2013).



SJB58

05/08/16

Figure 8. Cumulate textures: a) coarse-grained olivine orthocumulate (Black Swan) with some hollow 'hopper' morphologies, serpentinized with strong textural preservation of olivine, false-colour XRF element map (red = cpx, blue = disseminated sulfide, bright green = magnetite veinlets in lizardite pseudomorphs after olivine); b) olivine adcumulate, silica cap from weathering profile showing near-perfect textural preservation of original olivines (cut slab), Murrin Murrin; c) olivine adcumulate, completely fresh, thin section in crossed polars, Wildara; d) olivine harrisite from Kambalda, cut slab; e) olivine mesocumulate, as in b)

Two factors are necessary for in situ adcumulate growth: low degrees of supercooling to inhibit nucleation, and continuous mechanical breakdown of boundary layers of depleted liquid around the growing crystals. This combination permits continuous growth of large crystals. These conditions are best achieved at the interface between rapidly flowing (and possibly turbulent) lava and a bed of hot crystals at, or very close to, the liquidus temperature (Barnes et al., 1988; Hill et al., 1995). Orthocumulate textures, in contrast, reflect accumulation of transported olivine, or in situ nucleation and growth of new crystals, in an environment of moderate supercooling where the supply of new crystals or nuclei at the top of the cumulate pile exceeds the rate of growth of the existing crystals.

Field relationships in komatiite sequences

Komatiite sequences typically contain a range of lithologies, mainly defined by variable proportion and morphology of olivine. The majority of mineralized komatiite sequences contain a large excess of cumulus olivine, that is, a much higher proportion of olivine than could be expected to have crystallized from the observed volume of magma. This can only be the result of flow-through: cumulus crystals are left behind in the magma pathway as the magma flows on (Barnes et al., 1988), giving rise to a spectrum of lithologies from olivine cumulates to rocks representing solidified phenocryst-poor liquid. The proportion of these rock types varies enormously on a range of scales, as does the relative proportion of different varieties of cumulate and spinifex texture.

A large body of field evidence collected over three decades has revealed certain characteristic patterns of rock type distribution, defined by these variations. The consistency of these patterns led Hill et al. (1995) to propose a universal classification scheme and volcanological model for komatiites, based on the identification of distinctive spatial associations or 'facies'. Each facies contains individual or multiple packages confined by fine-grained, rapidly cooled or quenched cooling surfaces. These packages are defined as 'cooling units'. Characteristic assemblages of different kinds of cooling unit define the various facies. The following section describes some komatiite localities in the Yilgarn Craton and elsewhere that exemplify these facies and which have been used to construct a generalized model of development of large komatiite flow fields.

Spinifex-bearing compound flow sequences

The type komatiite localities of Munro Township and the Komati River Valley consist of multiple thin flow units, typically less than ten metres thick and forming overlapping lenticular lobes characterized by upper spinifex-textured 'A-zones' and lower cumulate-textured 'B-zones' (Pyke et al., 1973; Arndt et al., 1977). In a

number of well-studied localities, such as the Silver Lake Member at Kambalda, such spinifex-textured differentiated flow units are closely associated with thicker units dominated by olivine orthocumulates and mesocumulates. A stratigraphic reconstruction of a 'typical' Kambalda shoot is shown in Figure 9, modified from Beresford et al. (2002). The basal Silver Lake Member komatiites overlie the tholeiitic Lunnon Shoot basalts, separated by an intermittent thin unit of contact sediment, whose distribution is discussed in more detail below. Lava pathways are defined by the presence of homogeneous, olivine-rich cumulate sequences up to 200 m thick, an absence of contact sediment beneath the basal flow, and absence of overlying interflow sediments. Away from the pathways, flow units typically become thinner, and may be overlain by sediments (Gresham and Loftus-Hills, 1981; Lesher et al., 1984). The preferred pathways and flanking sheet flows correspond exactly to the 'ore' and 'non-ore' environment recognized very early in the development of the camp (Gresham and Loftus-Hills, 1981).

The pathways are closely associated with the ribbon-like ore shoots, and are strongly linear in geometry. The Silver Lake sequence passes up into the Tripod Hill Member, consisting of multiple thin flow lobes, mostly 1–5 m thick, with characteristic spinifex A zones and fine-grained olivine orthocumulate B zones. The upward progression from thick, cumulate-rich flow units to thin, layered spinifex-rich flow lobes is a common relationship, found in many komatiite sequences, which is attributable to declining emplacement rates with time at a particular point in a flow field.

Lenticular dunite bodies

Lenticular dunite bodies are of great economic significance in that they host the two largest accumulations of nickel sulfides in the Yilgarn Craton (and among the largest in the world): Perseverance, and Mount Keith (Barnes et al., 2011). They are found in two areas: the Agnew–Wiluna section of the Norseman–Wiluna greenstone belt, and the eastern komatiite belt of the Forrestania greenstone belt, where they also host mineralization (Perring et al., 1995b). The Maggie Hays deposit in the Lake Johnston greenstone belt (Heggie et al., 2012) is also associated with what is probably a lenticular dunite body. They are exemplified in the area covered by this guide by the unmineralized dunite body at Mount Clifford.

Lenticular dunite bodies are defined by a combination of olivine adcumulate lithologies and geometry. In three dimensions, they are elongate, flattened cigar-shaped bodies that appear as lenses in cross-section. The Perseverance area illustrates the defining relationship of this facies. The central 700 m-thick dunite lens is flanked to the north and south by a sequence dominated by homogeneous, medium-grained olivine orthocumulates. To the south, the flanking sequence contains packages of multiple, thin, differentiated spinifex-textured flows that extend between about one to about three kilometres to the south of the centre of the lens. Immediately south of the

lens, these flows are overlain by olivine adcumulate, which lenses out to the south as spinifex-textured flows make up a higher proportion of the section. The lens itself consists of remarkably pure, coarse-grained, monomineralic olivine adcumulate, much of which is fresh, lacking in chromite, and showing a gradual upward increase in the forsterite content of olivine from about Fo_{92.5} at the bottom to Fo_{94.8} at the top (Barnes et al., 1988). A similar trend is seen in the Mount Clifford dunite body (see below).

Sheeted dunite bodies

The dunite sheet facies consists of extensive, laterally homogeneous cooling units with a persistent, correlatable vertical sequence typically grading from dunites to cumulate and non-cumulate komatiitic gabbros. The Walter Williams Formation of the central Norseman–Wiluna greenstone belt (see Ghost Rocks locality description in this volume) contains the largest known example (Hill et al., 1995; Gole and Hill, 1990). The unit as a whole is exposed over an outcrop area of 130 km north–south and up to 35 km east–west, varies in thickness from less than 100 m to about 500 m, and is composed dominantly of olivine cumulates with a continuous central layer of olivine adcumulate extending over 100 km from Ora Banda in the south to Ghost Rocks in the north (Fig. 2). Farther north, in the Kurrajong area (Fig. 2), the sequence gives way to a differentiated profile, consisting of a lower zone of olivine mesocumulates overlain by a cyclically layered differentiated zone with a cap of pyroxene-spinifex textured komatiite and brecciated chilled upper margin. This differentiated upper zone is interpreted as a ponded lava lake.

An extensive sheeted dunite body is developed in the Murrin Murrin area (Fig. 2), between Leonora and Laverton (Hill et al., 2001). Here, a sheet-like body of olivine cumulate, consisting mostly of mesocumulate with some adcumulate, intermittently overlain by gabbro, is traceable over several tens of kilometres strike length, in many places relatively flatlying owing to intersection of regional cross folds, forms the protolith to the Murrin Murrin nickel laterite deposits. In the Kilkenny Syncline, at its southernmost extent, this sheet is steeply dipping, approximately 300 m thick, and capped by strongly layered olivine orthocumulates, thin pyroxene cumulate layers and gabbro, together forming a typical ‘dunitic differentiated cumulate subfacies’ profile. This sequence passes laterally along strike into a succession of multiple thin flow lobes, each a few metres thick, dominated by olivine and pyroxene spinifex textures, with intercalated layers of felsic tuff. This is a very clear example of a situation where coarse-grained olivine adcumulates can be traced laterally into demonstrably extrusive rocks, which are interpreted as a constructional levee sequence that ponded komatiite lava and allowed it to differentiate in situ within a lava lake.

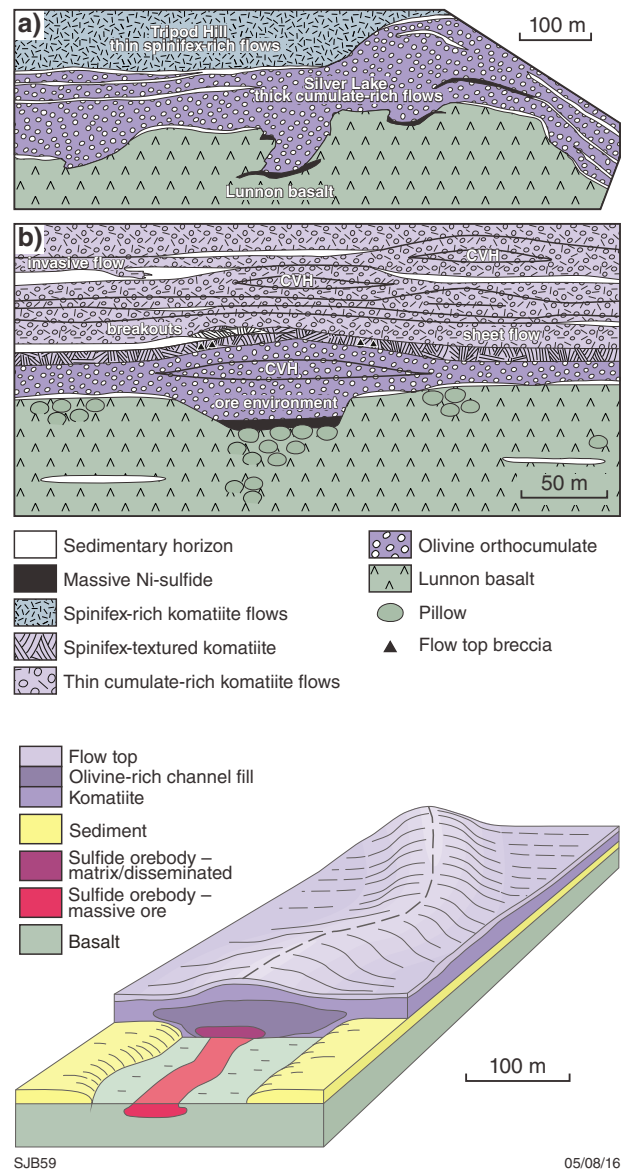


Figure 9. Kambalda facies model: a) simplified east-west cross-section through Lunnon Shoot, after Gresham and Loftus-Hills (1981); b) simplified facies distribution at the Long-Victor Mine after Beresford et al. (2002); c) schematic relationship of orebodies to basal komatiite flow geometry

Invasive flows or high-level intrusions in bimodal volcanic terranes

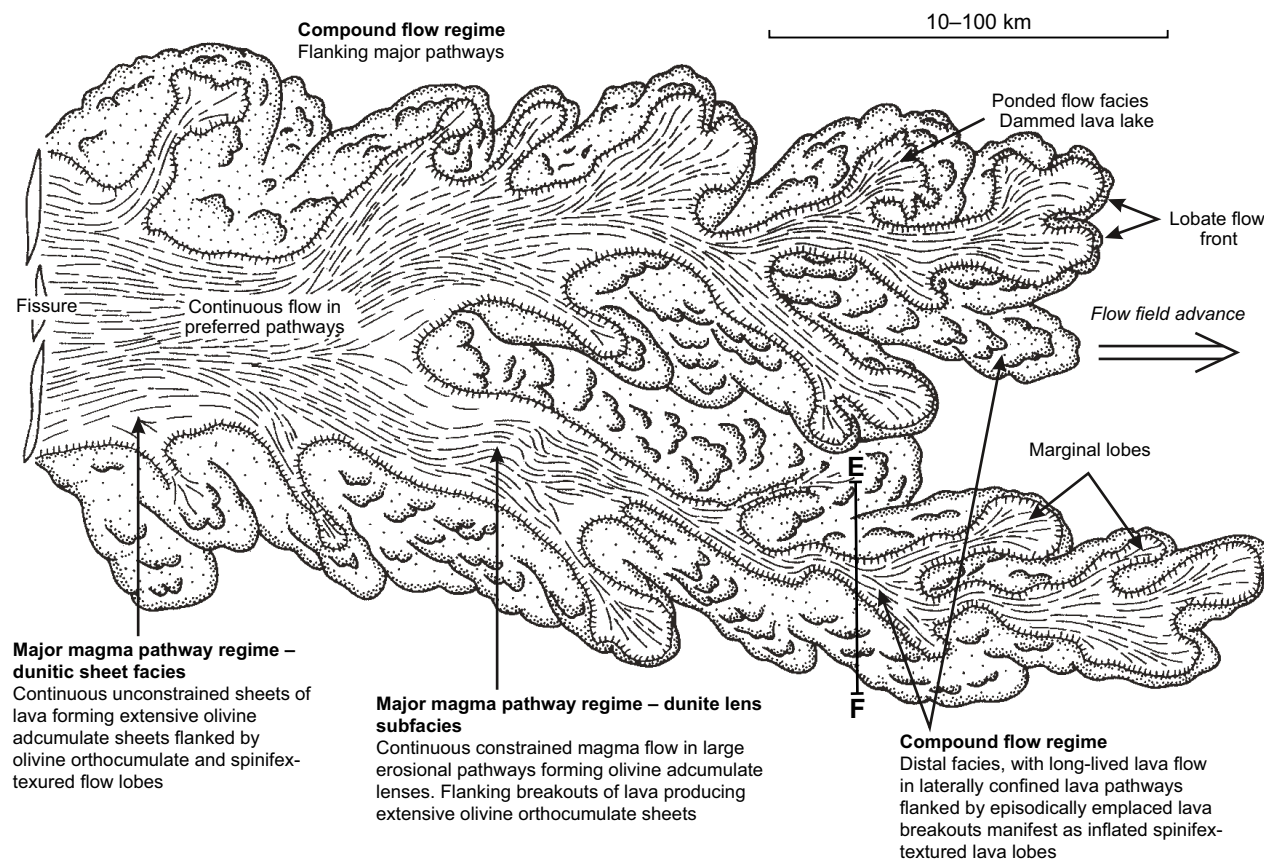
Trofimovs et al. (2004a,b) and later sections of this guidebook describe a number of localities to the south and west of the Black Swan nickel camp where complex intercalations between komatiite and dacite units are well exposed in lakebed outcrops. Two komatiite associations are described: typical asymmetric spinifex-textured flow lobes and complex, irregular bodies, which are decimetres to tens of metres thick and form irregular apophyses within porphyritic dacites, with spinifex textures at top and bottom contacts. Relationships are somewhat similar to those described from the Dundonald Beach area in the Abitibi Belt in Canada (Arndt et al., 2004), and are interpreted as the result of very shallow-level intrusion or invasion of komatiite magma into dacite. Magma mingling textures imply that the dacite was still hot at the time of komatiite emplacement, and that the two magma types were being erupted contemporaneously.

Evidence for bimodal komatiite–dacite volcanism is also reported from the Black Swan locality (Hill et al., 2004), where similar complex intercalations also occur, although in the Black Swan case these are inferred from close-spaced diamond drilling and detailed field

relationships are less evident (see Black Swan nickel mine locality). The Black Swan komatiites were interpreted by Hill et al. (2004) as extrusive based on the presence of differentiated spinifex flow lobes and vesicular textures within cumulates. The complex intercalations are interpreted as a combination of irregular topography, bimodal volcanism and thermomechanical erosion of dacite by komatiite.

Volcanic architecture of komatiite flow fields

Hill et al. (1995) proposed a composite komatiite flow field model (Fig. 10) that related all the facies associations described above, based on field relationships observed within the Norseman–Wiluna and Forrestania greenstone belts, and working on the hypothesis that the dunite bodies of both belts were dominantly extrusive in origin. Dunitic sheet facies and dunitic compound sheet facies were interpreted as the products of the highest flux inflated pathways, formed by upward accretion of adcumulates at the pathway floor. The lenticular dunite bodies were considered to have formed in laterally restricted pathways, constrained by original substrate topography and enhanced by entrenchment of the flow into linear erosional rills.



SJB60

18/08/16

Figure 10. Plan view of a hypothetical komatiite lava flow field fed by inflationary pathways, modified from Hill et al (1995)

These magma pathways were flanked by, and passed downstream into, compound flow facies rocks with similar overall geometry at smaller scales, representing more distal emplacement of lava at lower flow rates.

In a further development of the flow field model, Hill (2001) interpreted the characteristic relationships within the compound flow facies as a direct analogue of the inflationary basaltic flow model (Fig. 10), with thin spinifex lobes forming as breakouts at the propagating edges of the flow field, or subsequently by lateral breakouts and overflow from lava pathways or tubes.

The relative proportion of the different facies within the flow field was interpreted by Hill et al. (1995) as a function of lava flux: lower eruption rates resulted in compound flow facies forming closer to or at the source vent, and a higher proportion of thin spinifex flow lobes. The common observation of thick, compound cumulate-rich flows overlain by stacks of thin spinifex lobes was interpreted as a consequence of declining lava flux rate with time at any given point within the flow field.

Within this model, differentiated cumulate subfacies sequences represent downstream blockage of pathways and subsequent backing up and in situ differentiation of ponded magma. They are typically developed over former magma pathways — broad, sheeted pathways in the case of Kurrajong and Murrin Murrin; lenticular, dunite-filled pathways as at Mount Keith and Mount Clifford; and smaller, distributary pathways in compound flow facies sequences as at Flying Fox in the Forresteria Belt (Perring et al., 1995a; Barnes, et al., 2011).

Origin of adcumulate bodies

As noted above, there is an ongoing debate about the intrusive versus extrusive origin of komatiitic dunite bodies. Detailed field relationships exposed in the Mount Keith openpit led Rosengren (2004) and Rosengren et al. (2005) to conclude that this particular lenticular dunite body formed as a high-level sill emplaced into intermediate volcanoclastic rocks. This conclusion was challenged by Gole et al. (2013) on various grounds, most notably that dacites immediately overlying the upper contact of the Mount Keith body showed no evidence of thermal metamorphism or melting. The close association between dunite bodies and spinifex-textured rocks was the major line of evidence used by Hill et al. (1995) and Donaldson et al. (1986) to argue for an extrusive origin of the dunite bodies. In a number of localities, including Perseverance (Barnes et al., 1988), Kathleen East (Hill et al., 2001), Murrin Murrin (see Murrin Murrin locality description), the Cosmic Boy to Seagull section of the Eastern Forresteria Belt (Perring et al., 1995b) and the Cliffs (Central) Ultramafic Belt at Mount Keith (Hill et al., 2001), olivine adcumulates, coarse-grained mesocumulates and differentiated spinifex lobes occur within single continuous bodies of komatiitic rocks. In several of these cases, dunite bodies can be traced laterally along strike into multiple spinifex lobes. At Perseverance (Trofimovs et al., 2003) and Forresteria, the degree of deformation is such that it is not possible to discount tectonic juxtaposition of these rock types and there is no possibility

of making a definitive case for an extrusive origin for the dunites. At Murrin Murrin South (see Murrin Murrin locality description), the extensive exposure and general lack of major penetrative deformation makes it very likely that the observed field relationships are primary and not the result of a tectonic coincidence. The present state of knowledge is that some dunite-bearing komatiite bodies are quite possibly intrusive, some are probably extrusive, and most are indeterminate. Either way, the close association between dunite and demonstrably extrusive komatiites implies that komatiitic dunites were emplaced at least in shallow subvolcanic environments, as originally suggested by Naldrett and Turner (1977), roughly simultaneously with the emplacement of the flows, and are integral components of the volcanic architecture.

Critical to the interpretation of the dunites is the recognition that they must have formed largely in situ, for reasons relating to the kinetics of crystal growth, regardless of intrusive or extrusive origin. This implies that adcumulates form in an environment of rapid flow-through of magma crystallizing at very low degrees of supercooling very close to the liquidus temperature, and probably under turbulent conditions to allow sweeping away of depleted boundary layers around growing crystals.

From the point of view of mineral exploration, in komatiite flows as in conduit-hosted intrusive nickel sulfide deposits (Barnes et al., 2016), it is crucial to identify the site of maximum flux of magma. Thick dunite bodies define major magma pathways, whether intrusive or extrusive. The relative size and flux rate of the pathway is reflected in the grain size and concentration of olivine: the larger the pathway, the more closely packed and coarse grained the olivine, culminating in centimetre-scale, pure olivine adcumulates. These pathways provide thermally efficient, rapid delivery of magma and act as loci for thermal erosion.

Contrasting stratigraphic associations

Within the Kalgoorlie Terrane, komatiites occur in two distinctly different stratigraphic associations within the 2710–2690 Ma age range. In the Kambalda Domain in the southwest of the terrane (Fig. 1), komatiites form part of a plume-derived, basalt-dominated stratigraphy, which is underlain by low-Th tholeiites and overlain by intermediate-Th tholeiites and siliceous high-Mg basalts (Barnes and Fiorentini, 2012), with little or no felsic material. Elsewhere in the Kalgoorlie Terrane, in the Boorara Domain to the east of Kalgoorlie in the south and in the Agnew–Wiluna Domain in the north (Fig. 1), dacite flows and tuffs are intimately intercalated with komatiites (Hill et al., 2004; Trofimovs et al., 2004a,b; 2006). In the Kanowna – Black Swan region in the Boorara Domain (covered in this guidebook), the two magma types appear to have erupted simultaneously, forming complex peperite mingling textures and invasive pillow-like flow lobes of komatiite injected into soft or partially molten dacite (Trofimovs et al., 2004a) in a spectacular example of bimodal komatiite–dacite volcanism. Examples of this association are described in detail in the Breakaway

and Gordon Sirdar localities. Complex intercalations of komatiite and felsic tuffs and lavas are also inferred from closely spaced diamond drill sections through the Black Swan nickel deposit, 70 km northeast of Kalgoorlie (Hill et al., 2004). A similar intercalation of co-erupted komatiite and dacite is found within the Agnew–Wiluna Domain in the northern part of the terrane (Duuring et al., 2012; Fiorentini et al., 2012). This northern region hosts the largest amount of the known nickel sulfide mineralization in the Eastern Goldfields.

The two distinct stratigraphic associations — komatiite + siliceous high-Mg basalt (SHMB) and komatiite + coeval dacite — are mutually exclusive throughout the terrane. While local SHMB-like samples are found within the komatiite–dacite associations, as at Black Swan, they are clearly the result of local supracrustal magma mingling, peperite formation and within-flow contamination. Thick sequences of SHMB lavas are not found in the komatiite–dacite domains, and felsic volcanism (other than the overlying and significantly younger Black Flag rocks) is not found in the komatiite–SHMB domains. This may reflect a fundamental deep lithospheric control on magma generation and emplacement (Mole et al., 2014).

Komatiite-basalt associations

The Kalgoorlie Terrane is characterized by a belt of highly magnesian, cumulate-dominated komatiites and associated contaminated komatiitic basalts that extends

from Widgiemooltha in the south to Wiluna in the north, over a strike length of more than 500 km (Fig. 1), and erupted over a restricted time period between c. 2708 and 2690 Ma (Hill et al., 1995; Nelson, 1997; Barnes and Fiorentini, 2012; Fiorentini et al., 2012). The Kalgoorlie Terrane komatiites host the world’s third largest province of nickel sulfide ore deposits, after Sudbury and Noril’sk–Talnakh, and account for more than half of the total global endowment of komatiite-hosted Ni sulfide mineralization in a number of camps of which the major ones are Kambalda, Perseverance and Mount Keith (Barnes and Fiorentini, 2012). This belt is overwhelmingly the largest (by contained metal tonnes) nickel sulfide province associated with Archean komatiites. To the east in the Kurnalpi Terrane, komatiites are widespread but are marked by more evolved, lower MgO compositions, and a prevalence of compound spinifex-textured flows interpreted as the distal flanks of the major flow fields (Hill et al., 1995).

Associated with the komatiitic sequence in both terranes is a characteristic assemblage of distinctive basalt types, matching suites found in many other greenstone sequences worldwide (Barnes et al., 2012). Kalgoorlie Terrane basalts fall into three distinct geochemical categories, from stratigraphic bottom to top (Fig. 11): a Low-Th Tholeiite suite (Lunnon), an Intermediate Th Basalt suite (Devon Consols) and a High-Th Siliceous Basalt suite (Paringa), all defined on the basis of ratios of highly incompatible elements to moderately incompatible Ti (Fig. 12).

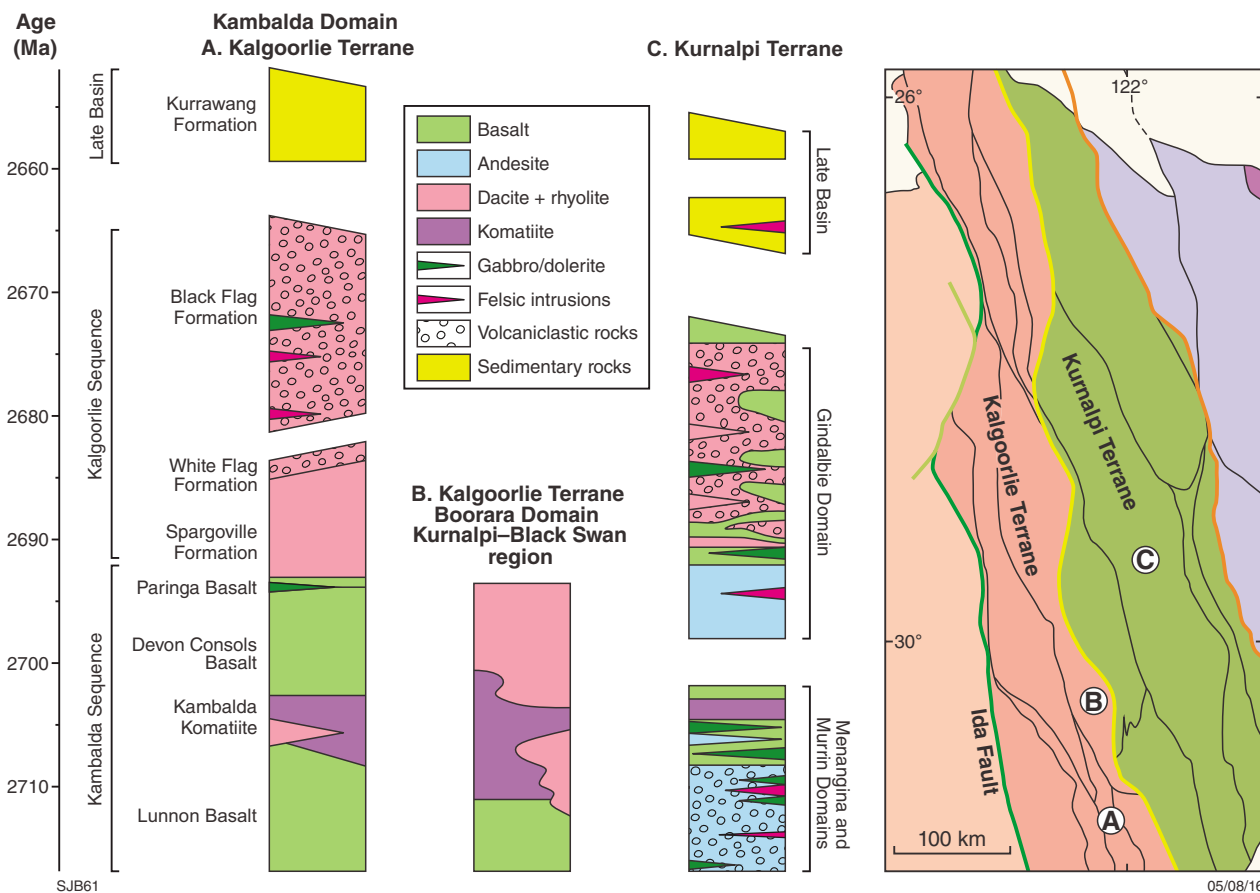
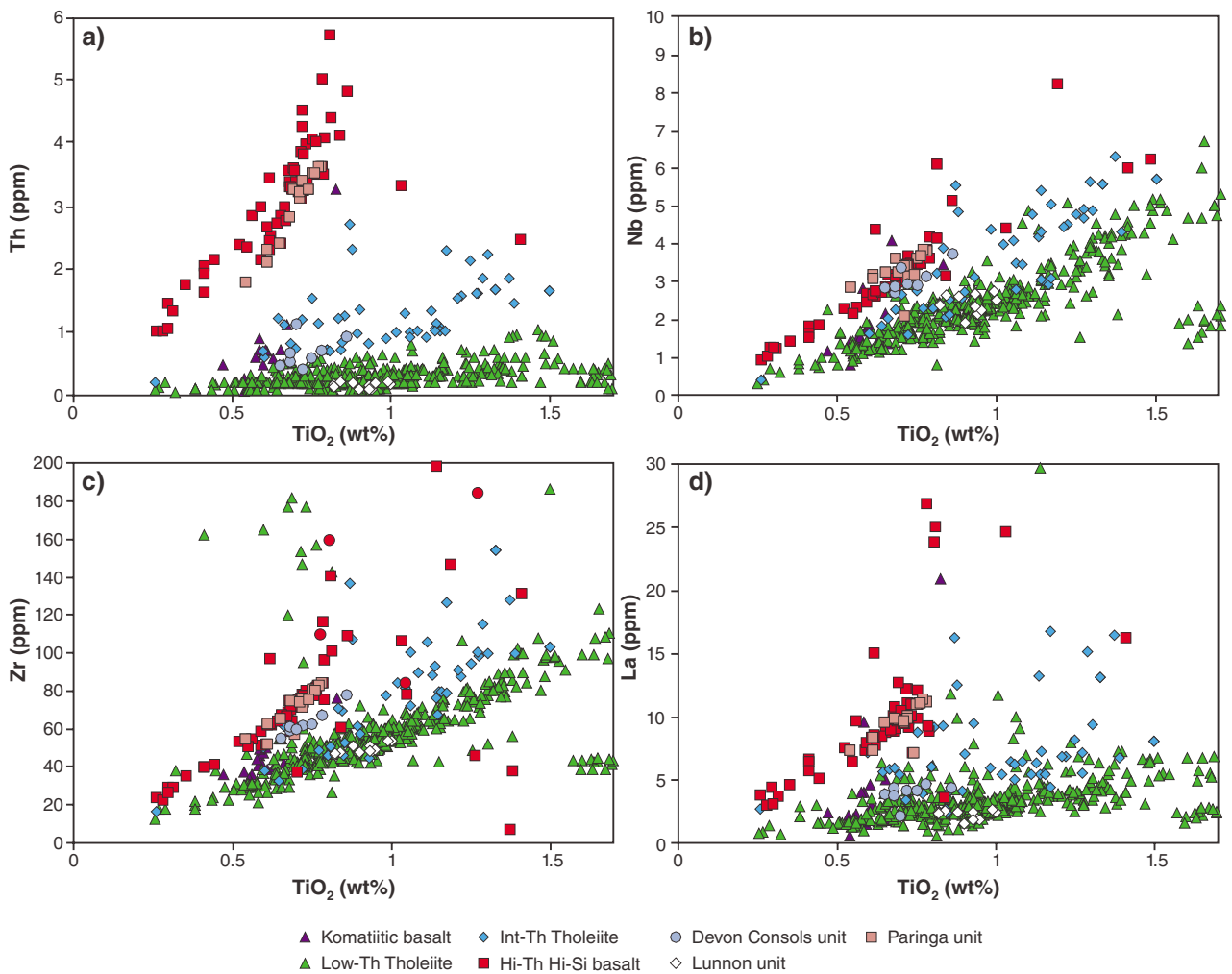


Figure 11. Stratigraphic columns for Kambalda and Boorara Domains of the Kalgoorlie Terrane, and for the Kurnalpi Terrane farther east, modified from Czarnota et al. (2010) and Barnes and Van Kranendonk (2014)



SJB62

08/07/16

Figure 12. Basalt chemistry summary

The Low-Th Tholeiite suite shows a tholeiitic affinity at SiO_2 between 50 and 53 weight %; moderate Al_2O_3 around 15 weight %; distinctly elevated Cr and Ni; MgO mostly between 5.5 and 8 weight %; and flat rare earth element – high field strength element (REE–HFSE) patterns with slight depletion in Th and small Nb anomalies. The High-Th Siliceous Basalt suite ranges from high-silica basalts to magnesian andesites with $\text{SiO}_2 > 52$ weight %; MgO between 6 and 9 weight % with higher values reflecting accumulated olivine or pyroxene; relatively low Fe and Ti; depleted Ni for given Mg#, strongly enriched light rare earth elements (LREE) and Th, strongly negative Nb anomalies and primitive mantle-like Zr/Nb, Nb/Y, Al/Ti and heavy rare earth element (HREE) ratios. The Intermediate Thorium Basalt suite is intermediate between these two end members in almost all respects. All three suites are represented across the entire Eastern Goldfields Superterrane, with their type examples in the Kalgoorlie–Kambalda region.

The most widespread suite, the Low-Th Tholeiite, shows limited spatial variation and is broadly homogeneous across the Eastern Goldfields Superterrane. It is interpreted as the Archean analogue of plume-head large igneous

province (LIP) basalts, similar to Phanerozoic oceanic plateau basalts and particularly to flood basalts associated with late-stage continental rifting, differing only in higher Ni and Cr attributed to a komatiite component in the plume. The High-Th Siliceous Basalt suite displays a distinctive signature, which is unique to Archean greenstone terranes. No similar compositions are found in Phanerozoic rocks from any setting. Derivation by contamination during fractionation of komatiites, probably deep in the crust, followed by mid-crustal homogenization in magma chambers, is the most likely hypothesis.

Basalts with characteristic island arc signatures of Nb depletion, high Al_2O_3 , low FeO and low Ni and Cr contents are rare or absent from the Eastern Goldfields Superterrane. This led Barnes et al. (2012) to conclude that the distribution of mafic and ultramafic magmatism across the Superterrane at c. 2700 Ma was caused by emplacement of a mantle plume under the ‘lid’ of what is now the Youanmi Terrane, which at that time formed part of the proto-Yilgarn Craton. Voluminous eruption of plume-tail komatiite was focused along the eastern margin of the Youanmi Terrane, in what is now the Kalgoorlie Terrane, while plume-head basalts and less voluminous

komatiites were erupted over a much wider area. The entire package of komatiites and basalts has many of the hallmarks of a LIP (Ernst, 2007).

Felsic and intermediate volcanic assemblages and relationship to komatiites and basalts

Volcanic and volcanoclastic rocks of andesitic to dacitic affinity are widespread across the Kalgoorlie and Kurnalpi Terranes. Much of the assemblage, including the areas covered by this guidebook in the Boorara Domain, falls within the same age range as the komatiite–basalt assemblage (Fig. 11). Rocks of andesitic to dacitic composition range from lavas to agglomerates and tuffs, and are commonly porphyritic with up to 25% phenocryst plagioclase, and locally amygdaloidal (Barley et al., 2006; 2008). Andesites underlie and overlie low-Th tholeiites and komatiites in the Kurnalpi Terrane, spanning an age range from c. 2720 to 2695 Ma (Blewett et al., 2010; Czarnota et al., 2010), although the older ages may be due to a component of inherited xenocrysts.

The felsic and intermediate volcanic rocks of the Kalgoorlie and Kurnalpi Terranes span a range of compositions from andesites to soda-rhyolites on the basis of silica and total alkali contents (Fig. 13a). Trace element characteristics of the felsic and intermediate volcanic rocks span a distinctive range that can be characterized by REE patterns and other lithophile immobile trace elements. According to Barnes and Van Kranendonk (2014) and Hollis et al. (2015), most of the felsic rocks fall within, or slightly on the low-Yb side of, the FI–FII categories of Hart et al. (2004).

The felsic rocks overall display a continuum of REE patterns, incorporating a broad trend of positive correlated La/Sm and Gd/Yb (i.e. light and heavy REE slopes) with a second flat trend toward variable and high Gd/Yb at high but roughly constant La/Sm (Fig. 13). The higher Gd/Yb character is indicative of an affinity with the tonalite–trondjemite–granodiorite (TTG) suite of magmas, usually interpreted as being moderate to high pressure partial melts of mafic precursors in the deep crust (Martin et al., 2005), although they are somewhat less enriched in Th and LREE and less depleted in Y and Yb than the ‘type’ TTG compositions as defined by Smithies (2000). A fourfold classification was proposed by Barnes and Van Kranendonk (2014): ‘Calc-alkaline low La/Sm’; ‘Calk-alkaline’ having La/Sm_n between 2 and 3.4; ‘TTG’ having La/Sm_n greater than 3.4 and Gd/Yb_n mostly greater than 1.5; and ‘TTG high Gd/Yb’ having La/Sm_n greater than 3.4 and Gd/Yb_n greater than about 3, where the subscript n refers to normalization to primitive mantle composition (Fig. 13). The TTG categories are dominated by dacites and rhyolites and have distinct negative Nb and Ti anomalies. The ‘Calk-alkaline’ categories are dominated by andesites; negative Nb and Ti anomalies are also evident, with the deeper Nb anomalies being associated with the stronger LREE enrichment. The entire intermediate to felsic assemblage is characterized by unusually high MgO, Cr and Ni contents compared with modern arc-related volcanic rocks at the same silica content.

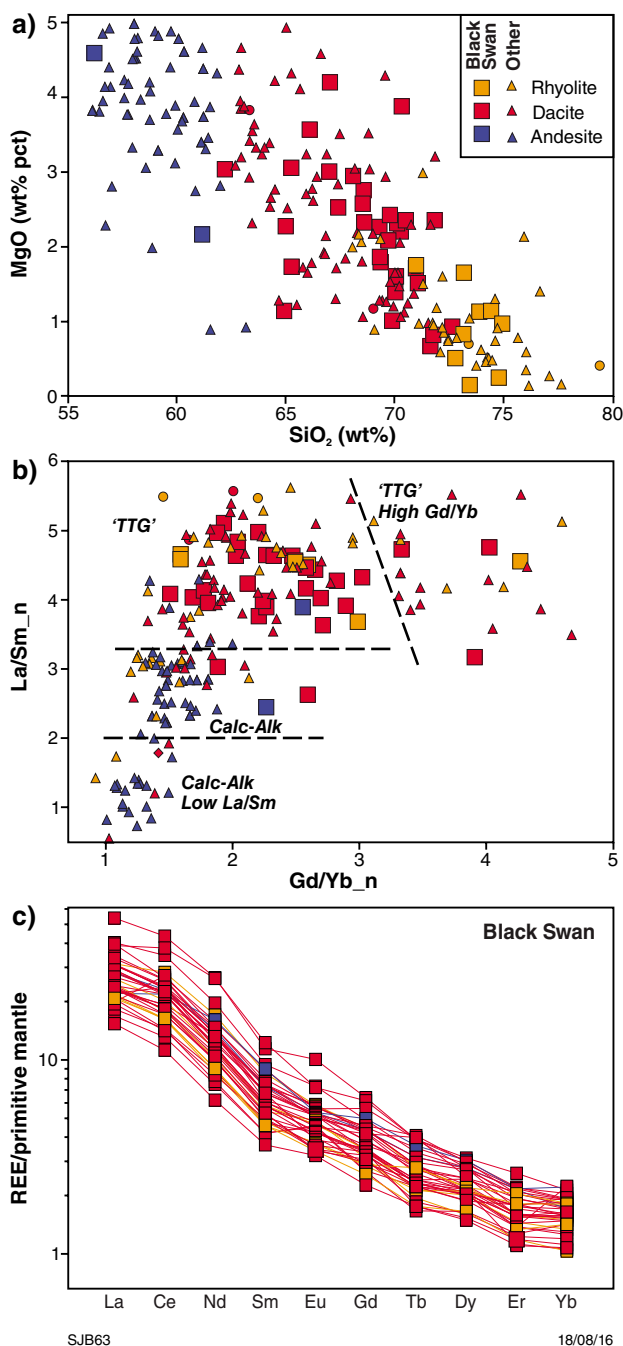


Figure 13. Geochemistry of Boorara Domain felsic rocks at Black Swan

Lithophile trace element concentrations in Eastern Goldfields Superterrane andesites closely match Phanerozoic calc-alkaline island arc andesites whereas the associated dacites and rhyolites have distinctly steeper patterns, higher ratios of middle REE to heavy REE (as represented by Gd/Yb ratios), and smaller negative Nb and Ti anomalies compared with Eastern Goldfields Superterrane andesites and with modern arc dacites and rhyolites.

Geochemical types of dacite are distributed without any obvious spatial control across both the Kalgoorlie and Kurnalpi Terranes, although a higher proportion of the TTG types are found within the Kalgoorlie Terrane. The andesite groupings are predominantly, although not exclusively, found within the Kurnalpi Terrane. The TTG-type andesites are rare and restricted to the Kalgoorlie Terrane and the low La/Sm variety is restricted to the northern part of that terrane. In summary, the various dacite types can be found anywhere across the two terranes but andesites of calc-alkaline type become dominant toward the east. Volcanogenic hydrothermal massive sulfide deposits (VHMS) in the Kurnalpi Terrane are associated with the calc-alkaline geochemical type, with the notable exception of the Ag-rich Nimbus deposit east of Kalgoorlie, which is uniquely associated with typical TTG dacite (Hollis et al., 2015). The dacites associated with komatiites in the Boorara Domain fall predominantly in the field of TTG type dacites (Fig. 13).

Excursion stops

Mount Hunt (MGA 356815E 6586475N)

Modified from Swager (1990) and Wyche (2007)

Hannan Lake and Mount Hunt

Most of the described stratigraphy of the southern Kalgoorlie Terrane, except for the lower basalt unit that is not exposed in the Kalgoorlie district (Figs 14 and 15), can be seen in the Mount Hunt area. The komatiite unit is represented by the Kambalda Komatiite (formerly called the ‘Hannan Lake Serpentinite’), and the Devon Consols Basalt. The Kapai Slate marks the top of the Devon Consols Basalt. The Paringa Basalt, which represents the upper basalt unit in the regional stratigraphy, occupies the highest part of Mount Hunt. The Black Flag Group, which outcrops on the western side of the Goldfields Highway, represents the upper felsic volcanic and volcanoclastic association. The late-basin succession is not exposed at Mount Hunt, but lies about 10 km to the west, where it is represented by the Kurrawang Formation.

The Hannan Lake – Mount Hunt traverse examines the stratigraphy of the Kambalda Domain, which is interpreted as a D_1 thrust sheet, repeating and overlying the sequence at Kambalda. The traverse crosses the axial plane of the regional F_2 anticline, the northern continuation of the Kambalda Anticline. The F_2 hinge is sheared out by the D_3 Boulder–Lefroy Fault. At Hannan Lake, the succession youngs eastward and is the continuation of the mineralized sequence south from Kalgoorlie. At Mount Hunt, the overall younging is to the west, but the succession is complexly folded and sheared.

The Hannan Lake – Mount Hunt traverse

Serpentine Bay

Extensive outcrops of serpentinite of the lowest exposed unit of the Kambalda Komatiite are found on the western shore of Hannan Lake (Locality 1 on Figure 16: MGA 358690E 6587100N). The rocks at Serpentine Bay are atypical in that they have been strongly affected by talc–carbonate alteration. However, this alteration has preserved spinifex textures indicating the extrusive nature of the ultramafic flows, which vary in thickness between one and 10 metres. Some flows show classic asymmetries in the spinifex textures (Fig. 17), indicating that the sequence youngs to the east. A typical cumulate base (B-zone) now consists of talc–carbonate–serpentine(–magnetite), which has replaced an original dunite or peridotite with 2–3 mm olivine grains. The spinifex zones, with coarse sheaf-spinifex blades up to 30 cm long followed by fine-grained, random spinifex and a thin aphanitic flow top, are now talc–carbonate–albite–chlorite(–magnetite). Albite content may be up to 15%.

To the west, the bulk of the Kambalda Komatiite is a strongly serpentinitized orthocumulate peridotite comprising medium-grained, granular olivine pseudomorphs with interstitial amphibole and chlorite. East of the headland (Fig. 16), islands in Hannan Lake contain east-facing pillow basalt (Devon Consols Basalt), cherty sedimentary rock (Kapai Slate), and komatiitic basalt (Paringa Basalt). Deep drilling below the lake has helped establish the regional stratigraphy (Travis et al., 1971).

Mount Hunt

The outcrop of Devon Consols Basalt at the start of the Mount Hunt traverse is best exposed in the creek immediately south of the track (Locality 2 on Figure 16: MGA 357824E 6586567N). Here it consists of variolitic basalt with well-preserved pillow structures. The pillows have a pale, feldspar-rich core and a greenish marginal phase with a groundmass of chlorite, clinzoisite, and tremolite (Hallberg, 1972). A transitional zone between core and margin consists of varioles made up of locally coalescing, spherical masses of radiating albite and amphibole plus chlorite, i.e. uralitized acicular pyroxene, whereas the marginal phase consists of plagioclase (An_{5-25}) in a felted groundmass of chlorite, clinzoisite, and tremolite (Hallberg, 1972). The origin of the varioles remains unresolved, but they are common in basalts at the lower end of the MgO range within high-Mg series (10–18 wt% MgO). Because they locally overprint primary volcanic structures, but have themselves been deformed during regional deformation events, the varioles may represent early alteration or devitrification textures.

A few metres west of the creek, the Kapai Slate, which overlies the Devon Consols Basalt, outcrops as a well-exposed chert marker (MGA 357785E 6586530N). At depth, the chert becomes carbonaceous and pyritic slate. Several episodes of deformation are indicated by the presence of small-scale, low-angle faults and two phases of steep-dipping, tight folds.

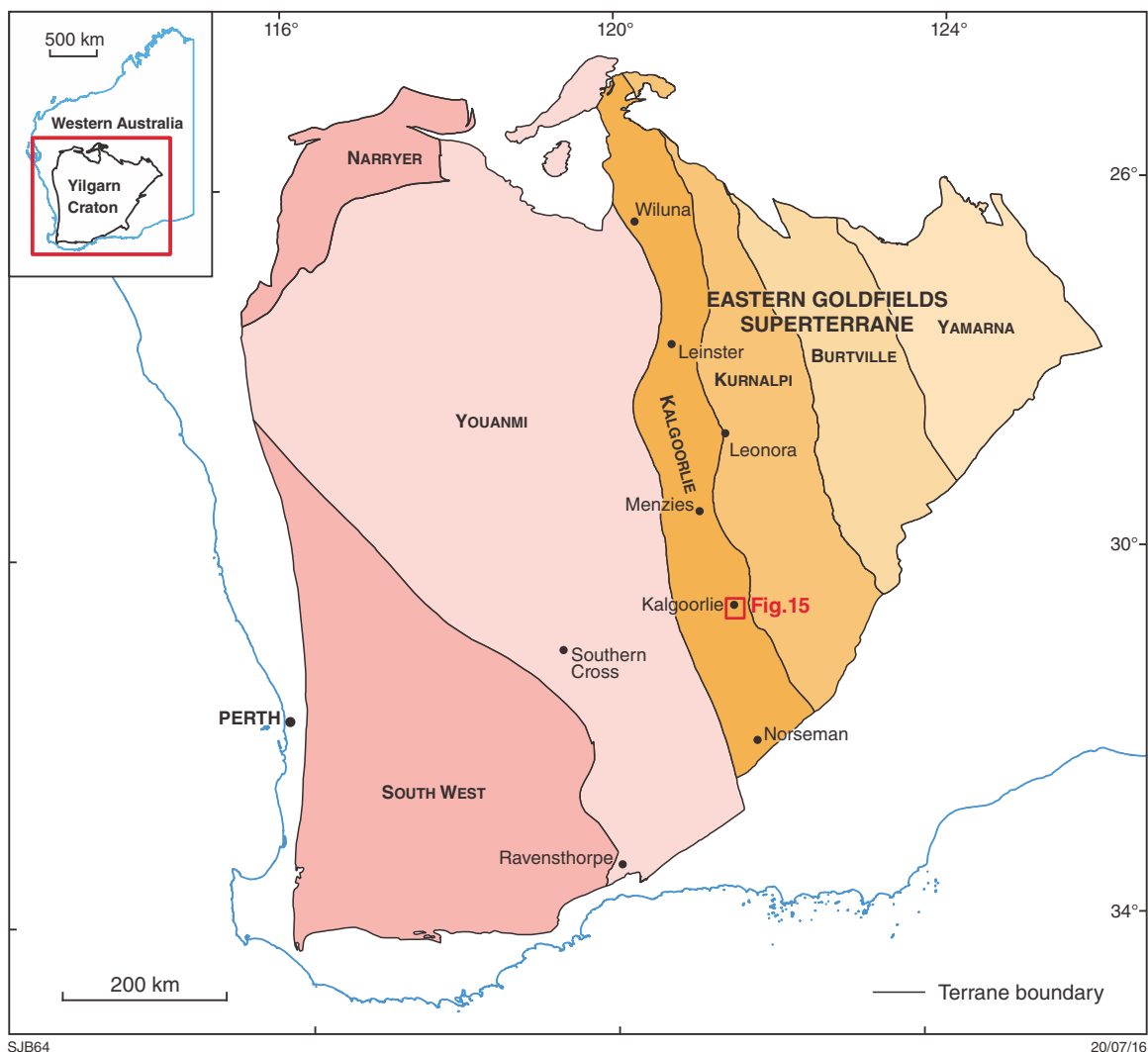


Figure 14. Subdivisions of the Yilgarn Craton

Immediately west of the Kapai Slate and south of the track, the base of the Williamstown Dolerite can be seen in small rubbly outcrops of peridotite, now a talc–tremolite–serpentine(–magnetite–apatite) rock. Euhedral olivine has been pseudomorphed by serpentine; euhedral prismatic orthopyroxene has been replaced by talc–tremolite; and intergranular clinopyroxene has been replaced by chlorite, serpentine, or both. Farther south, a more differentiated portion of the Williamstown Dolerite consists of gabbro in which pyroxene has been altered to fine, fibrous tremolite and chlorite, and to plagioclase that is partially altered to chlorite.

Williams and Hallberg (1973) studied the Williamstown Dolerite sill in some detail in the hinge of the major fold, about one kilometre to the north. They showed that the sill outcrops continuously over at least two kilometres, is bifurcated, has a thickness of about 400 m, and displays marked differentiation. All primary minerals are altered, but texture preservation allows recognition of the original mineralogy. A lower ultramafic zone consisted of a peridotite unit (olivine and orthopyroxene) overlain by a thin orthopyroxenite unit, followed by a mafic zone with

a lower norite–gabbro unit (orthopyroxene, plagioclase, and clinopyroxene) and an upper gabbro (plagioclase and clinopyroxene).

Continuing the traverse westward, the Kapai Slate is crossed again (MGA 357725E 6586490N) in what is interpreted as the west limb of a very tight D_1 syncline. Next are some small rubbly outcrops of Devon Consols Basalt. A major fault is crossed next and the whole sequence is repeated. A possible interpretation of the geometry is shown in Figure 18. According to this interpretation, an early, isoclinal fold pair (F_1), in which the short limb is thinned and sheared out, was tilted into a steep west-dipping orientation on the west limb of the regional anticline (F_2), and refolded by a discontinuous, asymmetric F_3 fold (Swager, 1989). In the side of the hill, extensive outcrop of variolitic Devon Consols Basalt contains large, weathered-out varioles (Fig. 19: MGA 357525E 6586500N). The overlying Kapai Slate is marked by a line of shallow gold workings that have now been infilled (MGA 357495E 6586475N). The Williamstown Dolerite is poorly exposed, being largely covered by talus from Mount Hunt. The final ascent to the summit

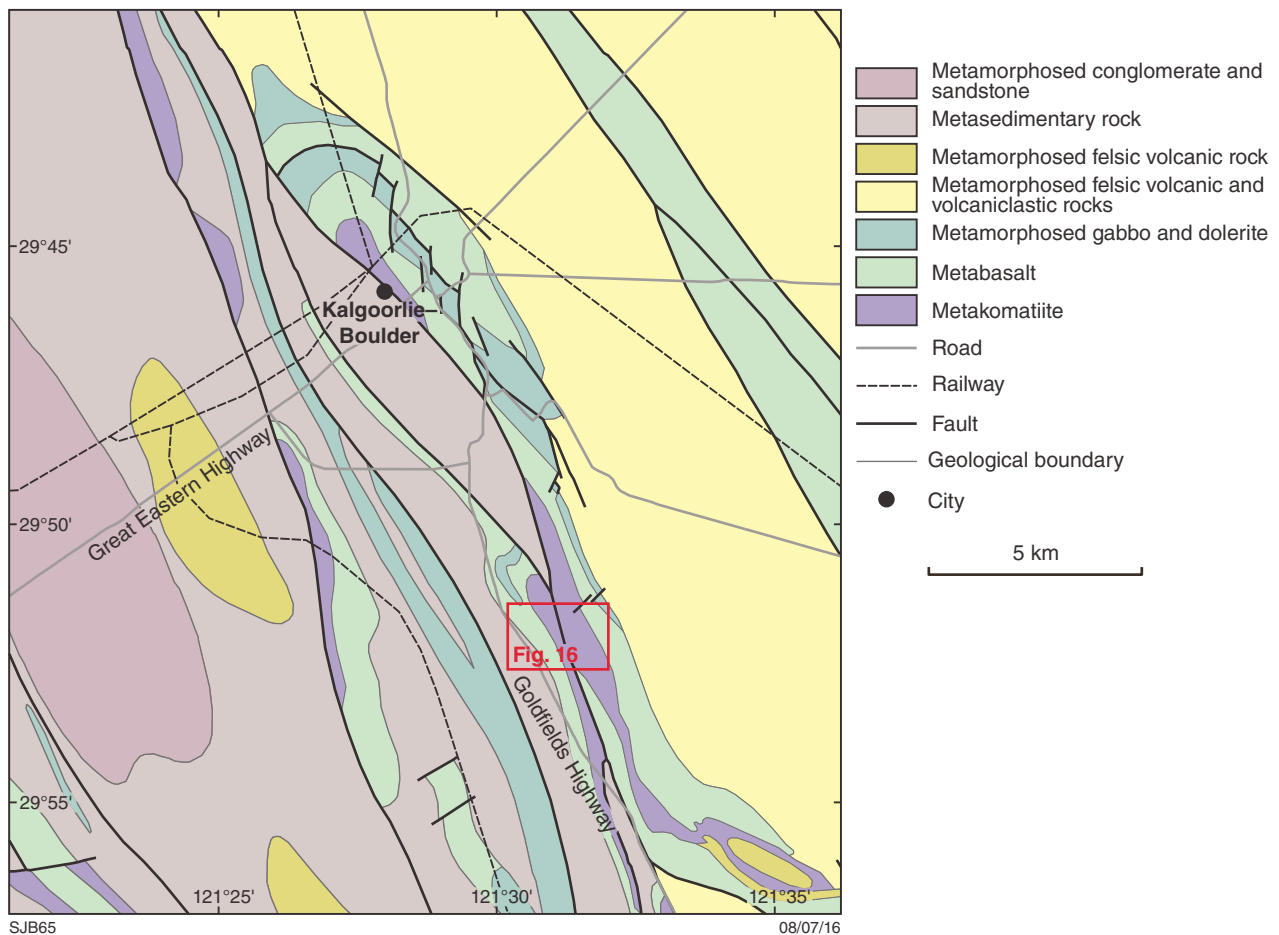


Figure 15. Interpreted bedrock geology of the Kalgoorlie area

of Mount Hunt crosses Paringa Basalt, which consists of metamorphosed pyroxene spinifex-textured basalt characterized by skeletal and acicular amphibole that pseudomorphs primary clinopyroxene, and minor biotite in a matrix of fine-grained amphibole, chlorite, clinozoisite, albite, and quartz. The acicular textures range in scale from a few millimetres up to 30 mm.

Just west of the summit (MGA 357293E 6586523), the Paringa Basalt contains a thin unit (<1 m) of olivine spinifex-textured komatiite. Scattered blocks of the komatiite can be traced along strike, suggesting the unit is in situ. The Paringa Basalt belongs to the high-Th siliceous suite of Barnes et al. (2012). This suite is interpreted to have been derived by the contamination of fractionated komatiitic magmas, thus allowing the possibility of local occurrences of uncontaminated parent magma.

Paringa Basalt

Deeply weathered, pillowed Paringa Basalt outcrops (Fig. 20) on the eastern side of the highway (Locality 3 on Figure 16; MGA 356815E 6586475N). Younging to the northwest is indicated by the pillows, whose weathered margins are marked by variolitic textures. Breccias, probably representing hyaloclastite (Fig. 21), are also preserved (MGA 356785E 6586300N). Fresher material

from the breakaway edge consists of metamorphosed komatiitic basalt like that in the rest of the Mount Hunt area.

Some pillows have well-preserved hyaloclastite textures. In particular, one pillow has an irregular, lobate margin with common angular fragments of fine-grained material that have jigsaw fit, and likely represents the remnants of the quench-fragmented chilled margin (in situ hyaloclastite).

The Paringa Basalt is more massive and homogeneous toward the southern end of the outcrop, with little evidence of the pillows that dominate the outcrop to the north. At one locality (MGA 356785E 6586300N), there are several thin (less than one metre thick) breccia units, one of which has a very irregular lower contact with relief of about 0.5 m. Here, the substrate appears to be breaking up in situ. There is a transition from cracking of the substrate and infilling of fractures, through angular blocks with jigsaw fit that match the substrate, to a clast-rich breccia over a distance of less than 30 cm. The breccia unit has a relatively planar top. The irregular base, the common in situ jigsaw fit, and the local deposition of the clasts, may indicate that fragmentation was due to local uplift by inflation of a flow unit. Based on the erosional lower contact of the fragmenting unit, the facing direction is toward the southwest, consistent with the pillow structures to the north.

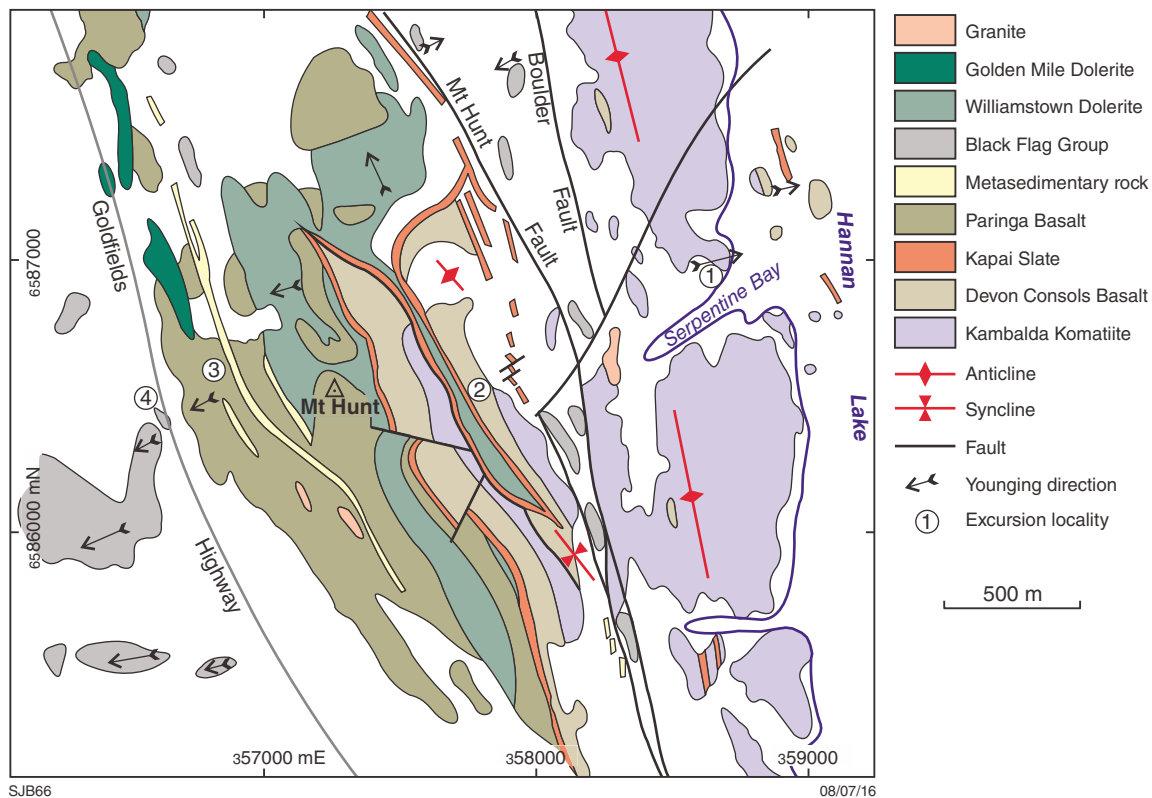


Figure 16. Outcrop sketch of the Mount Hunt – Hannan Lake area, adapted from Griffin et al. (1983) and Keats (1987)

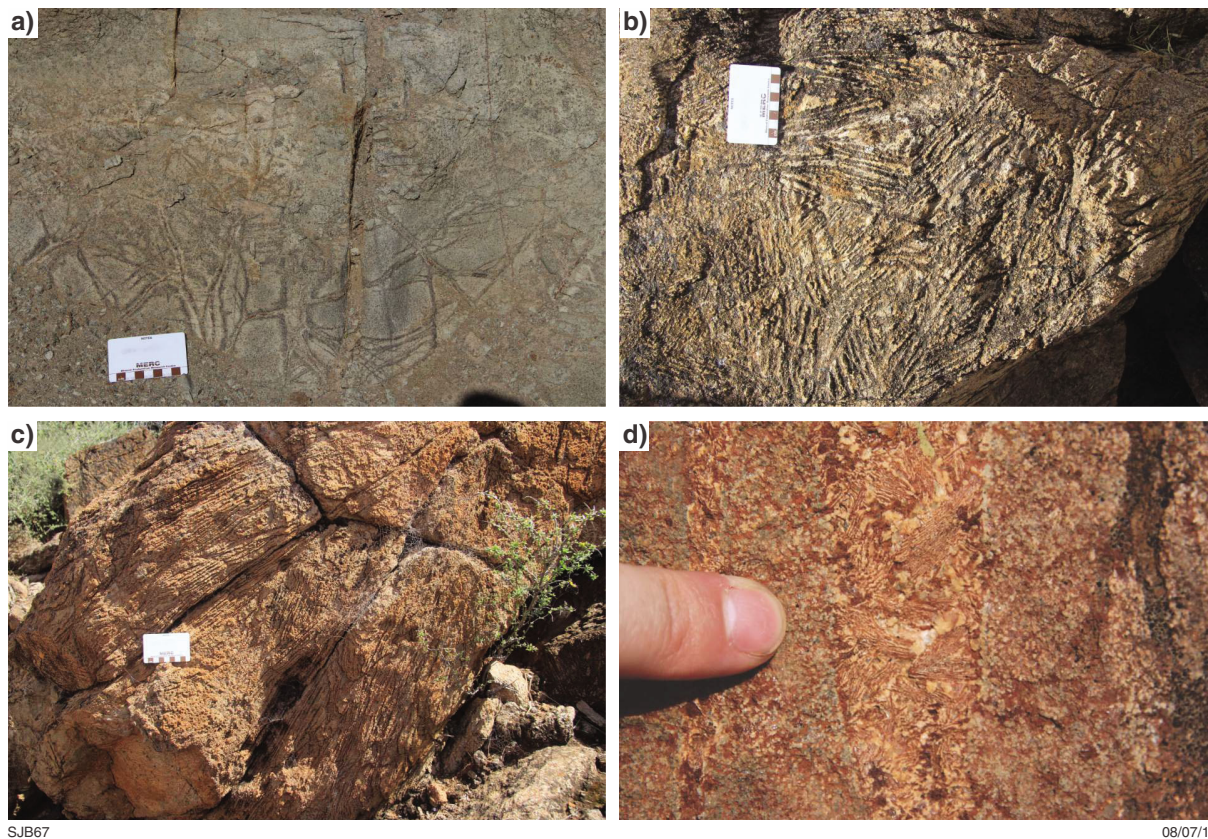
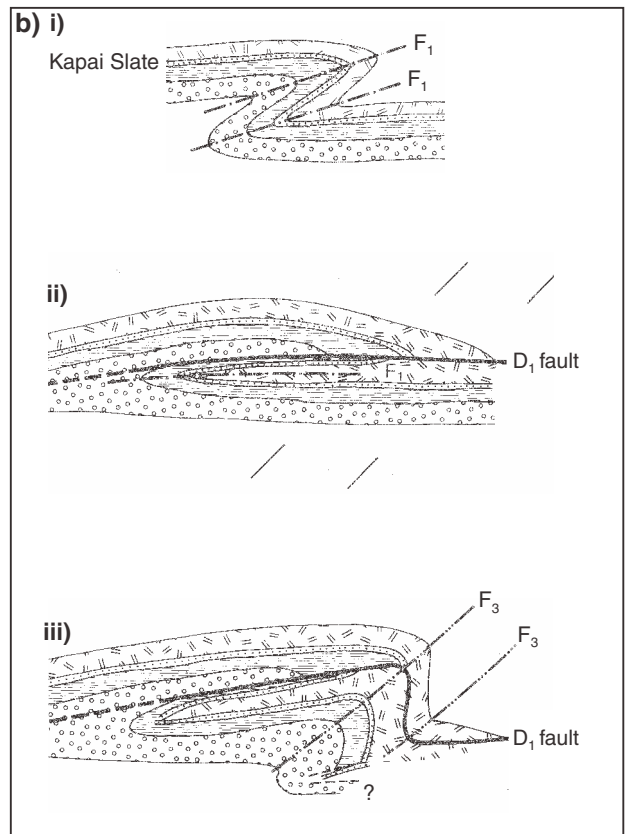
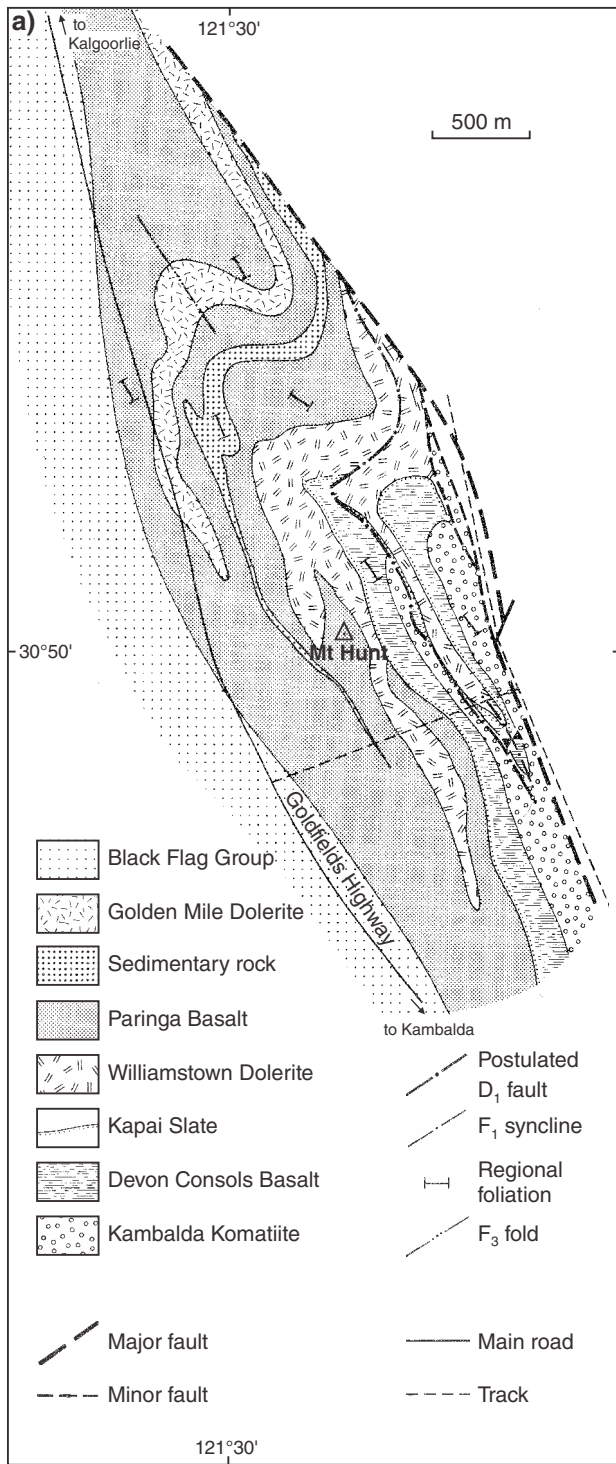


Figure 17. Serpentine pseudomorphs after platy olivine-spinifex texture in carbonate-altered, serpentinized komatiite at Serpentine Bay (MGA 358730E 6587070N): a) brecciated flow-top (A1 zone); b) randomly orientated spinifex (A2 transitional to A3 texture); c) large outcrop of oriented spinifex-textured komatiite (A3 zone); and d) small (2 cm wide) vein of randomly oriented spinifex



SJB68

08/07/16

Figure 18. a) Interpretative geological map of Mount Hunt, modified from Swager (1989, 1990); b) schematic development of fold structures at Mount Hunt: i) initial, asymmetric F₁ fold; ii) development of small-scale F₁ nappe structure, with largely sheared-out short limb; iii) F₃ refolding of the F₁ structure, after it was tilted into a steep orientation during the F₂ upright folding, after Swager (1989, 1990)



Figure 19. Variolitic Paringa Basalt on Mount Hunt (MGA 357525E 6586500N)

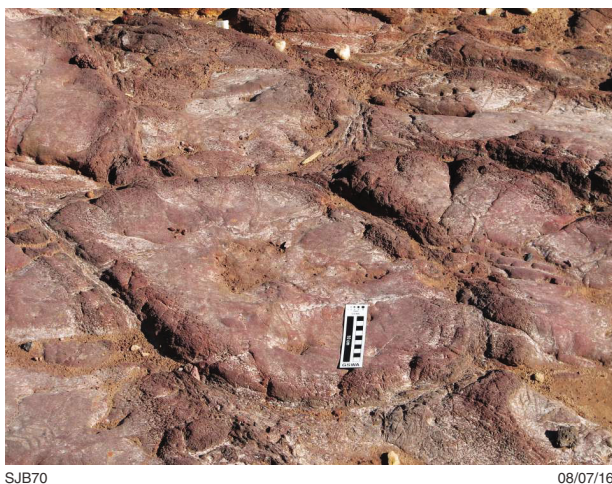


Figure 20. Relict pillow structures in saprolite after Paringa Basalt west of Mount Hunt (MGA 356815E 6586475N)

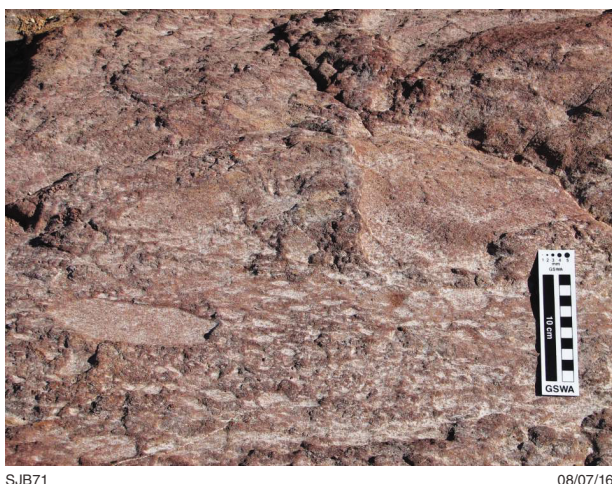


Figure 21. Relict hyaloclastite breccia in saprolite after Paringa Basalt west of Mount Hunt (MGA 356785E 6586300N)

Black Flag Group

Metasedimentary rocks of the Black Flag Group (Krapež and Hand, 2008; Squire et al., 2010) outcrop on the western side of the Goldfields Highway (Locality 4 on Figure 16; MGA 356695E 6586300N). Graded bedding, current bedding and scours indicate a consistent westward younging, except where there are local reverses due to minor folding. The basal beds contain zones of oligomictic conglomerate. Farther west, conglomerates are rarer and the sequence contains an appreciable felsic volcanoclastic component.

Minor folds in the sedimentary rocks (Fig. 22) have axial planes that are subparallel to the main bedding trend, with the folds forming a narrow zone bounded by a pair of metre-scale, layer-parallel shears. The shears have well-developed C-S planes and C' extensional shear bands that indicate a dextral sense of shear. The shears also contain abundant blocks of the sedimentary rocks, ranging from millimetre-scale up to 30 cm within a groundmass of very dark, fine-grained material. The blocks are typically elongate, commonly with shapes similar to mica fish and σ -porphyroclasts in mylonites.

The Long–Victor Mine and the Moran Shoot, Kambalda (MGA 373976E 6549856N)

The Kambalda deposits were the first discovered, and for many years the most closely studied, of all the Yilgarn Craton sulfide deposits (Gresham and Loftus-Hills, 1981; Gresham, 1986; Leshner, 1989; Barnes, 2006a). The deposits occur within a 30 km long, 10 km wide corridor between the Kambalda Dome (Fig. 23) and the Tramways Dome to the southeast, and are localized at, or very close to, the contact between the Lunnon Basalt and the overlying Kambalda Komatiite (Fig. 11). The deposits of the Widgiemooltha Dome to the southwest occur within the same stratigraphy and show broadly similar features.

The Kambalda Dome is a doubly plunging D_3 anticline on the crest of the major regional D_2 Kambalda Anticline, the D_2 episode being accompanied by extensive parasitic folding and thrusting. Much of this thrusting was localized along the zone of competency contrast along the komatiite–basalt contact, particularly where massive sulfide shoots are developed at this contact, to the point where undeformed magmatic contacts on massive ores are only rarely preserved. This relationship accounts for much of the observed diversity in ore geometry.

The conceptual 3D block model shown in the introductory section of this guide (Fig. 9) is a reconstruction of the inferred geometry of the stereotypical Kambalda Dome ore environment. It shows a number of common features: the antipathy between contact ore and sediment at the contact between Silver Lake Member komatiite and footwall Lunnon Basalt; the linear nature of ore shoots; the local presence of ores in successive flows within the corridors above contact ore; and the localization of massive contact ores within footwall trough structures. Much of the controversy around the Kambalda deposits relates to the origin of these trough features.



Figure 22. Folds in graded volcaniclastic beds of weathered Black Flag Group (MGA 356268E 6586122N)

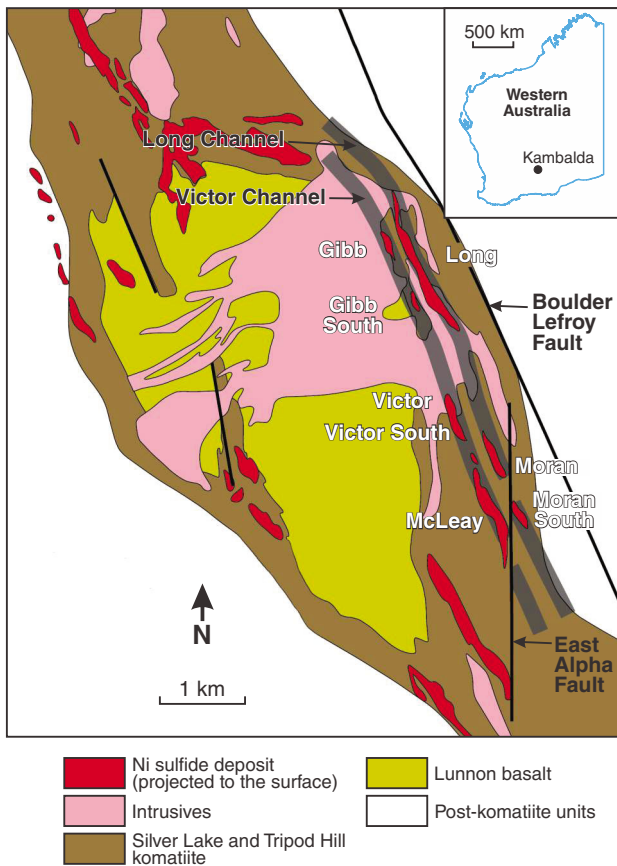


Figure 23. Map of Kambalda Dome showing location of Long-Victor Mine, after Staude et al. (in prep.)

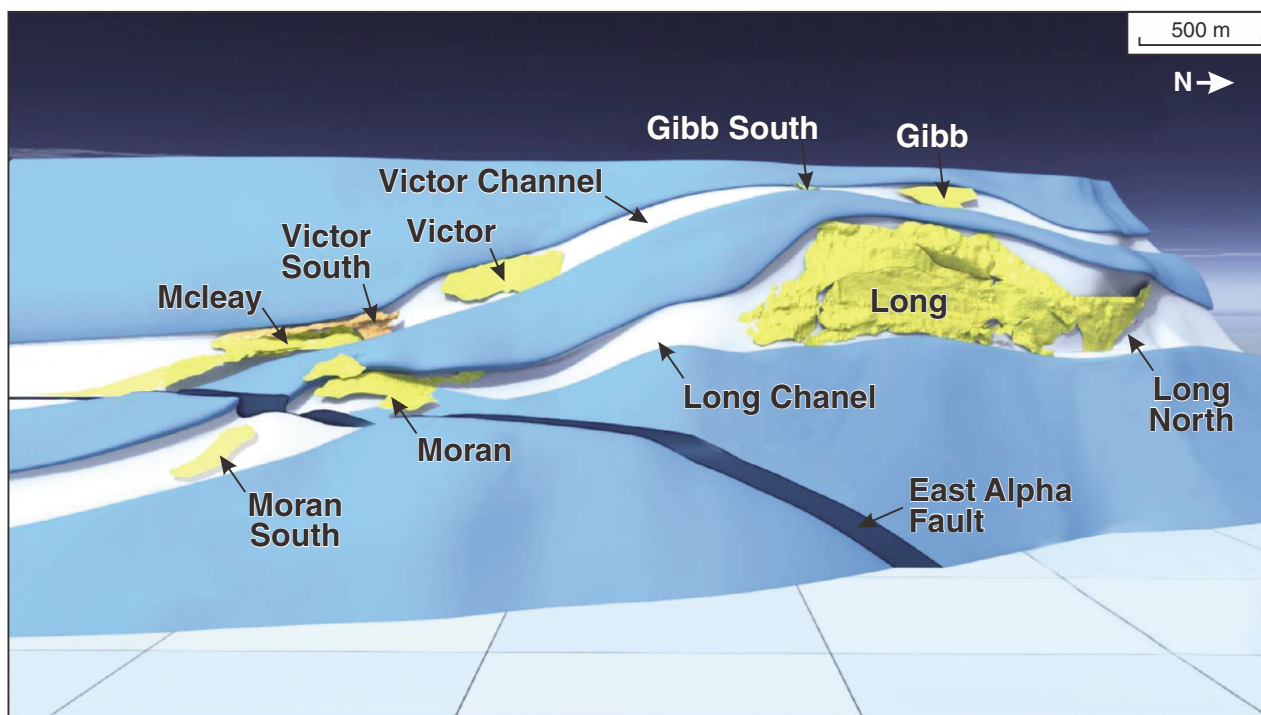
The facies architecture of the Silver Lake Member has been summarized in the introduction. This unit consists primarily of thick cumulate-rich flows 40–100 m thick, although thinner intercalated units are present and there may be as many as 20 distinct cooling units in the vertical section (Beresford et al., 2005; Stone et al., 2005). Mineralization is mainly (but not exclusively) restricted to the basal flow, which can be up to 100 m thick, is commonly the thickest flow, and contains the highest proportion of forsteritic olivine meso- to orthocumulates with MgO contents in excess of 45% (anhydrous). The pathway subfacies is defined by a thickening of the flow unit associated with linear troughs in the underlying Lunnion Basalt, and by absence of an underlying sedimentary layer, and is typically traceable over up to 15 km in length and 500 m in width (Leshner et al., 1984; Stone and Masterman, 1998). The host komatiites are typically extensively reconstituted to talc carbonate assemblages with no preservation of original texture in cumulates and local preservation in spinifex zones. Serpentinites are preserved in rare pockets, such as at Victor and Durkin Shoots.

More than 80% of the resources at Kambalda are contained within contact ore, defined as massive or matrix ore located at the basal contact of the Silver Lake Member. About half the ore shoots consist of massive ore overlain by matrix ore: some have massive and disseminated ore only, some have matrix without massive ore but most have a halo of low-grade disseminated ore which, in some cases, displays spherical, buckshot or blebby textures described below.

Orebodies typically have strongly linear, ribbon-like geometries, up to 3 km long, 300 m wide, are typically less than 5 m thick and range from less than 0.5 to 10 Mt (Stone and Masterman 1998).

Most of the ore shoots of the Kambalda–Tramways corridor are completely or partially confined within linear trough-like features in the upper contact of the Lunnion Basalt (Figs 9, 10, 24, 25). All the trough features are substantially overprinted by and, in some cases, defined by tectonic deformation, giving rise to a long-standing controversy as to their origin.

The troughs have been classified by Gresham and Loftus-Hills (1981) and Stone and Archibald (2004) into re-entrant and open varieties. Re-entrant troughs, such as the excellent example preserved at Moran are typically wider at the bottom than at the top, and show a marked tectonic asymmetry depending on their position relative to the axis of the Kambalda Dome. They are elongate, up to three kilometres in strike extent, and up to 100 m deep, with relatively flat floors which, in at least some cases, can be shown to be shear zones. Massive ore commonly occurs in ‘pinchout’ structures (Fig. 25) where ore is developed entirely within Lunnion Basalt. In most cases, these structures are primarily the result of D₂ thrusting but Leshner (1989) and Staude et al. (2015) provide textural evidence (e.g. undeformed contacts decorated with skeletal ferrochromites) for a primary origin in some cases.



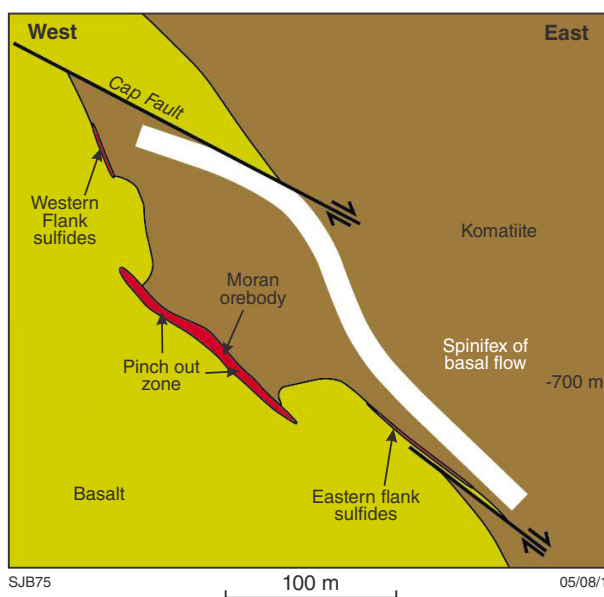
SJB74

05/08/16

Figure 24. 3D geology model showing morphology and relationship of the various ore shoots in the Long and Victor channels, after Staude et al. (in prep.)

In a number of documented cases, there is an association between troughs, ore and the petrographically and geochemically distinct pathway subsurfaces of the overlying flow (Leshner, 1989; Barnes et al., 2013). In some other cases, such as the Ken and Gellatly ore shoots on the generally more tectonized northwestern segment of the Kambalda Dome, evidence for primary volcanological controls are lacking.

Historic mining within the Long–Victor mine was focused on three main ore shoots: the Long, Victor and Gibb shoots (Fig. 24). The pre-mining resource at Long is estimated at 4.6 Mt at 3.72% Ni for 173 000 t nickel, and at Victor 0.8 Mt at 3.83% Ni for 30 000 t nickel (Western Australian Department of Mines and Petroleum, quoted by Barnes and Fiorentini, 2012). Exploration in the mine environment since 2005 has identified down-plunge extensions of both the Long and Victor systems. The shoots can be grouped together into two subparallel discontinuously mineralized channels (Fig. 24), termed the Long and Victor Channels (Barnes et al., 2013), plunging shallowly to the north and south, with an identified strike length of approximately three kilometres. Total resources, including Measured, Indicated and Inferred Resources across all deposits at the Long operations, stood at 1.379 Mt at 4.8% Ni containing 66 400 t nickel at 30 June 2015 (Independence Group NL, 2015).



SJB75

05/08/16

Figure 25. Simplified cross-section showing the morphology of the Moran orebody and its containing trough feature, after Staude et al. (in prep.)

The Moran Shoot (Fig. 25) has been the target of most recent mining and development. The Moran deposit, containing approximately 50 000 t of nickel, occurs within an elliptical embayment that is approximately 40 m deeper than the sediment-covered flanks relative to the original horizontal contact surface. The deposit is flanked around its entire margin by a basalt–sulfide–basalt pinchout. Ore in the centre of the embayment includes 20 cm of massive sulfides and up to five metres of matrix sulfides (Fig. 26), whereas ore in the pinchout includes up to four metres of massive sulfides and no matrix sulfides, similar to other embayments at Kambalda. Detailed underground observations have revealed some remarkable delicate primary features at sulfide–silicate contacts, including partially detached basalt melt plumes at the basal contact, and accumulations of chromite-bearing basaltic xenomelt at upper contacts in pinchouts (Staude et al., in prep.). These features, at Moran in particular, provide some of the most compelling evidence yet seen for a primary origin of both troughs and pinchouts, and indicate that the sulfide liquid itself has played a major role in deepening and widening the original thermal erosion channels that host the ore (Staude et al., prep.).

Breakaway locality, Kanowna (MGA 367575E 6616985N)

This is one of a number of localities within the Boorara Domain (Fig. 27) illustrating complex relationships between komatiites and co-erupted TTG dacites and volcanoclastic sediments. A detailed description and interpretation of the Breakaway locality (Fig. 28) is given by Trofimovs et al. (2004a). High-resolution orthophotos of a portion of the outcrop (geo-rectified photomosaics collected using drone-based photogrammetry) are shown in Figures 29 and 30.

As described by Trofimovs et al. (2004b):

... the locality preserves continuous, texturally well-preserved outcrop exhibiting both coherent and fragmental komatiite–dacite associations. These rocks outcrop over a 600 × 600 m area and the sequence dips steeply (75°) to the southwest providing a cross-sectional view of the preserved volcanic facies (Fig. 29). The coherent dacite and komatiite associations are preserved within metre- to hectometre-scale megablocks that form the ‘block’ facies of a volcanic debris avalanche deposit (Trofimovs et al., 2004a).

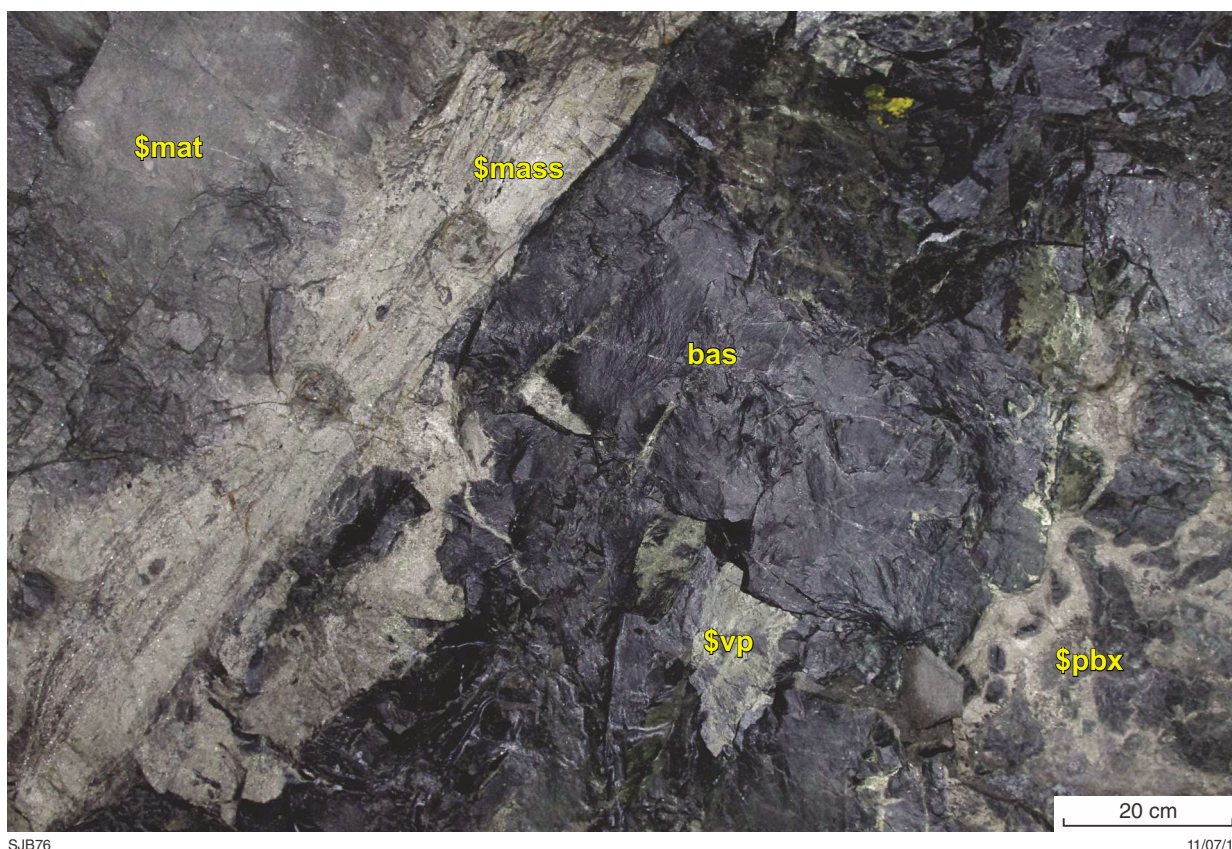


Figure 26. Moran underground face. \$mat = matrix (net-textured) ore; \$mass = massive sulfide (pn rich); bas = footwall basalt; \$pbx = sulfide-matrix breccia with pillow fragments; \$vp = sulfide paint on fracture surface

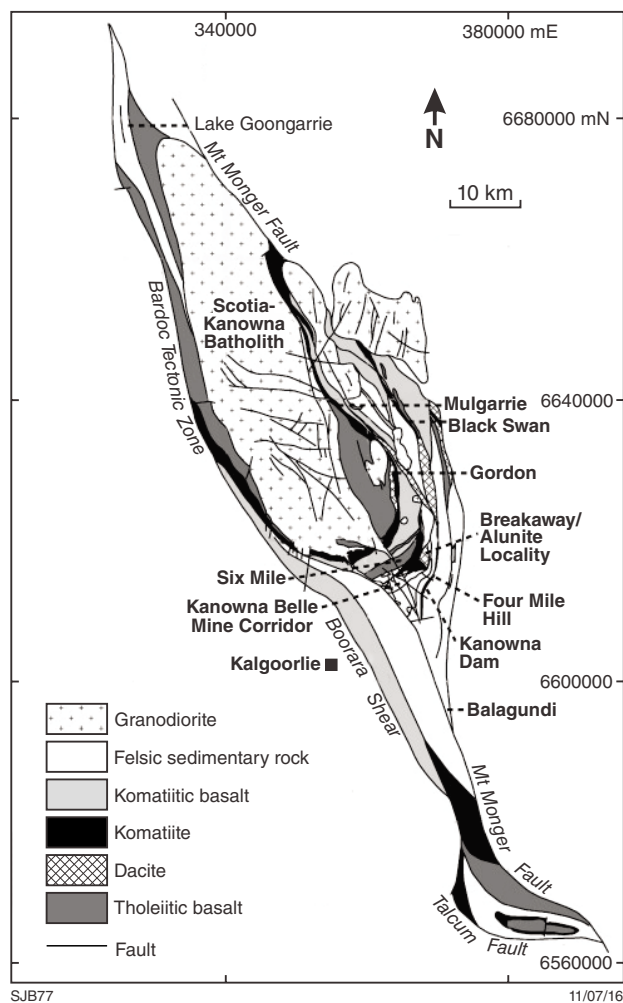


Figure 27. Boorara Domain map, after Trofimovs et al. (2004b). Published with permission

The megablocks within this primary volcanic breccia (Fig. 29) preserve original lithological and stratigraphic contact relationships and primary igneous textures and structures. Surrounding these megablocks is a brecciated facies comprising quartz- and subordinate feldspar-phyric dacite and komatiite-derived fuchsite granule- to boulder-sized angular clasts, supported by a predominantly quartzofeldspathic, with subordinate fuchsite (1–2%), coarse-grained matrix. The brecciated matrix exhibits the same composition as the megablocks (quartz- and feldspar-phyric dacite and komatiite). The matrix is interpreted to have formed by abrasion and grain-to-grain collision of the large volcanic megablocks during transport. Previous work at the Breakaway/Alunite Locality describes the breccia as an olistostrome deposit, where large olistoliths have gravitationally collapsed into a pre-existing conglomeratic matrix (Ahmat, 1995; Hand 1998). The genetic relationship established between the megablocks and surrounding matrix disputes this interpretation and features such as jigsaw-fit textures between blocks and the lack of internal stratification in the deposit are indicative of a volcanic debris avalanche origin (Trofimovs et al., 2004a).

The coherent dacite megablocks at this locality are characterized by 15% relict quartz phenocrysts, with subordinate (2–5%) relict plagioclase phenocrysts, preserved in 80% fine-grained, originally quartzofeldspathic groundmass. Phenocrysts are euhedral and on average 2–4 mm in size. However, rare (~2%) quartz phenocrysts up to 0.8 cm are observed. The groundmass shows intense, pervasive clay alteration, which has obliterated the original feldspar content, groundmass grain size and texture. Autobrecciation and flow banding are commonly preserved within the dacite unit.

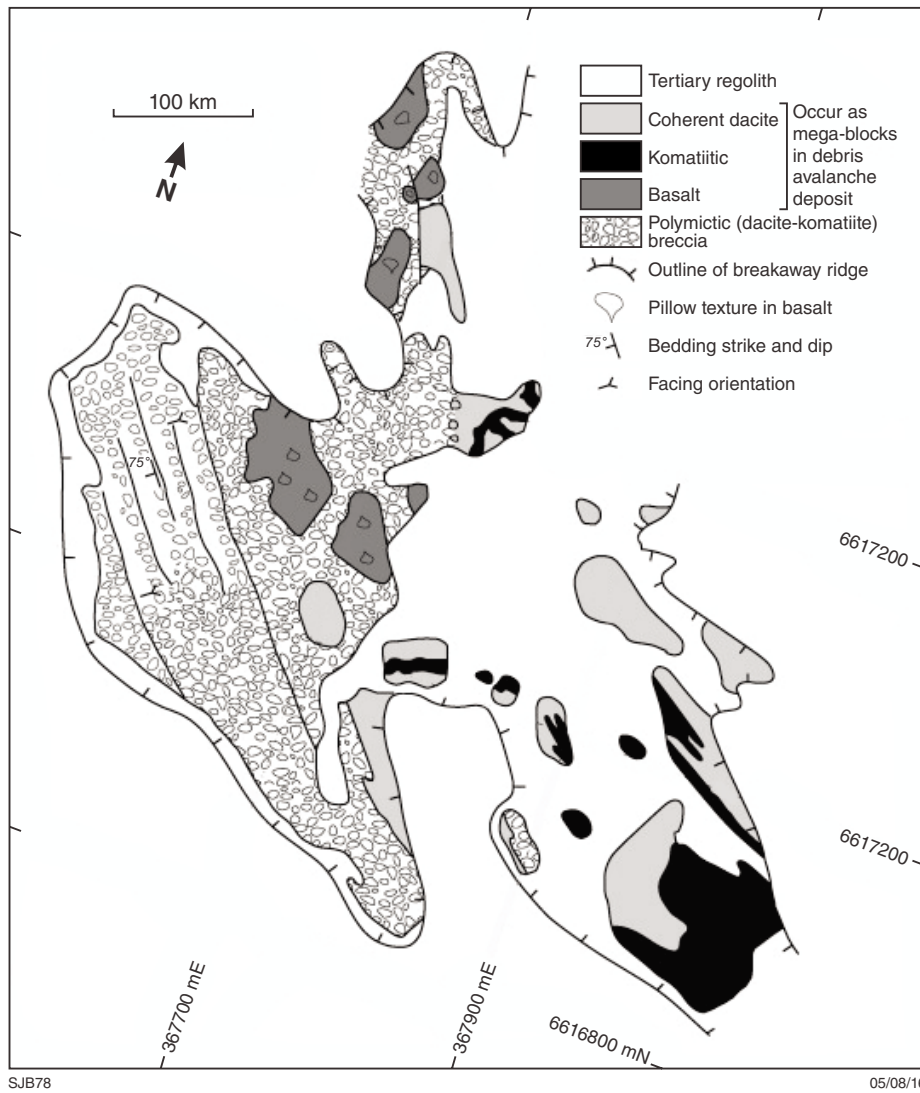
Komatiite is intercalated with the coherent dacite, the primary contact relationships preserved within the large volcanic debris avalanche blocks. Komatiite at the locality shows much variation in preservation of primary texture and is most commonly represented as fuchsite–talc–carbonate–chlorite schist. However, low-strain pockets preserve small (0.5 – 2 cm), randomly oriented spinifex texture along the margins of komatiite units. The random spinifex texture grades toward the centre of the komatiite into larger (3–10 cm) oriented pseudomorphed olivine (now chlorite) spinifex blades.

Contacts between the dacite and komatiite in places appear extremely irregular (Fig. 31), exhibiting morphologies suggesting both were fluidal at the time they were juxtaposed (Fig. 31; Trofimovs et al., 2004b). Komatiite apophyses have injected centimetres to metres into the dacite unit (Fig. 31). The apophyses are randomly aligned and distributed along the komatiite–dacite boundaries with each apophysis preserving centimetre-scale lobate and flame-like structures along its margins. Spinifex texture is observed along some of the komatiite margins adjacent to contacts with the dacite unit. However, the majority of boundaries have been altered to fine-grained assemblages, largely consisting of fuchsite. A small, 2 × 2 m, zone of magma mingling, where both lithologies were physically intercalated as liquids, is observed along a komatiite–dacite contact.

Harper Lagoon (MGA 364230E 6623120N)

At Harper Lagoon, the succession is described by Trofimovs et al. (2006):

... consists of a minimum thickness of 30 m of ultramafic olivine orthocumulate to mesocumulate, pseudomorphed by serpentine with a chromite oxide component, grades into pyroxene spinifex textured, high-Mg, komatiitic basalt. Tabular serpentine crystals grade into acicular pseudomorphed pyroxene crystals then into ~3 m of centimetre-scale randomly oriented pyroxene spinifex textured high-Mg basalt. The original clinopyroxene phenocrysts are pseudomorphed to an actinolite–chlorite mineral assemblage. Chlorite is observed in the centre of the acicular crystals, while amphibole and subordinate plagioclase rim the pseudomorphed phenocrysts and fill the interstitial voids. A gradational change to an ophitic gabbro unit



SJB78

05/08/16

Figure 28. Breakaway map, after Trofimovs et al. (2004b). Published with permission

occurs at the top of the clinopyroxene-dominant basalt. The ~4 m-thick gabbro, contains primary, 5–20 mm, euhedral, acicular, and bladed clinopyroxene crystals that have been pseudomorphed by actinolite, associated with euhedral to subhedral plagioclase crystals. A second clinopyroxene (now amphibole) spinifex-textured horizon (Trofimovs et al., 2006) overlies the gabbro. This pyroxene spinifex textured unit is ~2–4 m thick and exhibits randomly oriented 2–3 cm spinifex blades together with larger, 4–6 cm oriented spinifex blades that form radial patterns.

Shearing truncates the top of the spinifex textured zone, and a 7–10 m-thick breccia horizon comprising high-Mg basalt clasts stratigraphically overlies the shear zone and the basalt – komatiitic basalt sequence. Angular, 5–10 cm, amygdaloidal basalt clasts are bound together by a recrystallized carbonate, with subordinate chlorite and amphibole, cement. The clasts appear to be the fragments of the overlying, coherent, pillowed,

amygdale-rich, high-Mg basalt lavas (Fig. 32). In these overlying lava flows, well-preserved pillow structures indicate a southeast younging direction (125–130°) and clearly show that the basalt forms the stratigraphic top of the sequence. A high abundance of amygdales (40–50%) is typical in the pillows, particularly around the pillow rims. Concentric layering is defined by amygdale zonation, with variations between amygdale-rich and amygdale-poor zones (Fig. 32). Amygdale-rich zones exhibit spherical to coalesced albite-filled vesicles. The amygdale-poor layers and pillow cores exhibit an amphibole-dominant (tremolite) mineralogy with chlorite (Mg-rich) and subordinate carbonate, plagioclase and epidote. The size of the pillow structures decreases upsequence through the pillow basalt pile. Large, 1 – 1.5 m pillows directly overlie the basaltic breccia, whereas the average pillow size decreases to 30–50 cm, 15 m upsequence. Associated amygdale-rich, high-Mg basaltic dykes are also observed within the pillowed basalt pile.



SJB79

11/07/16

Figure 29. High-resolution orthophoto mosaic of the southern section of the Breakaway outcrop: geo-rectified photomosaics collected using drone-based photogrammetry. Note the 50 x 25 m rounded dacite block. Inset shows detailed image of area a).

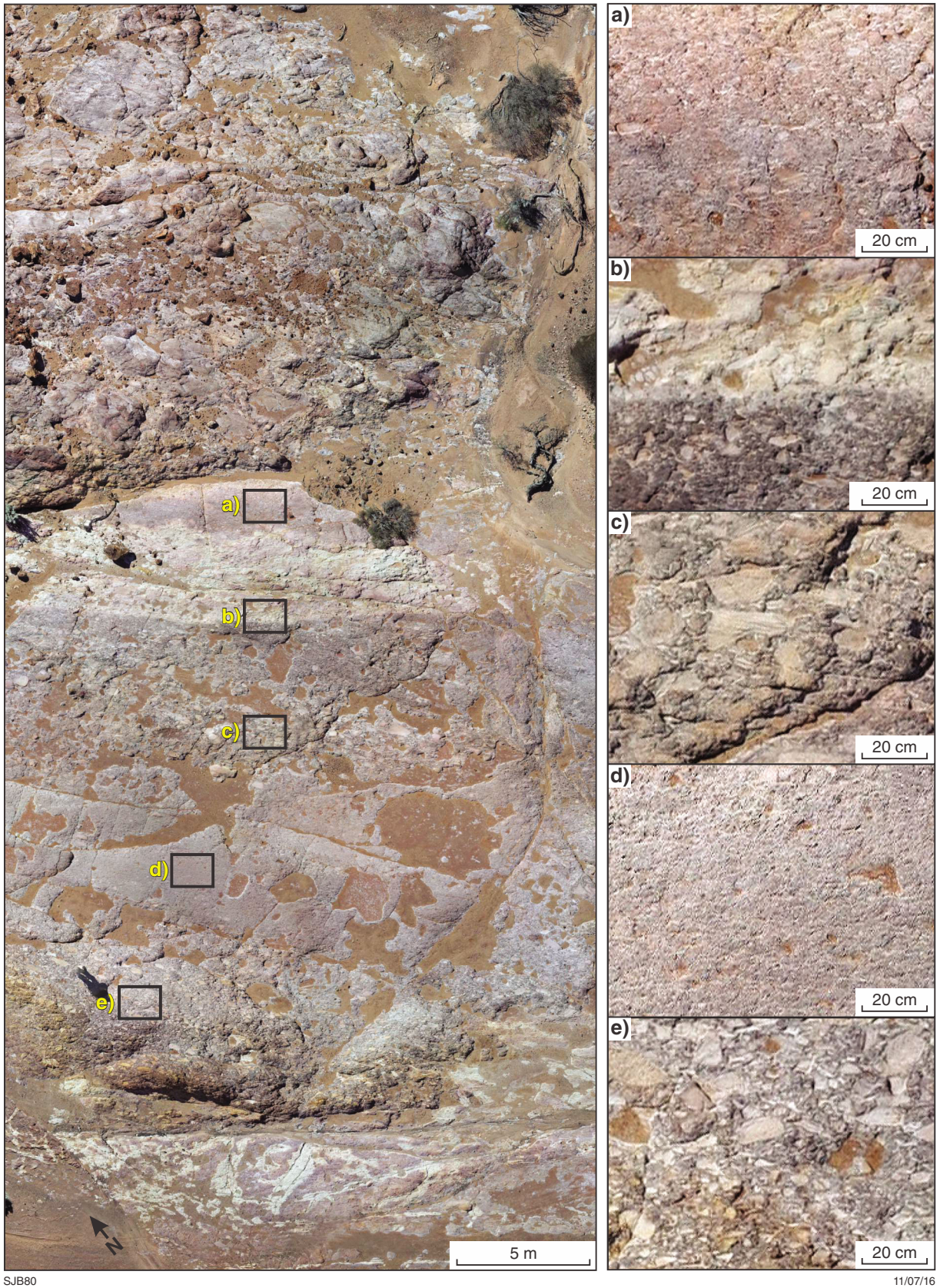


Figure 30. Orthophoto of a complete section of epiclastic sediments (from top left of area shown in Figure 29), with enlargements showing details of individual units

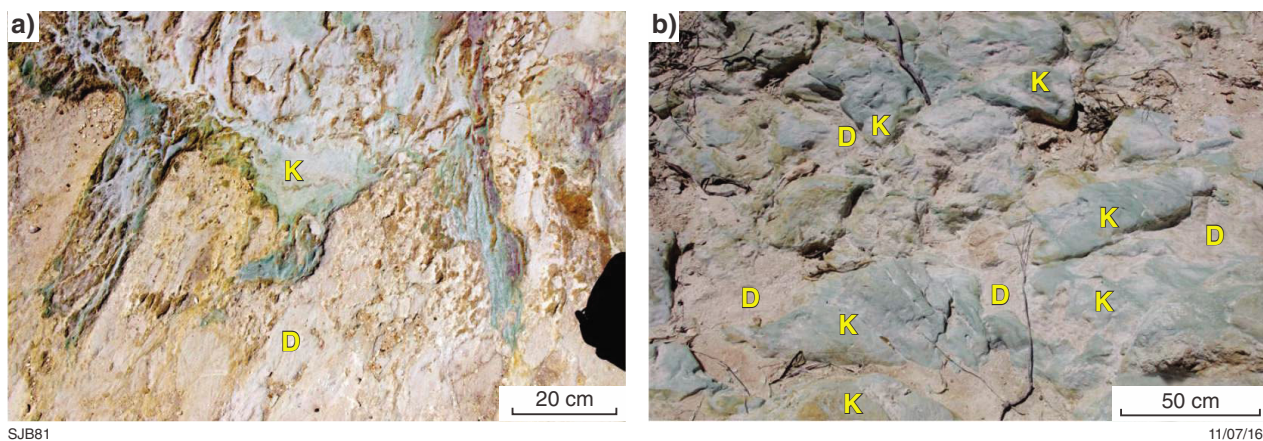


Figure 31. Komatiite (K) dacite (D) mingling textures in outcrops, Breakaway locality

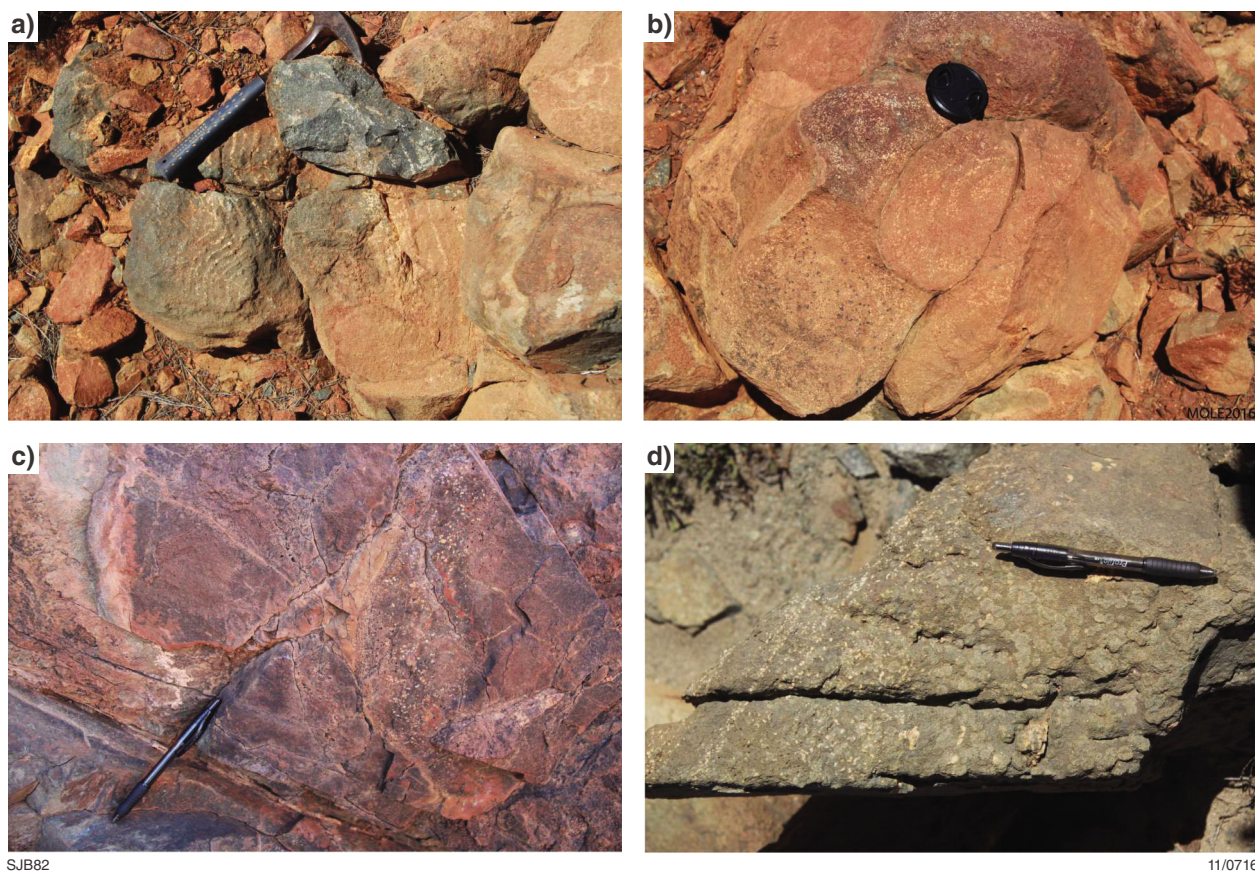


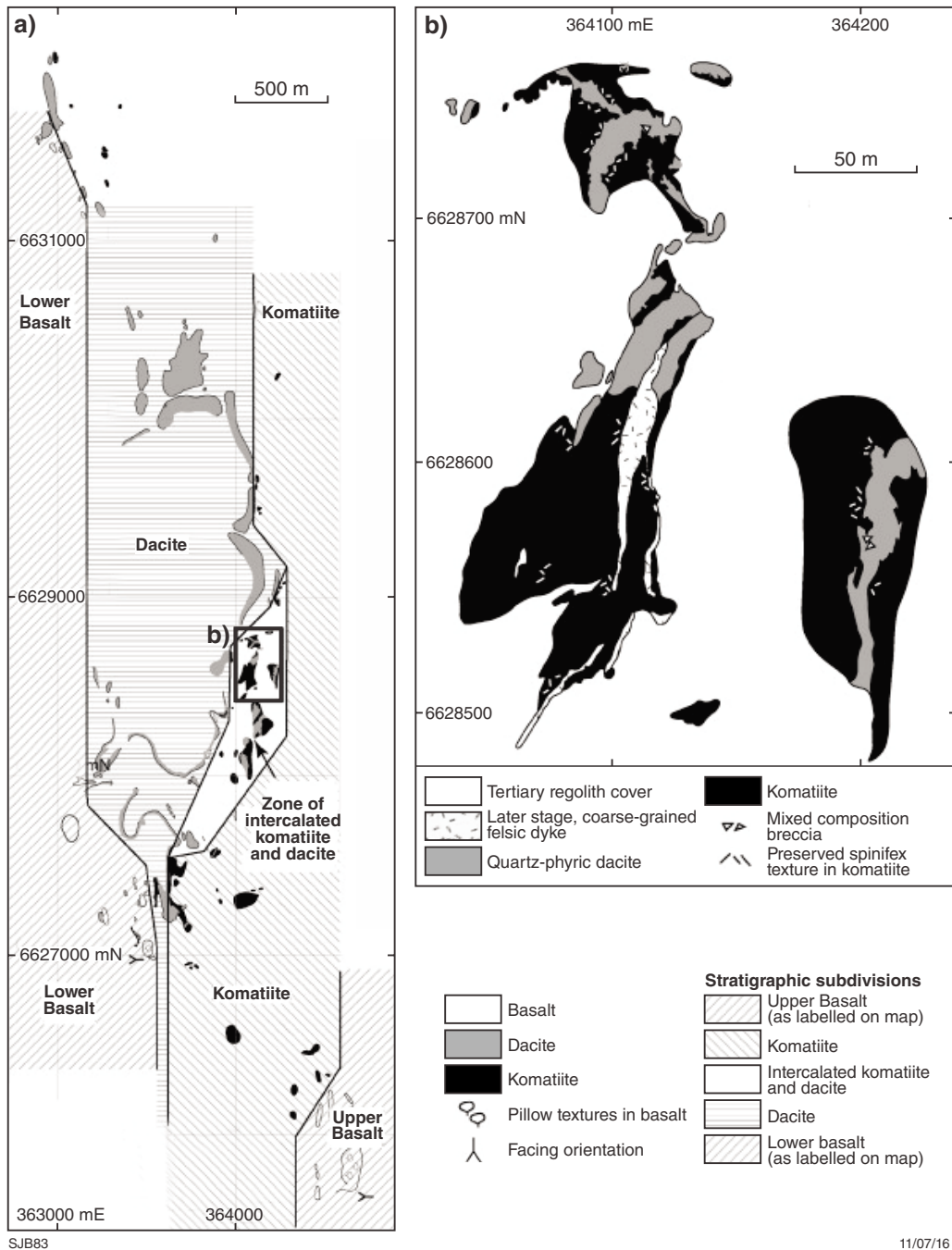
Figure 32. Photographs from Harper Lagoon: a,b) basalts demonstrating a radial pattern of amygdales, a rare feature common at this locality; c) triple point between three basaltic pillow lavas (edges are vesicular); and d) variolitic basalt

Gordon Sirdar (Kanowna) (MGA 364100E 6628600N)

Modified from Trofimovs et al. (2004b)

The Gordon area of the Boorara Domain, located approximately 40 km north-northeast of Kalgoorlie (Fig. 2), preserves the Lower Basalt, Dacite, Komatiite and Upper Basalt stratigraphic units in discontinuous outcrop over a north–south strike length of 6 km (Fig. 33). Primary contact relationships between the Lower Basalt and Upper Basalt and adjacent strata are poorly preserved within this

region. However, well-preserved lithological relationships are recorded between the dacite and komatiite stratigraphic units (Fig. 34) in weathered outcrops in a playa lake bed close to the Gordon Sirdar gold mine. The extent and quality of these exposures is variable depending on recent water flows into the lake and, at the time of writing (2016), was somewhat less extensive than those existing at the time of the 2004 Trofimovs study. Clear relationships can still be discerned, and were captured in 2016 in a program of high-resolution (down to 1 cm pixels) aerial photogrammetry using a drone-mounted camera. Results are shown in Figures 34, 35, and 36.



SJB83

11/07/16



Figure 34. High-resolution orthophotos of dacite–komatiite intercalations in the Gordon Sirdar lake bed outcrops: geo-rectified photomosaics collected using drone-based photogrammetry

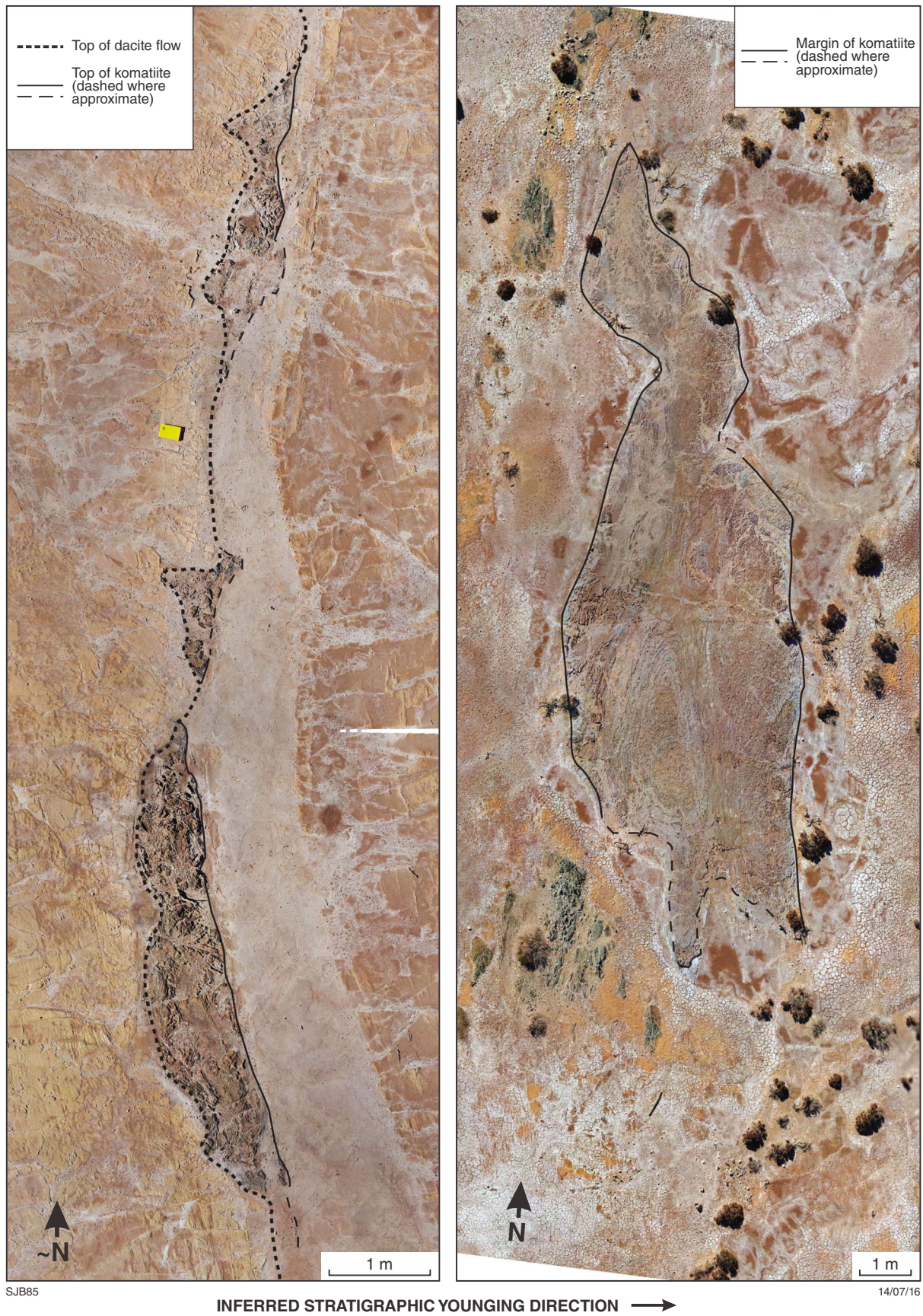
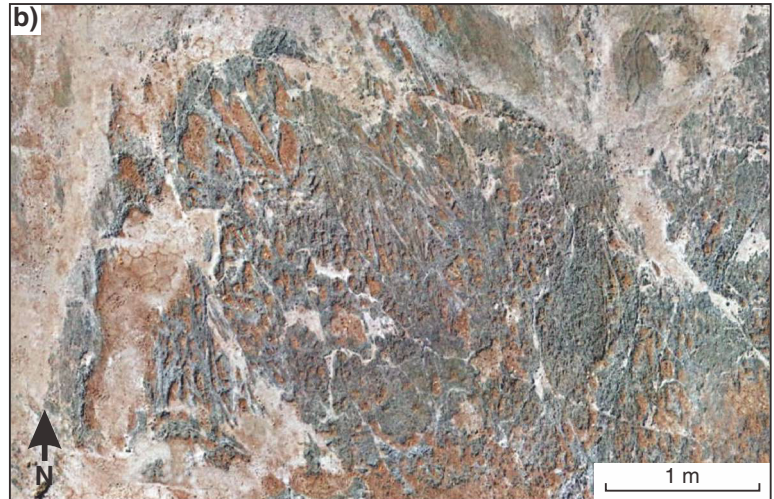


Figure 35. Gordon Sirdar orthophotos showing field relationships between thin komatiite flow lobe ‘fingers’ and intercalated dacite flows



Figure 36. High-resolution orthophotos of dacite–komatiite intercalations in the Gordon Sirdar lake bed — overview, and details: a) carbonate-filled fracture patterns compared with (centre of b) true spinifex textures; c) detail showing inflated section of komatiite flow lobe or shallow subvolcanic sill



SJB86b

11/07/16

Figure 36. continued

Irregular komatiite–dacite contacts with well-preserved textures are observed within a 300 × 200 m area where komatiite is intercalated with quartz- and feldspar-phyric dacite. The komatiite at the Gordon Locality has been serpentinized and subsequently altered to chlorite and talc. Spinifex texture is locally preserved through the pseudomorphing of original olivine. In many places, crosscutting carbonate veins within the original talc–carbonate rock look superficially similar to spinifex texture and are, in some cases, very hard to distinguish from spinifex texture (Fig. 34). A porphyritic texture is observed in the dacite, with small (3 mm), euhedral quartz, and subordinate feldspar phenocrysts distributed within a pervasively sericitized, quartzo-feldspathic groundmass. Pervasive weathering is interpreted to have obscured a percentage of the feldspar phenocrysts, producing a bias in their preserved abundance.

Contacts between the komatiite and dacite lithologies at the Gordon Locality have a variety of morphologies (Fig. 37). In some cases, flame-like protrusions of komatiite are injected upward into overlying dacite, clearly indicating a shallow invasive or intrusive arrangement of komatiite sills into pre-existing tuffs producing peperite-type contacts. In other places, upper komatiite contacts are planar or gently domed and clearly represent the tops of inflated lenticular flow lobes. A small proportion of

these exposed flow tops exhibit a 4–8 mm thick, fine-grained chilled margin grading into small (0.5 – 2 cm), randomly oriented spinifex blades that grade into oriented (serpentine, chlorite) spinifex plates, up to 30 cm in length. Within the main body of the komatiite, primary cumulate textures have largely been destroyed by pervasive chlorite–talc–carbonate alteration. Rare relict orthocumulate to mesocumulate textures are observed in thin section. Trofimovs (2004a) reported a symmetrical zonation within some komatiite bodies in that the zones of spinifex are observed along all contacts with the dacite, including the irregular lobe margins, but in many cases the textures on lower contacts are more likely to be intersecting carbonate-filled fractures. In other places, very thin komatiite apophyses, interpreted as the propagating finger-like fronts of advancing thin flow lobes, drape gently domed dacite flow tops (Fig. 35).

The complex relationships at this locality are consistent with Trofimovs' interpretation that the komatiites and dacites were erupted essentially simultaneously as a mixture of dacite flows and tuffaceous sediments, small intrusive dacite bodies, lobate komatiite flows and invasive high-level komatiite sills. The intrusive bodies are similar in many respects to those reported from the Dundonald Beach area of the Abitibi belt, Canada (Houlé et al., 2008).

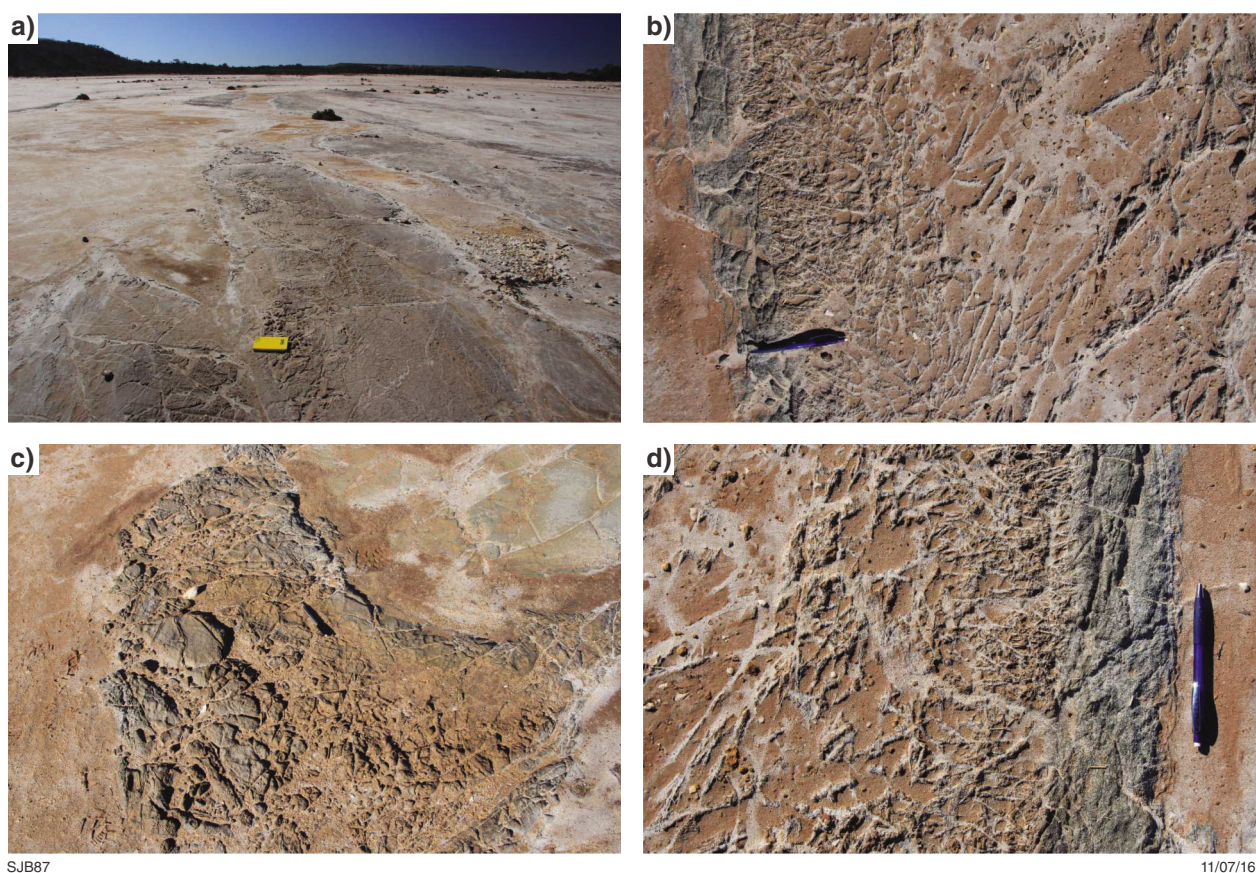


Figure 37. Photographs of komatiite flow features at Gordon Sirdar: a) view of a differentiated komatiite flow lobe within dacite (way-up to the right); b) top of a komatiite flow lobe (way-up to the left) with a very thin, quenched, brecciated top, followed by 20 cm of random spinifex, and finally around a metre of deeply weathered-out oriented spinifex; c) flow-top breccia and polygonal jointing characteristic of extrusive komatiite flows; and d) similar to b) but with way-up to the right

Black Swan nickel mine (MGA 369225E 6636965N)

The Black Swan succession is a particularly well-preserved example of bimodal komatiitic and calc-alkaline dacitic volcanism. The complex komatiite stratigraphy hosts a number of orebodies, including the Silver Swan massive ore shoot and the larger disseminated Black Swan and Cygnet orebodies. The following account is summarized from RET Hill and co-workers (Barnes et al., 2004; Dowling et al., 2004; Hill et al., 2004).

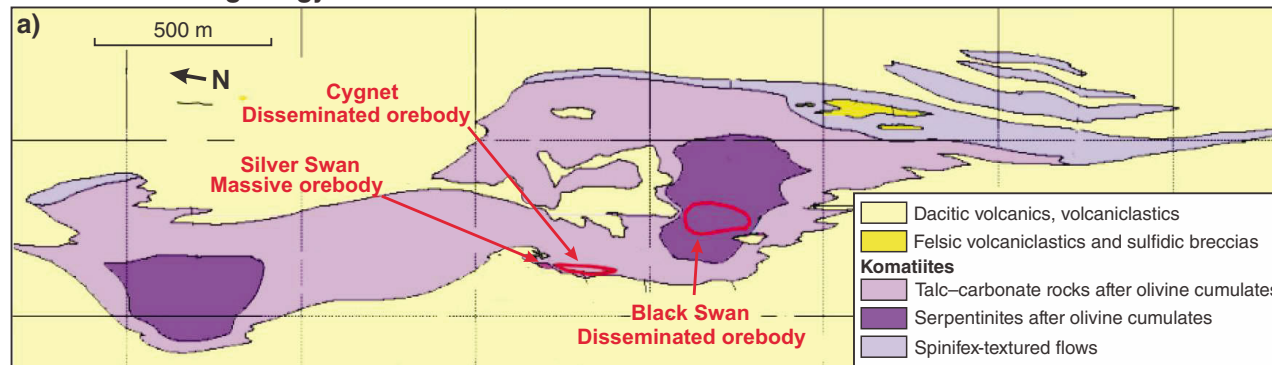
Stratigraphy and host rocks

The komatiite stratigraphy at Black Swan can be divided broadly into two units (Fig. 38). The lower unit extends for about two kilometres along strike, has a maximum thickness of at least 300 m, and overlies plagioclase-phyric dacitic breccias at an irregular, locally non-tectonized contact. Internally, it consists of two thick pathways occupied by olivine mesocumulates, separated along strike by a broad central zone dominated by less magnesian olivine orthocumulates. The planar spinifex-textured top of the lower ultramafic unit is overlain by an upper sequence of quartz–plagioclase phyric dacite breccias and tuffs, and

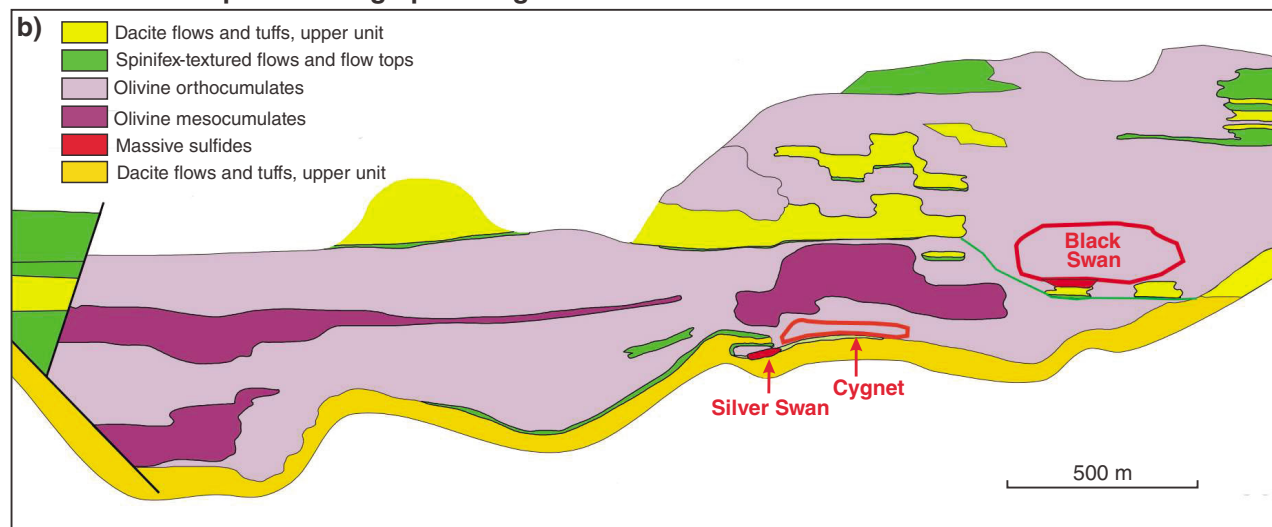
an upper komatiite sequence complexly intercalated with the dacites. A range of komatiite textures at Black Swan is shown in Figure 39.

The upper komatiite sequence has a central pathway, which hosts the Black Swan disseminated orebody. It rests directly on the lower komatiite unit. To the north, dacites are complexly intercalated with irregular komatiite units with spinifex-textured upper zones and highly irregular bases, interpreted as flow lobes by Hill et al. (2004), ranging in thickness from 30 cm to 50 m and in width from 10 to 100 m. To the south, the Black Swan pathway is flanked by a sequence of differentiated flows with abundant spinifex-textured upper zones, intercalated with dacitic lithic tuffs in the upper part. Some of these tuff units contain abundant pyrite-rich clasts. The upper komatiite unit and upper dacitic unit have relationships broadly similar to that between the lava pathway and flanking environments at Kambalda (Leshner et al., 1984), except that the intervening volcanoclastic units are much thicker and more irregular in geometry than the Kambalda interflow sediments. This complexity is interpreted by Hill et al. (2004) as the result of the simultaneous eruption of komatiite and dacite lavas during continuous lava flow through the Black Swan pathway.

Black Swan area geology



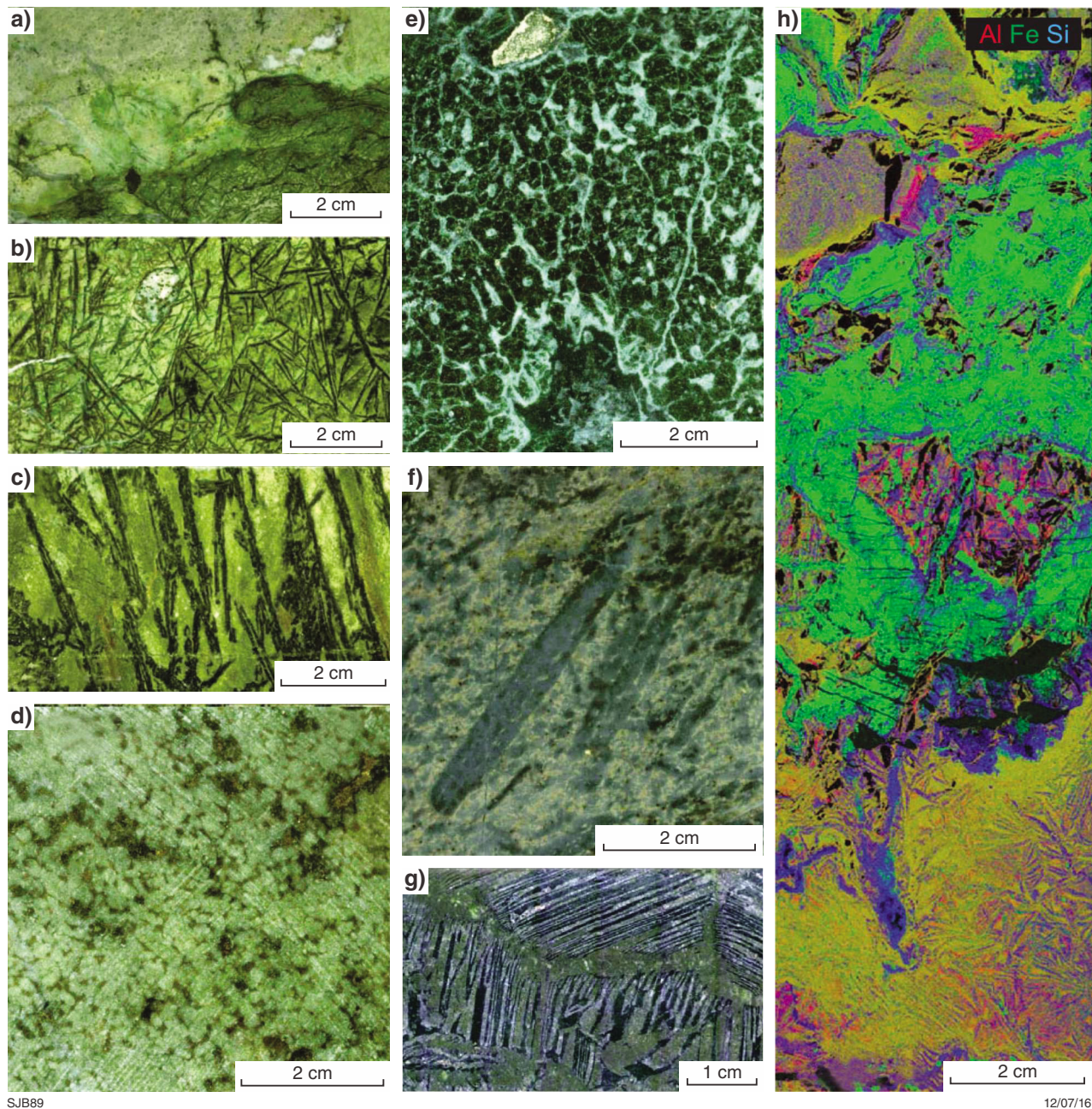
Black Swan Complex – stratigraphic long section



SJB88

05/08/16

Figure 38. a) Black Swan geology, showing distribution of alteration type within the ultramafic rocks; b) reconstructed stratigraphic long section of the Black Swan Complex, after Hill et al. (2004)



SJB89

12/07/16

Figure 39. Black Swan komatiite textures: a–c) A1 to A3 pyroxene-spinifex textured flow top (a) shows contact with dacite, white); d) typical medium-grained ‘sago textured’ olivine orthocumulate, replaced by carbonate–quartz assemblage, olivine pseudomorphs appear white; e) serpentinized olivine orthocumulate showing subskeletal rounded olivine morphologies; f) bimodal/porphyritic olivine orthocumulate with large, weakly laminated olivine plates in a matrix of finer grained orthocumulate; g) spinifex vein, pocket of very coarse, chevron-textured dendritic olivine developed in a decimetre-scale vein with relatively sharp walls against enclosing coarse orthocumulate; h) false-colour three-element XRF map (Al red, DFe green, Si blue) of a peperite contact between fragmented microspinifex-textured komatiite and ferruginous siliceous sediment

The Silver Swan orebody

The Silver Swan orebody is a vertically plunging, ribbon-shaped feature, which is up to 20 m thick, 20 to 75 m wide, at least one kilometre long, and open at depth (Fig. 40). It lies at the base of the lower ultramafic unit, close to the northern limit of the southern pathway, and is locally separated from the mesocumulate rocks by a thin, discontinuous layer of fine-grained, quenched orthocumulates. The orebody itself has a convex-up morphology, with a relatively flat basal contact and a primary upper contact with essentially barren olivine orthocumulate. This contact is commonly marked by a narrow zone rich in distinctive skeletal ferrian chromite (Figs 39 and 40).

The most remarkable feature of the Silver Swan orebody is the presence of abundant xenolithic inclusions of dacite in the ores (Dowling et al., 2004). These inclusions show

clear evidence of partial melting at their margins and, in the interior of the orebody, are disaggregated into irregular sinuous blobs and plumes (Fig. 39). The morphology, internal textures and compositions of the inclusions leave no doubt that they are partially molten fragments of the immediate dacite footwall. They extend throughout the lower five metres of the massive ore shoot. Where the total thickness of the shoot is less than five metres, they extend all the way through and, in places, accumulate to form a layer of ‘xenomelt’ separating the top of the massive ore from overlying ultramafic rock. Where the ore zone is thicker than five metres, the plume-bearing zone is overlain by pure, inclusion-free, massive ore, a feature attributed to breaking away of ascending plumes from a three-dimensional network connected to the floor. The major and trace element geochemistry of the plumes indicates that they range from pure dacite to hybrid compositions with up to 30% komatiite melt component.

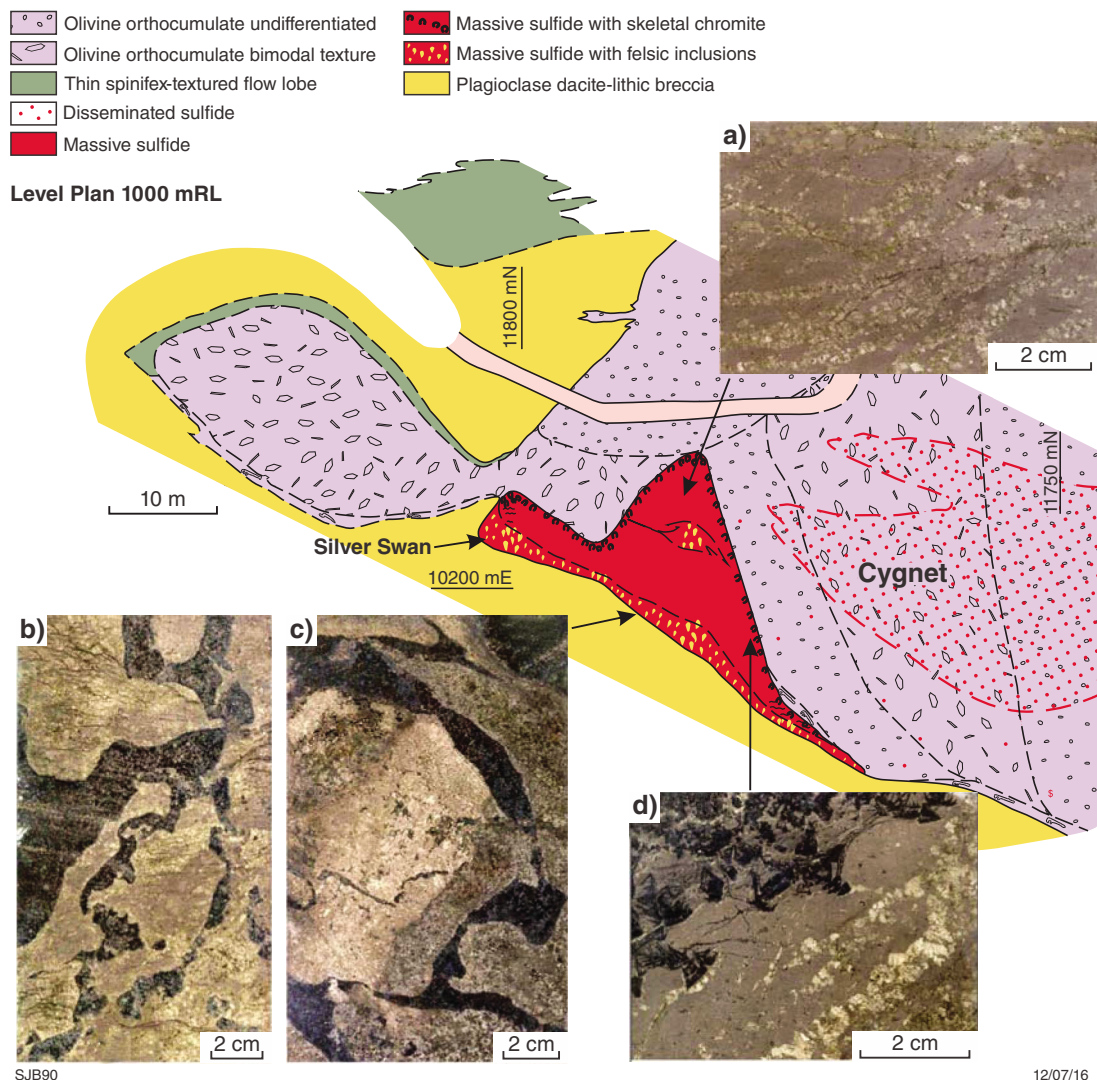


Figure 40. Silver Swan orebody plan and massive ore textures: a) inclusion-free massive ore from upper part of the orebody showing coarse trellis-like chains of pentlandite (Pn) within pyrrhotite (Po); b,c) disaggregating 'plumes' of molten dacite (dark) within lower zone of orebody; d) skeletal chromite developed along upper contact of massive sulfide against komatiite

The massive sulfide orebody shows strong internal differentiation with respect to the platinum group elements (PGE) (Barnes, 2004), being enriched in the iridium-group PGE (IPGE) in the middle and upper part, and depleted in IPGE and enriched in Pt and Pd at the base. This zonation is attributed to magmatic fractionation of monosulfide solid solution (MSS) from the sulfide liquid pool. The accumulation of Pt and Pd enriched, Ir-depleted, fractionated sulfide liquid at the base of the massive sulfide layer is difficult to explain, but may be suggestive of crystallization of the sulfide liquid pool from the top down. The bulk composition of the massive ore is enriched in IPGE but depleted in Pt and Pd relative to typical bulk ore compositions of comparable Ni tenor, implying that the ores may be enriched in cumulus MSS relative to the original sulfide liquid composition.

The basal contact of the lower ultramafic unit north and south of the orebody is highly irregular, distinctly non-planar, and marked by a zone several metres thick of distinctively hybridized rocks (Fig. 39) that shows evidence for localized assimilation and back veining.

The Cygnet and Black Swan disseminated sulfide orebody

The Black Swan komatiite succession also hosts two separate disseminated sulfide orebodies: Cygnet, adjacent to Silver Swan; and the Black Swan disseminated orebody hosted with the Eastern Ultramafic Unit (Fig. 38; Dowling et al., 2004).

The Cygnet shoot is a broad, steeply plunging lenticular zone of heavily disseminated and locally matrix (net-textured) sulfide, predominantly olivine–sulfide mesocumulate, occupying a broad linear trough in the basal Western Ultramafic Unit contact (Dowling et al., 2004). The highest grade mineralization (>1.5% Ni) is heavily disseminated grading to matrix ore, which occupies the lower central portions of the mineralized zone and is flanked and overlain by an envelope of progressively lower grade mineralization. The mineralization is separated from the footwall contact (and from Silver Swan massive ores) by a roughly 10 m thick basal zone of barren olivine orthocumulate, and the basal rind of highly contaminated, hybridized, mixed material described above. The sulfide mineralogy shows strong evidence of modification during talc–carbonate alteration.

The host rocks of the Cygnet orebody are a series of equigranular- and bimodal-textured olivine orthocumulates and mesocumulates, altered to talc–carbonate and quartz–carbonate assemblages with intermittent preservation of primary igneous textures. The irregularly distributed sulfide occurs as fine disseminations, coarse-grained patches, and lobate blobs scattered throughout all varieties of cumulate, some of which contain carbonate pseudomorphs after amygdals.

Cygnet is distinctive in containing a variety of felsic and ultramafic xenoliths. Partly resorbed and disaggregated sulfidic felsic inclusions are present throughout the high-grade zone, ranging in size to tens of centimetres.

The most distinctive feature of the ore is the presence of abundant, approximately golf-ball-sized, spherical or near-spherical inclusions of net-textured olivine–sulfide cumulate developed within more sparsely disseminated ore and rare inclusions of spinifex-textured ore. The distinctive textures of the Cygnet ores are interpreted by Dowling et al. (2004) as evidence for reworking and redeposition of pre-existing massive and matrix sulfides up-channel.

The Black Swan orebody is characterized by an association of sulfide blebs with segregation vesicles (Fig. 41), and by unusually coarse-grained olivine. It is interpreted as the result of transport of sulfide droplets within lava charged with a suspended load of coarse olivine crystals (Dowling et al., 2004). The sulfide mineralogy in the Cygnet and Black Swan disseminated ores is primarily the result of oxidation and re-equilibration that accompanied serpentinization and later talc–carbonate alteration of the ultramafic host rocks (Barnes et al., 2009). The disseminated sulfide grains are intimately intergrown with carbonate, talc, and chlorite. Primary coarse intergranular lobate sulfide blebs are now intergrowths of coarse-grained ferroan carbonate and sulfide. The sulfide mineralogy varies systematically with sulfide mode and grade. There is a systematic change in sulfide mode and mineral assemblage from top to bottom of the Cygnet ore zone, corresponding to a gradual increase in sulfide mode from less than one percent to 25–35%. The upper nickeliferous assemblages are rich in vaesite and hematite, and give way with increasing sulfide mode to polydymite–millerite with magnetite, and ultimately millerite–pentlandite. Pyrite is a ubiquitous phase.

In contrast to Cygnet, the Black Swan ores are dominated by millerite–pyrite–(polydymite) assemblages in both serpentinites and talc carbonates, with no evident relationship to the progression of carbonation. Sulfides show three types of intergrowth with gangue minerals, which can occur separately or all together: intergrowth with magnetite, at least some of which appears to be primarily magmatic in origin; fine intergrowth with interlocking lath-textured antigorite, and intergrowth with carbonate minerals. Pentlandite assemblages are interpreted as slightly modified survivors of the original magmatic event, while the millerite–pyrite assemblages formed during the earliest stages of serpentinization. Overprinting of the early serpentinization event by talc–carbonate had essentially no effect on sulfide mineralogy, other than inducing intergrowth with carbonate (Barnes et al., 2009).

An unusual feature of the Black Swan orebody is the rare presence of the mineral szaibellyite, a manganese-bearing hydrated magnesium borate (Fig. 42) found along fractures within the serpentinized portion of the orebody. This is likely to be due to interaction with seawater-derived boron during serpentinization but it has not been reported from any of the other komatiitic rocks in the Yilgarn.

Detailed sampling of the entire komatiite complex reveals that the Black Swan komatiites are pervasively contaminated by crustal material. Contamination signatures (high LREE:HREE ratio, Zr/Ti, Th/Yb,

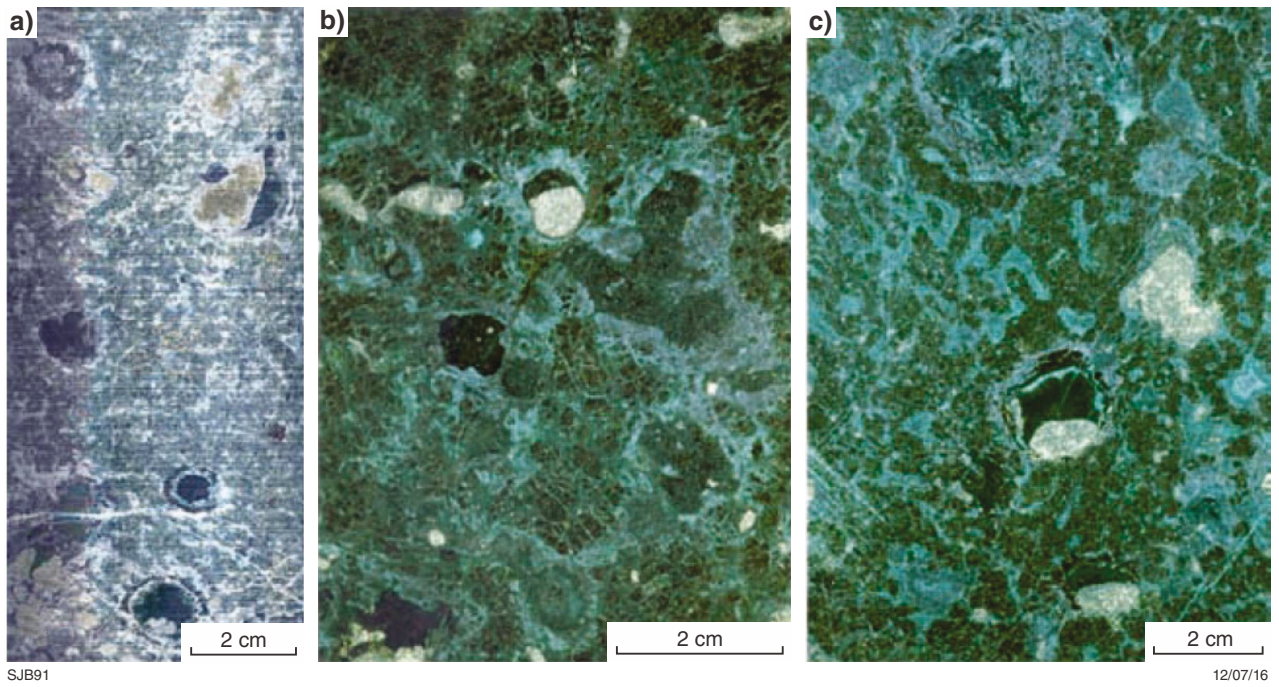


Figure 41. Disseminated ore textures, Black Swan deposit. Capped sulfide globules associated with segregation vesicles in olivine orthocumulate, Black Swan komatiite-hosted deposit. Drillcore samples showing globules occupying lower portion of segregation vesicles, after Dowling et al. (2004)

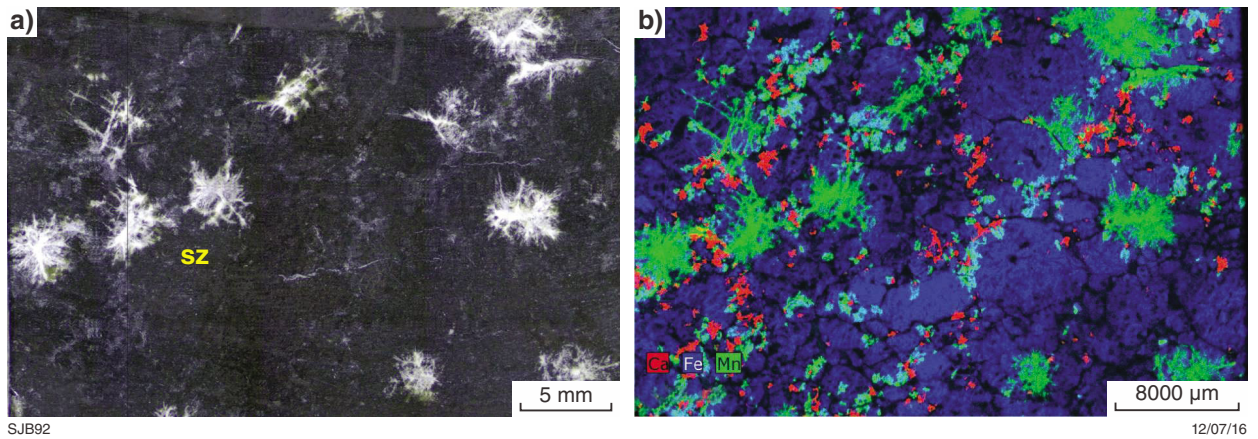


Figure 42. Szaibellyite (hydrated magnesium borate – sz) in serpentinite from within the Black Swan orebody: a) reflected light on cut slab; b) false-colour XRF map of same sample

Th/ Nb etc.) are observed both at flow margins and in internal olivine orthocumulate zones in lava pathways, and in talc-carbonate rocks as well as in serpentinites (Barnes et al., 2004). Komatiites are contaminated with as much as 50% dacite in obviously hybridized basal zone rocks, and up to 20% in komatiites with no obvious textural features of contamination. A suite of samples from throughout the succession shows no evidence of PGE depletion, implying that the magmas were undersaturated in sulfide on emplacement.

Kanowna Town Dam (MGA 367310E 6609870N)

The Kanowna Town Dam locality preserves spectacular examples of volcanoclastic turbidites (Fig. 43), which are considered to be within the Black Flag Group, although their spatial and stratigraphic relationship to nearby komatiites suggests they may be older (Kambalda Sequence). They were described by Trofimovs et al. (2006) as:

... texturally well-preserved sedimentary rock deposits comprising laminated siltstone and mudstone, centimetre- to metre-scale graded beds of coarse sand to granule-sized particles and pebble-sized conglomerate lenses. The deposit dips moderately, 40–55°, towards the east. Sedimentary structures, such as graded beds, flame structures, load casts, and scour-and-fill structures, indicate an east-younging direction (Fig. 44).

The succession coarsens up-sequence. The basal sedimentary layers comprise graded sandstone and mudstone in 2–100 cm-thick beds. Intraformational slumping is commonly preserved in the basal units, together with abundant flame structures and load casts, pseudonodules and dewatering conduits. The middle of the sequence is dominated by coarse-grained quartzofeldspathic (with a minor fuchsitic component) sandstone beds, observed on a metre scale, together with lensoidal felsic porphyry clast-dominated conglomerate channels that have scoured into the underlying sandstone sequence. Amalgamated beds of sandstone and conglomerate form the top of the sequence.

The dominant clast population in the conglomerates comprises ~90% quartz-phyric felsic porphyry clasts with subordinate ultramafic- and mafic-derived fuchsitic clasts (~8%) and siliceous metapelite clasts (~2%). Clasts are rounded and poorly sorted. Intense weathering has altered the primary mineralogy in the matrix to a predominantly phyllosilicate-rich assemblage. Individual volcanic quartz crystals in the matrix are observed. These quartz grains are commonly fragmented, although rare embayment structures are preserved, indicating a volcanic or high-level intrusive provenance.

An open, macroscopic, southeasterly plunging fold (about 100 m across) can be seen in the western and southern sides of the exposure.

East of the Kanowna Town Dam, a thin sequence of komatiite flows overlies the turbidites. Trofimovs et al. (2004b) recognized five distinct komatiite flow units in this area. The komatiites range from medium-grained, equigranular cumulate rocks to very coarse-grained, olivine spinifex-textured komatiite. The contact between the turbidites and the komatiites is poorly exposed (MGA 367750E 6610110N) but can be constrained to within 10 m. Immediately above the contact, ultramafic rocks are pale brown, equigranular altered rocks that are likely after olivine cumulates. These rocks are relatively massive, with little deformation, although there is a variably developed spaced foliation near the contact.

Toward the breakaway, the outcrop alternates between equigranular cumulate textures and olivine spinifex-textured rocks, representing the sequence of stacked komatiite flow units which were recognized by Trofimovs et al. (2004b). Primary textures are well preserved, despite the intense alteration, in the breakaway (MGA 367778E 6609989N) where medium-grained cumulate ultramafic rock grades up into a coarse-grained, randomly oriented, olivine spinifex-textured rock, which then grades into a very coarse olivine spinifex-textured rock with blades up to 30 cm long. The textural zonation in the komatiite flow suggests the top is to the east.

Kalgoorlie Terrane stratigraphy at Ghost Rocks (MGA 298330E 6724968N)

At Ghost Rocks (Fig. 45), a short southwest to northeast traverse crosses a mafic-ultramafic succession that is correlated with the Kalgoorlie Terrane stratigraphy at Kalgoorlie (see Mount Hunt locality, this volume). This traverse includes a section across the regionally extensive Walter Williams Formation, interpreted by Gole and Hill (1990) and Hill et al. (1995) as an extensive komatiite sheet flow complex that is traceable over an area at least 100 km long and up to 35 km wide (Fig. 45). It is characterized by a very extensive unit of coarse-grained olivine adcumulate: the most extensive body of olivine adcumulate known in the Yilgarn Craton. It can be traced continuously from southwest of Siberia to the shores of Lake Ballard northwest of Menzies and, arguably, to the Kurradjong Anticline in the Mount Ida greenstone belt (Fig. 45).

The Walter Williams Formation is a layered body consisting of a lower zone of olivine cumulates and an upper zone of gabbroic rocks (Gole and Hill, 1990; Hill et al., 1995). The proportion of olivine cumulates to gabbro varies along strike as does the igneous porosity within the lower olivine-cumulate zone. The formation is interpreted as part of a very large komatiite flow field.



Figure 43. High-resolution orthophotos collected using drone-based photogrammetry of a portion of the outcrop of turbidites at the Kanowna Town Dam locality: a) enlargement of inset area

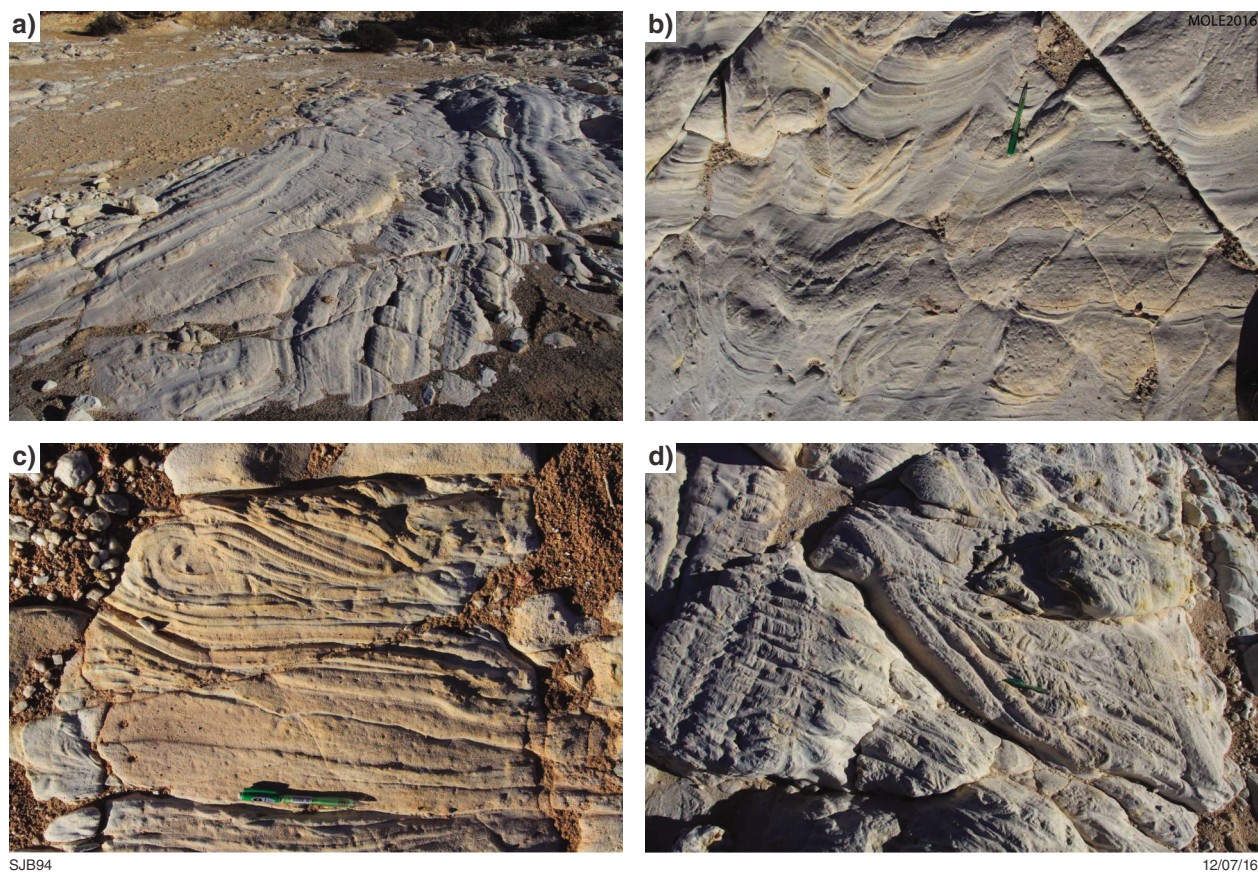


Figure 44. Photographs of sedimentary features at Kanowna Town Dam locality: a) pavement turbidite outcrop at Kanowna Town Dam; b–d) soft-sediment deformation features are common in these sediments, suggesting an active tectonic environment during deposition.

The southern part formed as a vast sheet lobe, resulting in the development of an extensive thick pile of olivine cumulates. In the north, the flow underwent ponding, in situ fractionation, and repeated influxes of new batches of lava (Gole and Hill, 1989, 1990). Stratigraphic profiles through the Walter Williams Formation (Fig. 46) show the gross layering and lateral lithological variations. South of Ghost Rocks, the lower ultramafic zone of the Walter Williams Formation is dominated by a thick olivine-accumulate layer, which grades laterally to olivine mesocumulates and orthocumulates to the north between Ghost Rocks and Lake Ballard and at Kurrajong. North from Yundaga, the upper zone of the Walter Williams Formation is a layered gabbro, which thickens from approximately 30–40 m at Yundaga to 100 m at Ghost Rocks and 180 m at Kurrajong.

Estimates of the true thickness of the unit are greatly hampered by the lack of dip information, and the relative thicknesses shown in Figure 46 are conjectural. At Vettors Hill, the estimated thickness is about 200 m, just south of Menzies it is only 50 m, and at Ghost Rocks it is again 100–200 m. The unit certainly appears to thin from an area about 10 km south of Menzies northward to Lake Ballard, although this may in part be due to deformation, as some of the rocks in this area are highly strained.

For convenience in the following discussion, the Walter Williams Formation is considered in two segments: the southern segment extending from Siberia around the Mount Pleasant anticline to Menzies, and the northern segment in the Kurrajong Anticline (Fig. 45).

The Ghost Rocks locality, along and beside the track across the southwestern limb of a syncline (Fig. 47), is described as follows:

1. From the main road, there are small outcrops of basaltic schist (Missouri Basalt of Swager et al., 1995). Along the track, this passes into metagabbro and cumulate-textured metapyroxenite.
2. A narrow layer of olivine cumulate (MGA 298330E 6724968N) which is serpentized and silicified (at a prominent mesa to the northwest). This is the Walter Williams Formation of Gole and Hill (1990) and Hill et al. (1995). A strongly cleaved grey shale/slate unit within the ultramafic unit (MGA 298532E 6724977N) was probably an interflow sediment.
3. Across a small gully there is common outcrop and float of coarsely spinifex-textured komatiite (MGA 298399E 6724948N). Although foliated in places, the platy olivine-spinifex texture is well preserved. This is the Siberia Komatiite of Swager et al. (1995).

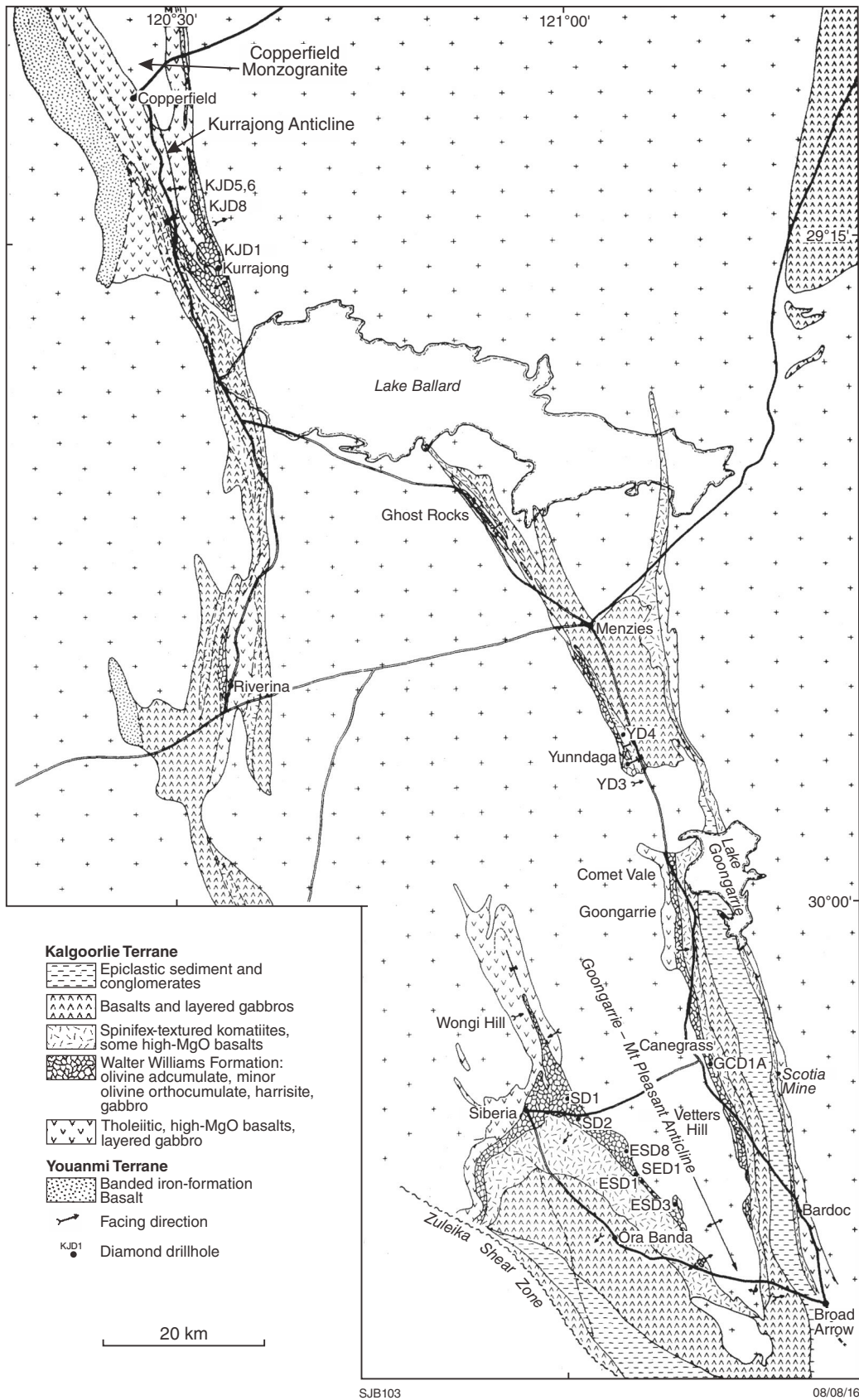


Figure 45. Regional geology of the Walter Williams Formation, after Gole and Hill (1990) and Hill et al. (1995)

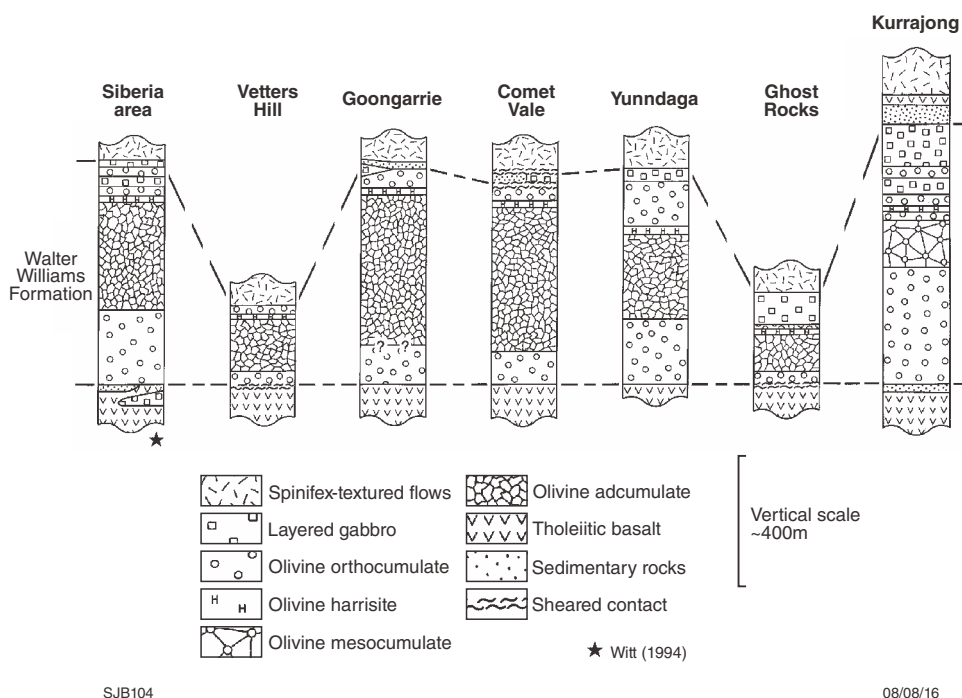


Figure 46. Stratigraphy of the Walter Williams Formation, after Hill et al. (2001)

Two shallow pits in the komatiite on top of the rise (MGA 298469E 6724949N; 298456E 6724937N) have exposed small patches of copper mineralization.

4. Metagabbro above the komatiite (MGA 298503E 6724944N).
5. Above the contact with the overlying metabasalt (MGA 298609E 6724962N), strongly cleaved metabasalt becomes more massive and locally very coarsely feldspar-phyric (MGA 298670E 6724962N).

Comet Vale ultramafic rocks (MGA 319710E 6685732N)

Modified from Hill et al. (2001)

Note: Participants are requested not to use hammers or remove sample material from this outcrop.

At this locality, the upper sections of the Walter Williams Formation (see Ghost Rocks locality description) and the overlying spinifex-textured flow sequence (Siberia Komatiite) are seen. At the beginning of the traverse (Fig. 48) on the old WMC grid baseline, and on the flat area immediately to the east, the adcumulate is covered by ferruginous laterite cap and adcumulate textures are preserved only in a few places. Down the eastern slope of the hill, lower down the laterite profile, adcumulate textures are well displayed in siliceous laterite. The olivine harrisite and its abrupt contact with the adcumulate can be seen just before the steep drop on the eastern side of the

hill (MGA 319950E 6685657N). The harrisites have been etched by weathering and their three-dimensional shapes are shown.

Down the slope, fine-grained orthocumulate with several 30 cm-thick pyroxenite layers outcrop (MGA 319960E 6685690N). On the flat ground farther east, only patchy low outcrop of orthocumulate is present. The rocks here are highly sheared and numerous pegmatites are present. Two major shear zones intersect in this area. Across the shear zones to the northeast are unstrained spinifex-textured flows that form part of the Siberia Komatiite volcanic rocks. These are part of a rotated block, striking southeasterly, bounded to the south by a shear zone and to the north by intrusive granite.

Veters Hill ultramafic rocks (MGA 329397E 6651857N)

Modified from Hill et al. (2001)

A complete section through the Walter Williams Formation (see Ghost Rocks locality description) is seen in the siliceous laterite that caps Veters Hill. The ultramafic unit is unusually thin at this locality, having an apparent thickness of about 150 m compared to 600–900 m elsewhere in its southern outcrop area. The facing is easterly and we shall walk down stratigraphy (at least initially). From the road to just past the fence are serpentinites with fine-grained orthocumulate and uncommon spinifex textures. Rubble covers the lower

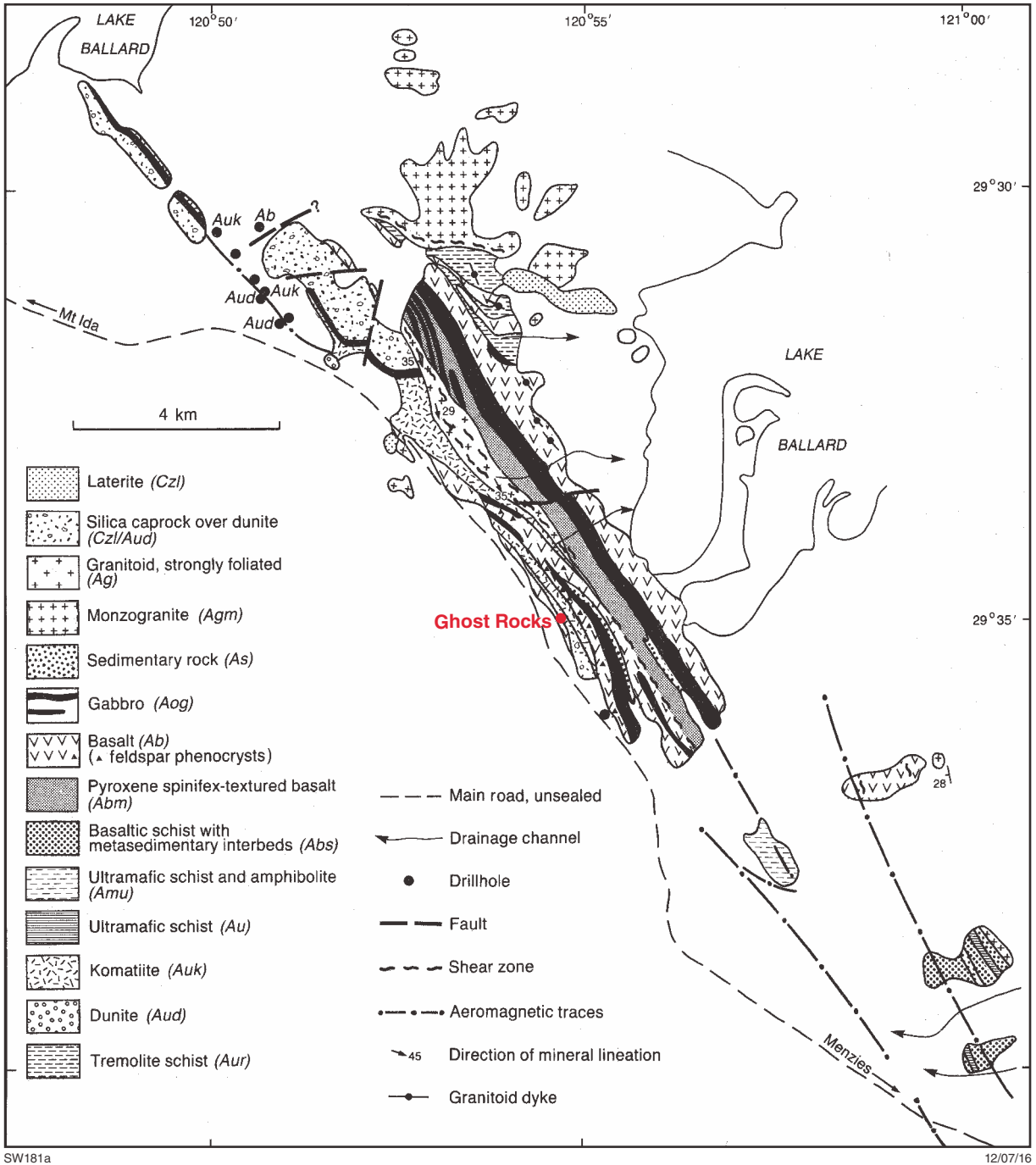


Figure 47. Ghost Rocks geology map, modified from Swager (1994)

part of the hill, although there are a few low outcrops of orthocumulate. About three-quarters of the way up the hill (MGA 329397E 6651857N) there are olivine harrisites in thin rubbly outcrop. Above these and extending to the back slope is adcumulate-textured siliceous laterite. Laterite with orthocumulate textures is present just above the contact with strongly foliated metabasalt (MGA 329257E 6651927N). There is a marked contrast in the preservation of igneous textures for the ultramafic and mafic rocks over this contact. From the top of the hill, the dump at the Sand King openpit mine, near the western extent of the Walter Williams Formation, is visible. Well-developed, dark-brown silica cap over olivine adcumulates is developed around the northern end of the hill.

Western Mining Corporation SM7 nickel laterite pit (MGA 307372E 6652923N)

Modified from Hill et al. (2001)

Exposures of the Walter Williams Formation (see Ghost Rocks locality description) in the Western Mining Corporation (WMC) SM7 nickel laterite pit provide a spectacular illustration of the unique style of weathering of very olivine-rich rocks in the Tertiary laterite profile. Adcumulates have been converted to a ‘silica cap’ that contains more than 90% chalcedonic silica but perfectly preserves the original adcumulate texture and, commonly, the textures associated with serpentinization of olivine. Pseudomorphs of adcumulate with fine-bladed antigorite along grain boundaries are present on the northern side of

the openpit. This is the best locality for collecting samples of silica cap. The openpit was mined for silica flux (with a bonus of up to 2% Ni) for the WMC nickel smelter. The nickel laterite mining operations elsewhere in the Yilgarn Craton (as at the nearby Cawse deposit) mine the nickeliferous clays from the profile overlying the silica cap layer, which have been eroded in this locality.

The Murrin Murrin komatiite complex in the Kilkenny Syncline (MGA 380772E 6795244N)

The Murrin Murrin area is the site of the largest nickel-laterite mining project in Australia. The distribution of these laterites, their preserved profiles, and the nature and extent of nickel enrichment are the result of a complex interplay between supergene processes, regolith profile erosion, and variation in ultramafic protoliths (igneous and metamorphic).

A detailed mapping study carried out by CSIRO in the mid-1990s found that the Murrin Murrin ultramafic cumulates are komatiitic in origin, and that their large lateral extent is the result of widespread areas of shallow dip associated with fold-interference structures. The Kilkenny Syncline (Fig. 49), in the southern part of the lease area, shows steep dips and excellent exposure, and is one of the best areas in the Yilgarn Craton to examine the field relationships between thick adcumulate bodies, spinifex-textured flows, and gabbroic cumulates formed from differentiated komatiite lava.

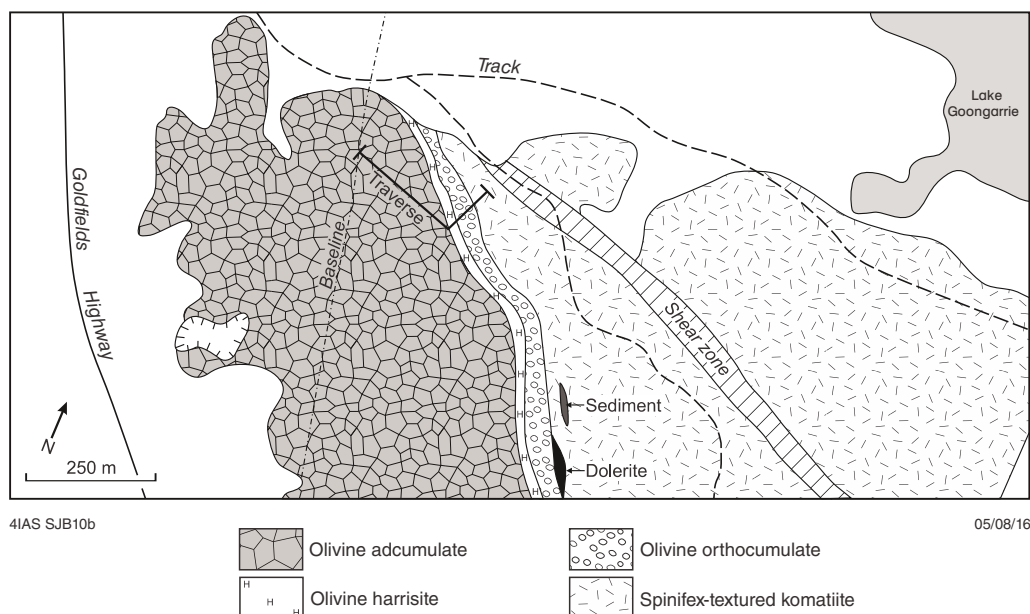


Figure 48. Geological map of the Comet Vale area, modified from Hill et al. (2001)

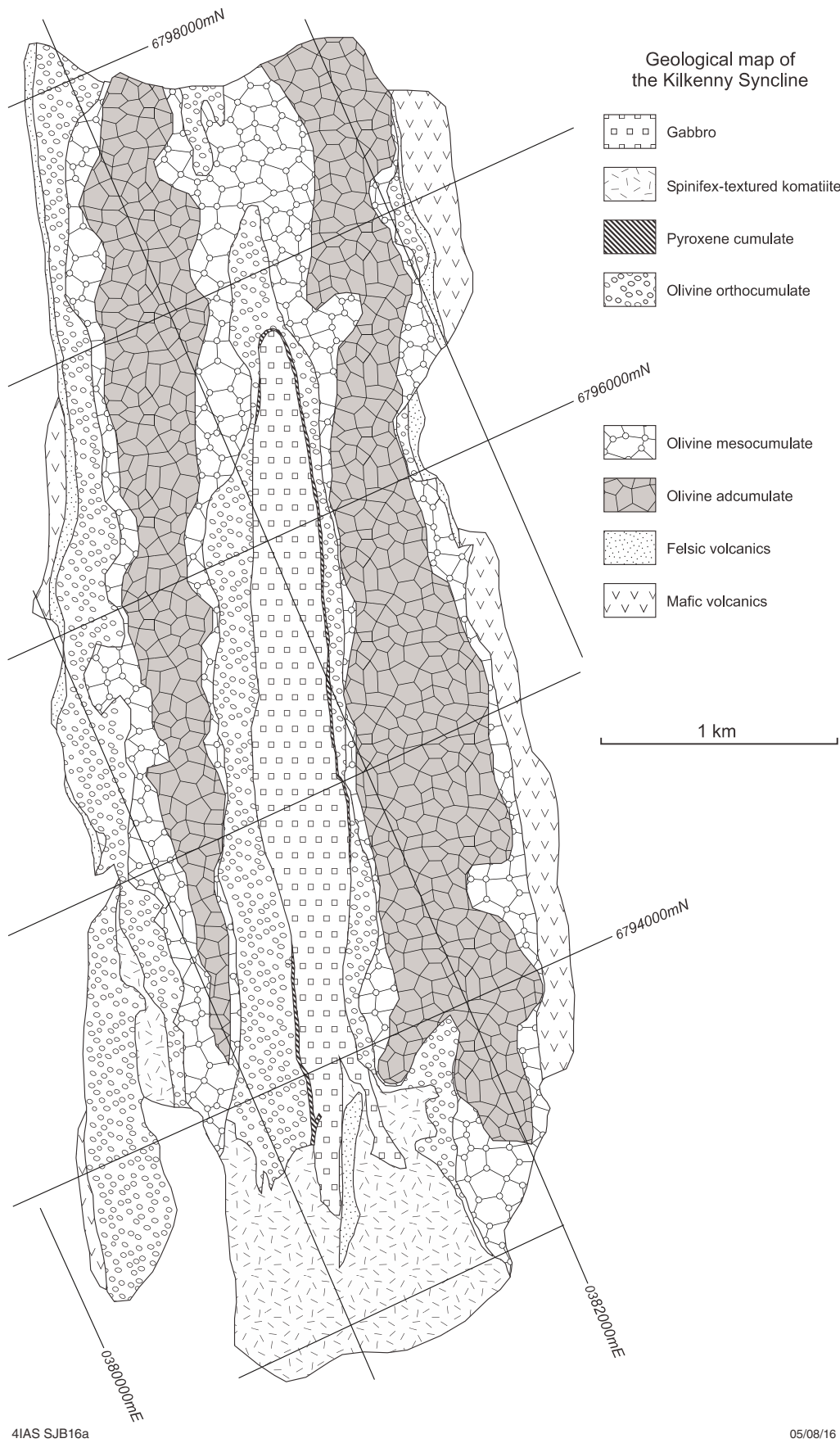


Figure 49. Geology of the Kilkenny Syncline, showing the Murrin Murrin komatiite complex, after Hill et al. (2001). Note that coordinates on the figure refer to the Australian Map Grid 1984 (AMG84).

Regional geology

The Murrin Murrin area is in the central part of the Norseman–Wiluna greenstone belt, between Laverton and Leonora, and lies within a sequence of dominantly intermediate, felsic, and mafic volcanic rocks with intercalated epiclastic sediments, all of which are deformed by at least two phases of folding. The dominant structure in the Murrin Murrin area is a series of isoclinal or near-isoclinal north-northeasterly trending synclines and anticlines.

The regional stratigraphy comprises ‘Association 2’ of Hallberg (1985) and can be interpreted as an intercalation of basalt and high-Mg basalt flows with epiclastic felsic volcanic rocks derived from a number of emergent felsic volcanic centres. The rocks of the Murrin Murrin Ultramafic–Mafic Complex are derived from high-Mg basalt lavas and overlie a thick sequence of tholeiitic pillow basalts, with a thin, discontinuous layer of felsic tuff at the contact.

The rocks of the Murrin Murrin Ultramafic–Mafic Complex in the Murrin Murrin area are folded into the near-isoclinal south-southwest-plunging Kilkenny Syncline. The internal stratigraphy is made up of a thin basal chill zone, which is overlain by an ultramafic cumulate section that is several hundred metres thick, with olivine orthocumulates at the top and bottom and mesocumulates to adcumulates in the centre. This is overlain by gabbroic differentiates, either in direct contact or separated by one or more thin layers of pyroxene cumulate. The core of the syncline in the northern part of the excursion area is occupied by gabbroic rocks, grading laterally to the south into multiple small flow lobes of spinifex and ocellar-textured high-Mg komatiitic basalts.

The critical features of the Murrin Murrin Ultramafic–Mafic Complex to be visited are the basal chill zone, layered olivine orthocumulates, the contact zone between ultramafic and gabbroic layers, the lateral gradation within the ultramafic zone into spectacular pyroxene spinifex-textured komatiitic basalt flow lobes, and the lateral gradation between gabbro and high-Mg basalt lobes. The area provides one of the best known examples of a thick pile of olivine cumulates that can be traced laterally in outcrop into demonstrably extrusive spinifex-textured rocks.

The excursion examines critical parts of the stratigraphy in the area of best exposure, in the southwestern part of the map area. A detailed outcrop map based on CSIRO mapping by M Hunter, J Liimatainen, R Hill, and S Barnes is shown in Figure 50. The access track from the main dirt road traverses well-developed pillow basalts in the footwall of the Murrin Murrin Ultramafic–Mafic Complex. The following localities are identified.

1. Basal chill zone

The first stop shows exposures of olivine-spinifex rocks forming the basal chill zone of the Murrin Murrin Ultramafic–Mafic Complex. The northernmost of the two outcrops (MGA 380918 6795600) exposes this zone almost directly in contact with a thin unit of bedded felsic tuffs, dipping at approximately 70° to the east. The basal

chill zone (MGA 380910 6795400) shows well-developed fine-grained olivine-chevron spinifex textures, in a rock of high-Mg basalt composition with around 12 wt% MgO.

The basal chill zone is no more than five metres thick, and is overlain by a layer of olivine orthocumulate, which in places contains thin discontinuous harrisite layers. The thickness of this layer is unknown in the absence of detailed knowledge of dips, but the combination of rare dip indications on the footwall felsic tuffs and the overall outcrop pattern implies that dips are 70° or more, and the true thickness approximates the outcrop width of around 300 m. This orthocumulate layer is overlain by a central core of olivine mesocumulate and adcumulate, which is approximately 500 m thick, forming the substrate to the economically significant nickeliferous laterites that cap the hills in the area.

2. Layered olivine orthocumulates

The Tertiary weathering profile can be seen well in places. The central adcumulate band is commonly weathered to highly siliceous hardpan or ‘silica cap’ covered by lateritic clays. This central olivine-rich band is stratigraphically overlain by a continuous 200 m-thick layer of very well layered coarse-grained olivine orthocumulates (MGA 381585 6795375), characterized by a strong layer-parallel preferred orientation of olivine grains and an abundance of hollow ‘hopper’ grains, very well exposed at Locality 2 on Figure 50. Layers are defined by flat alignment of olivine crystals with no preferred lineation.

3. Contact between ultramafic and gabbroic cumulates

The contact zone between the ultramafic and gabbroic cumulates is exposed here (MGA 381800E 6795810). Over about a 30 m strike width there is an interlayering of olivine orthocumulate, pyroxene-rich gabbro, and a porphyritic olivine websterite, consisting of 80–90% cumulus clinopyroxene grains with larger orthopyroxene and rare olivine phenocrysts. The precise thickness of these pyroxenite layers is difficult to determine because of the rubbly nature of the outcrop. However, it is clear that the transition from olivine to pyroxene plus plagioclase was rapid, and there was a very small crystallization interval of only pyroxene. This is consistent with the known phase equilibria of evolved komatiite liquids, and explains the common relationship in many komatiitic cumulate sequences where olivine-rich cumulates pass very rapidly into gabbros.

A common rock type at this locality is an unusual calcium-rich metasomatic rock called rodingite. This rock has a strongly bladed texture and is superficially reminiscent of olivine-spinifex texture. In this section, it is evident that the rock consists mainly of diopside, prehnite, and an abundance of other calc-silicate minerals. It also contains graphic eutectic-like textures (Fig. 51) that suggest a felsic granophyre protolith. The rodingite units are in places semiconformable and clearly crosscutting in other places, and are interpreted as a network of calcium-metasomatized felsic dykes.

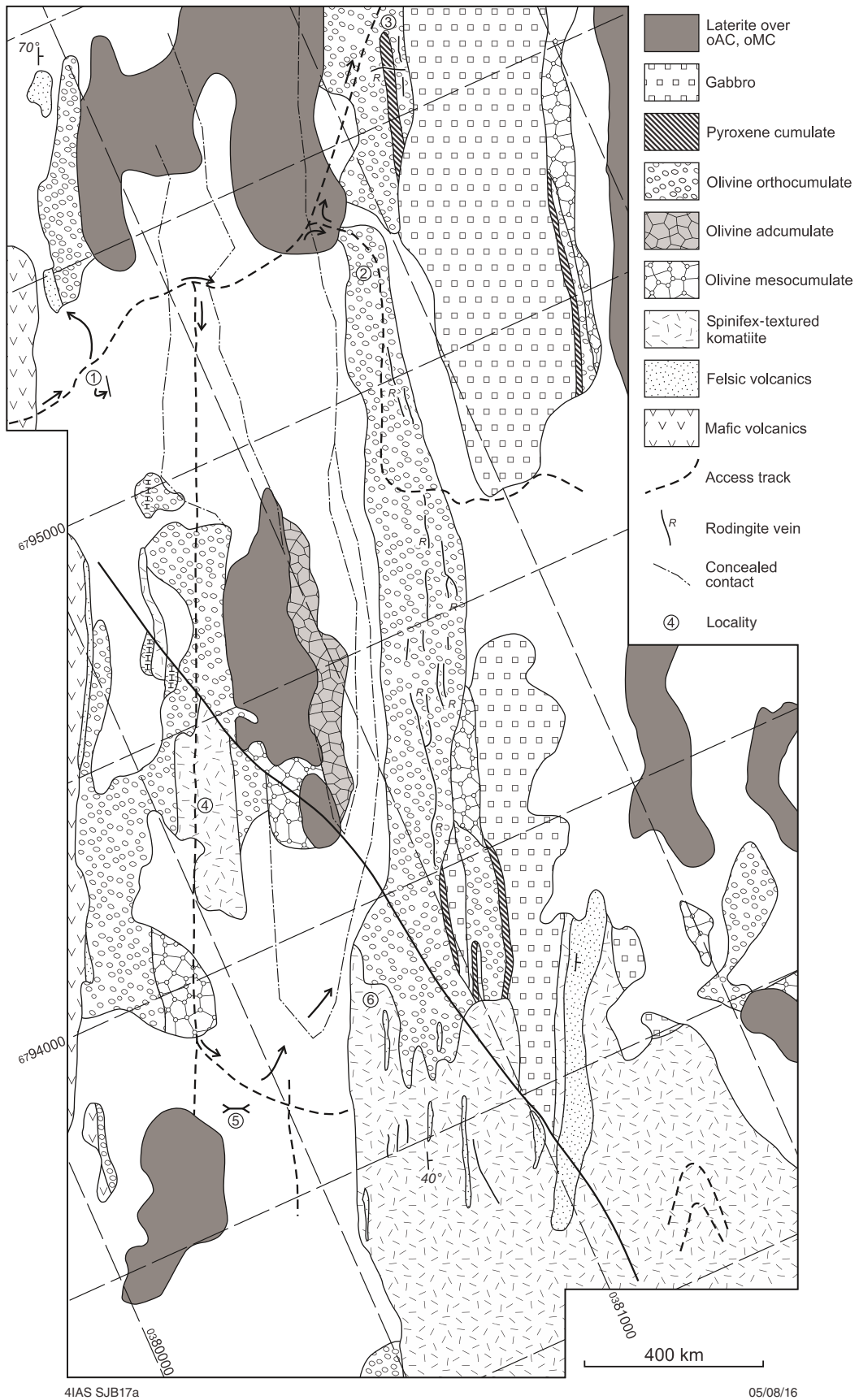


Figure 50. Detailed outcrop map of the southwestern part of the Kilkenny Syncline area, showing the access track, after Hill et al. (2001). Locality numbers are referred to in the text. Abbreviations: oAC = olivine adcumulate; oMC = olivine mesocumulate. Note that coordinates on the figure refer to the Australian Map Grid 1984 (AMG84).

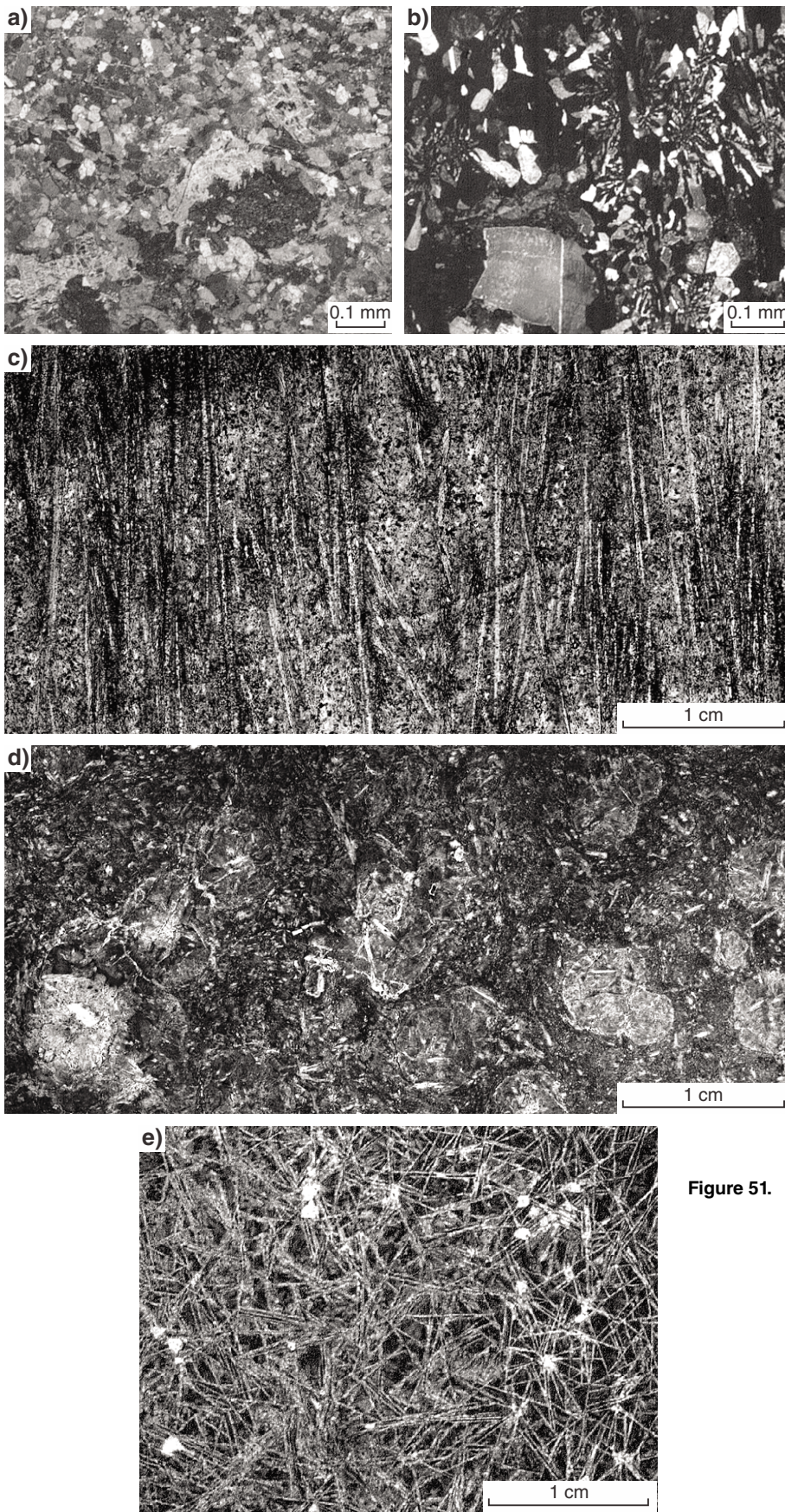


Figure 51. Photomicrographs of Murrin Murrin ultramafic rocks: a) websterite, containing clinopyroxene orthopyroxene mesocumulate from Locality 3 on Figure 50 (crossed polars); b) rodingite from Locality 3 on Figure 50, showing relict granophyric texture, presumably inherited from the original felsic intrusive; c) coarse pyroxene 'string-beef' spinifex, Locality 4 on Figure 50; d) spheroidal ocellar texture in basalt, Locality 6 on Figure 50; e) chevron olivine spinifex in basal chill zone, Locality 1 on Figure 50. After Hill et al. (2001)

SJB98

12/07/16

4. Spinifex-textured komatiitic basalt flow lobe

Outcrops running across the main baseline track (MGA 380722 6794495) expose spectacular ‘string beef’ pyroxene-spinifex textures in a well-differentiated flow lobe. From top to bottom, the lobe consists of about 50 cm of quenched vesicular flow-top autobreccia grading down in a random pyroxene-spinifex A2 zone, which itself grades down into an A3 zone, up to seven metres thick, consisting of spectacular downward-flaring sheaves of pyroxene needles, individually a metre or more long. This is underlain by a cumulate B zone, consisting of highly altered, fine-grained olivine orthocumulate. Spinifex rocks contain 11–13% MgO (anhydrous). The lobe was overlain by a thin unit of bedded felsic tuff containing accretionary lapilli, indicative of a subaerial origin, but this outcrop was largely destroyed during geochronology sampling.

This lobe is one of a series of similar lobes occupying a stratigraphic thickness of up to 50 m, which is overlain, underlain, and flanked at either end by medium- to coarse-grained olivine orthocumulates and mesocumulates. This clearly extrusive unit is completely surrounded by the main mass of the Murrin Murrin Ultramafic–Mafic Complex cumulate pile.

Proceeding to the south from this location, outcrops along the baseline track are of conventional olivine mesocumulate with 1–3 mm green ‘knots’ visible on the surface. These knots are composed of clusters of small cumulus chromite grains mantled by secondary chlorite.

5. Test costean in lateritic clays

This is a test costean in lateritic clays after olivine mesocumulates (MGA 380559 6793865). Relict textures of the igneous protoliths can be seen in the pit spoil.

6. Lateral gradation between gabbro and high-Mg basalt lobes

The traverse starting at MGA 380890 6794060 is approximately 250 m to south and back, over lateral transition between layered olivine orthocumulates and flanking high-Mg basalt flow-lobes with spinifex textures (MGA 380830 6793800) and well-developed ocellar textures in places. This sequence of flow lobes broadens out to the south and forms the core of the syncline; thin interbeds of felsic tuff up to one metre thick are also exposed.

Summary and interpretation

The Kilkenny Syncline exposures illustrate two important relationships:

1. The crystallization history is characteristic of high-Mg mafic liquids derived by fractionation of komatiites. Parent magmas to the complex were komatiitic basalts, having between 12 and 16% MgO, and crystallizing olivine with compositions between Fo₈₇ and Fo₉₁ (Fig. 52). Liquidus relations were such that clinopyroxene and orthopyroxene replaced olivine on the liquidus very close to the point where plagioclase also began to crystallize. This accounts for the rapid transition from olivine cumulates to gabbros with thin, discontinuous intervening pyroxenite layers.
2. The lateral stratigraphic variation is interpreted as the product of a ponded differentiated lava lake flanked by episodically emplaced thin flow lobes. The Kilkenny Syncline exposures provide some of the clearest field evidence yet seen for the extrusive origin of a thick komatiitic cumulate sequence.

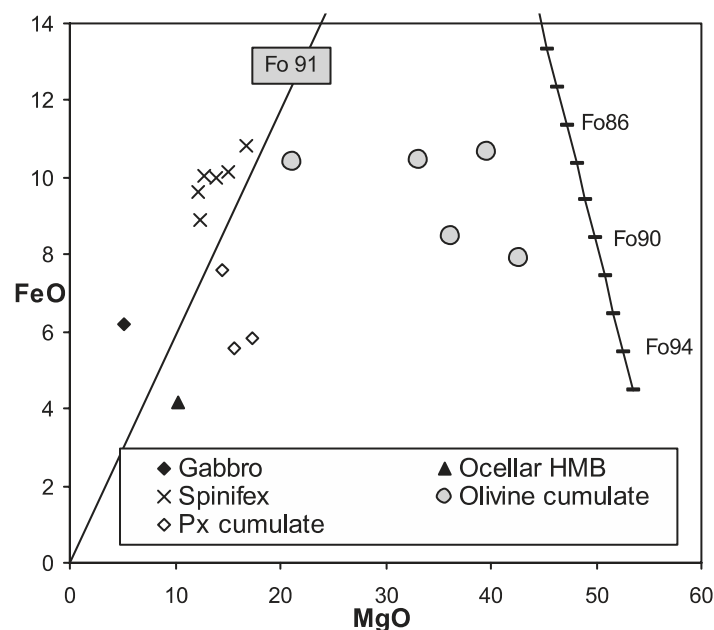


Figure 52. Plot of FeO v. MgO (recalculated anhydrous wt%) for samples from the Murrin Murrin Ultramafic–Mafic Complex. The sloping solid line on right shows pure olivine compositions; the line labelled ‘Fo₉₁’ shows compositions of liquids in equilibrium with Fo₉₁ olivines. After Hill et al. (2001)

Komatiites in the Mount Clifford – Marshall Pool area (MGA 303100E 6850500N)

Regional geology

The Mount Clifford – Marshall Pool area forms the southward extension of the Agnew–Wiluna greenstone belt, an attenuated greenstone belt (Fig. 53) characterized by intercalations of komatiites, dacites and basalts (Fig. 54) extending over more than 200 km, with at least two phases of complex folding, and commonly steep dips. Conditions of peak metamorphism increase southward from prehnite–pumpellyite facies in the Wiluna area to lower amphibolite facies in the Perseverance area, and decrease again to lower greenschist facies near Mount Clifford. Probably correlative stratigraphy, including the Sullivans komatiite unit, extends south almost to Leonora (Thébaud et al., 2012).

Faulting in the Agnew–Wiluna greenstone belt has produced elongate tectonic slices within which lithological correlation is relatively easy given sufficient outcrop, exploration drilling, and aeromagnetic data. There is a general lack of exposure and, in places, extensive fault imbrication and steep plunges combine to render stratigraphic reconstruction difficult. Komatiite rocks are almost continuous over at least 200 km of strike.

The Mount Clifford – Marshall Pool ultramafic complexes are 50 km north of Leonora (Fig. 2), within the southern extension of the Agnew–Wiluna greenstone belt. Definitive correlation with the stratigraphy farther north is not possible due to the structural complexity but the nature of the komatiites is consistent with correlation with the upper part of the greenstone sequence in the Agnew–Wiluna greenstone belt farther north (Hayman et al., 2015).

The Mount Clifford – Marshall Pool block is characterized by gently folded sequences of mafic, ultramafic, felsic volcanic and epiclastic rocks. Peak metamorphic grades range from lower amphibolite facies at the northern end of the block to lower greenschist facies at its southern extremity. An interpretive geological map of the area (Fig. 55) has been compiled from mapping by Thom and Barnes (1977), exploration data generated by Western Mining Corporation, and detailed descriptions of ultramafic rocks from Geological Survey of Western Australia Bulletins and other publications (Barnes et al., 1974; Travis, 1975; Donaldson, 1982b; Donaldson et al., 1986).

The ultramafic successions at Mount Clifford and Marshall Pool are similar in character and, although they have undergone extensive, low-grade pervasive alteration, they have retained spectacular primary igneous textures. The ultramafic succession, which is exposed in a pair of open synclines, includes a large, poorly outcropping olivine-accumulate body overlain by a thick sequence of spinifex-textured flows and olivine orthocumulates. The olivine-accumulate body conformably overlies a thick sequence of pillowed tholeiitic basalts, although they are separated by

a thin chloritic sedimentary unit. The Mount Clifford and Marshall Pool cumulate bodies are tentatively correlated on the basis of aeromagnetic data and percussion drilling (Donaldson et al., 1986).

Mount Clifford area

The supracrustal lithologies define an asymmetrical fault-bounded syncline plunging 45° to the northeast (Fig. 55). At the base of the ultramafic stratigraphy, a one kilometre-thick olivine-accumulate body outcrops sporadically as jasperoidal silica cap exhibiting pseudomorphed igneous textures. Overlying the accumulate is a sequence of coarse-grained olivine orthocumulates with sporadic development of harrisitic textures, overlain in turn by a layered gabbroic body with a fine-grained and locally pyroxene spinifex-textured flow top. This layered unit is in turn overlain by a komatiite sequence comprising a laterally restricted 150 m-thick olivine orthocumulate unit (the Marriotts nickel prospect) and an arcuate, one kilometre-thick pile of thin spinifex-textured flows. Directly above the Marriotts olivine-orthocumulate unit are two sedimentary horizons (Fig. 56).

The Mount Clifford olivine-cumulate body dips to the north at about 30° (Fig. 56) and consists of several units, of which only the basal one is well defined. A one kilometre-thick layer at the base, composed of chlorite and amphibole, is interpreted as an altered chilled margin in contact with the chloritic metasediment (Donaldson et al., 1986). Above this layer, igneous textures are clearly discernible and define a gradual change, with increasing olivine, from rocks with oikocrystic pyroxene to olivine accumulate over the next 50 m. This marginal zone is similar to the olivine-orthocumulate units at the base of the Walter Williams Formation between Ghost Rocks and Siberia. Above this level, abundant relict colourless olivine is preserved. Fine-grained disseminated subhedral chromite crystals are a common accessory mineral. At a height of 343 m above the base there is a thin Mg-augite pyroxenite layer, which marks the top of the basal olivine-accumulate unit. Above this layer the olivine accumulate continues to the upper-orthocumulate marginal zone in contact with the layered gabbro. There is a gradual increase in the forsterite content of olivine upward, from the base to the top of the accumulate body (Fig. 57): a feature common to many of the accumulates of the Norseman–Wiluna greenstone belt. This variation is irregular on a smaller scale, crudely reflecting the presence of cryptic layering (Donaldson, 1983). In the lower basal dunite unit there is a definite in situ fractionation trend from Fo_{90.5} to Fo_{86.5} over the upper 100 m. A gradual increase in forsterite content upward through the accumulate crystal pile is also exhibited by the olivines at Perseverance (Barnes et al., 1988), Six Mile Well, and Yunndaga, and is probably common to most of the accumulate bodies. In the lower basal dunite, chromite is a prominent accessory phase (up to 2 wt%) as ubiquitous disseminated subhedra. Above the pyroxenite layer, where olivine compositions are higher than Fo₉₂, chromite is very rare and grains exhibit an irregular anhedral shape, interstitial to olivine.

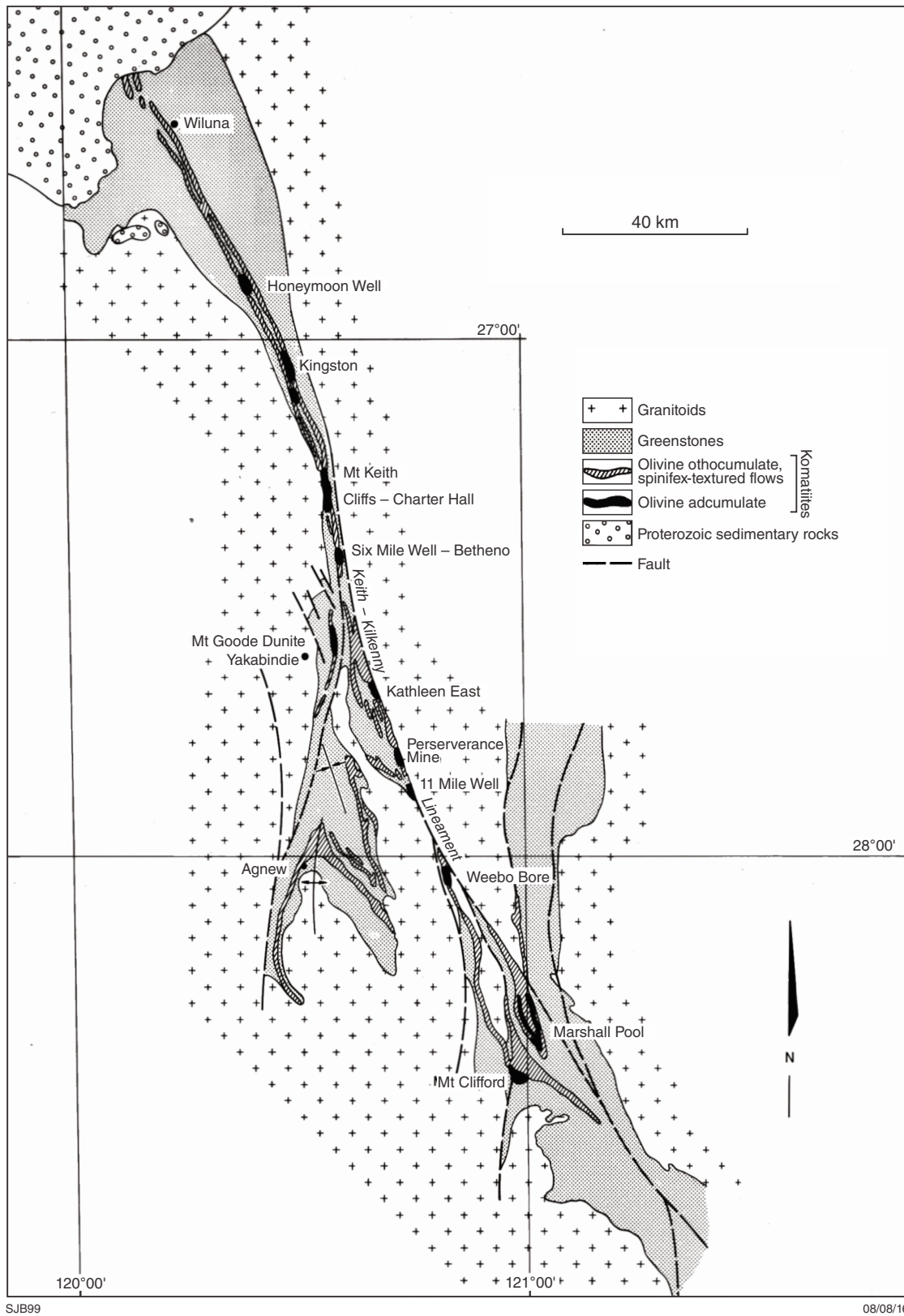


Figure 53. Regional geology of the Agnew–Wiluna greenstone belt from Mount Clifford to Wiluna, showing the distribution of komatiites and komatiitic dunite bodies, after Hill et al. (2001)

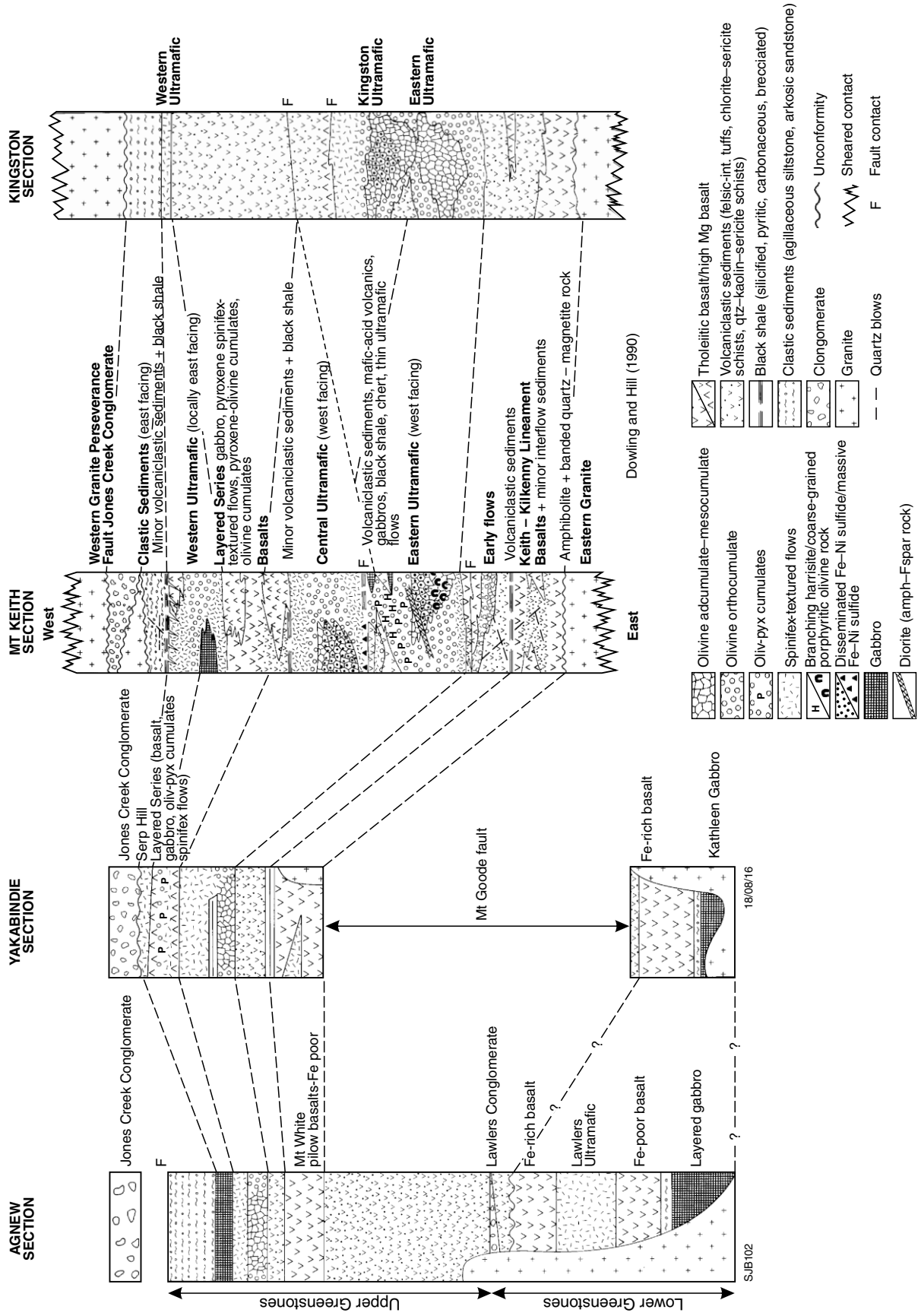


Figure 54. Schematic geological sections across the Agnew-Wiluna greenstone belt, after Hill et al. (2001)

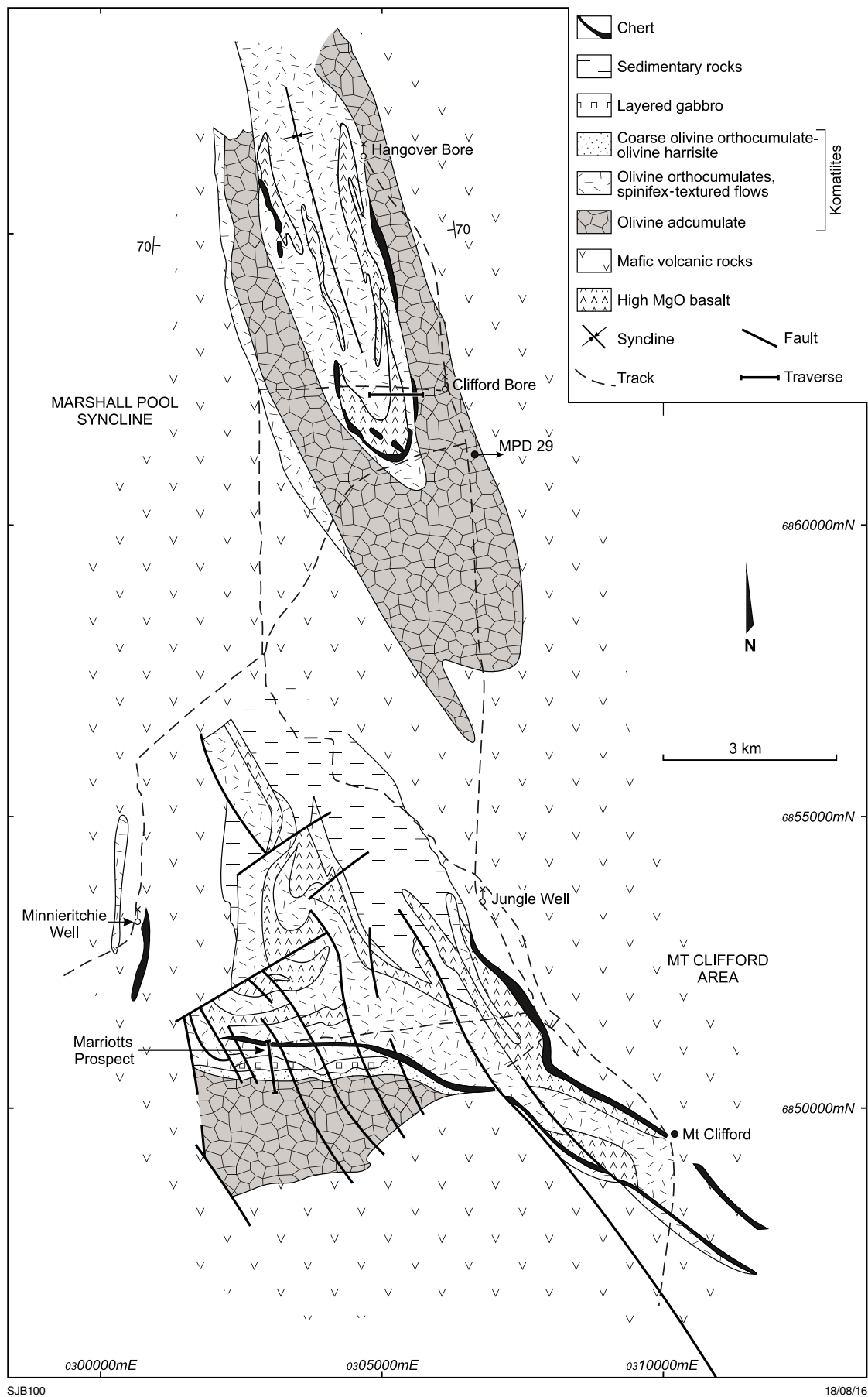


Figure 55. Regional geology of the Mount Clifford – Marshall Pool area, after Hill et al. (2001). Note that coordinates on the figure refer to the Australian Map Grid 1984 (AMG84).

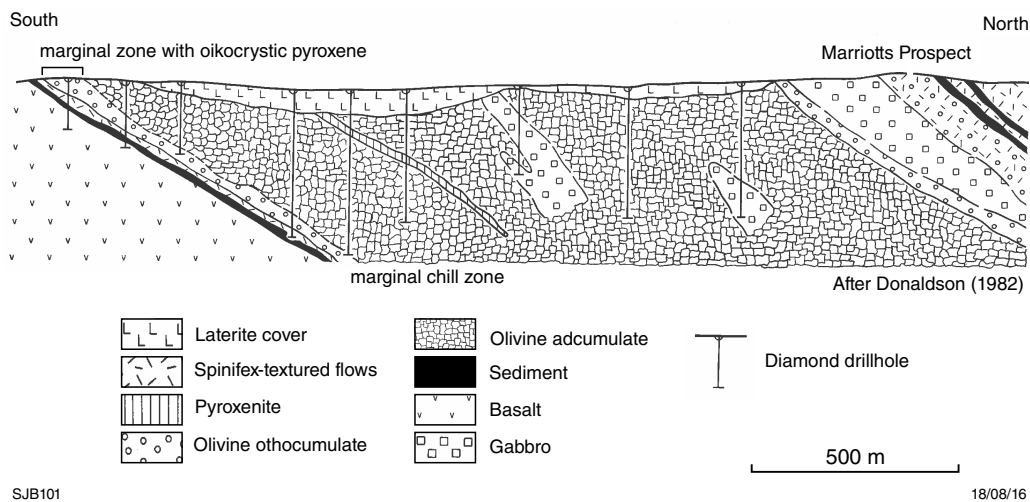


Figure 56. Geological cross-section through the Mount Clifford complex and the Marriotts Prospect, after Hill et al. (2001)

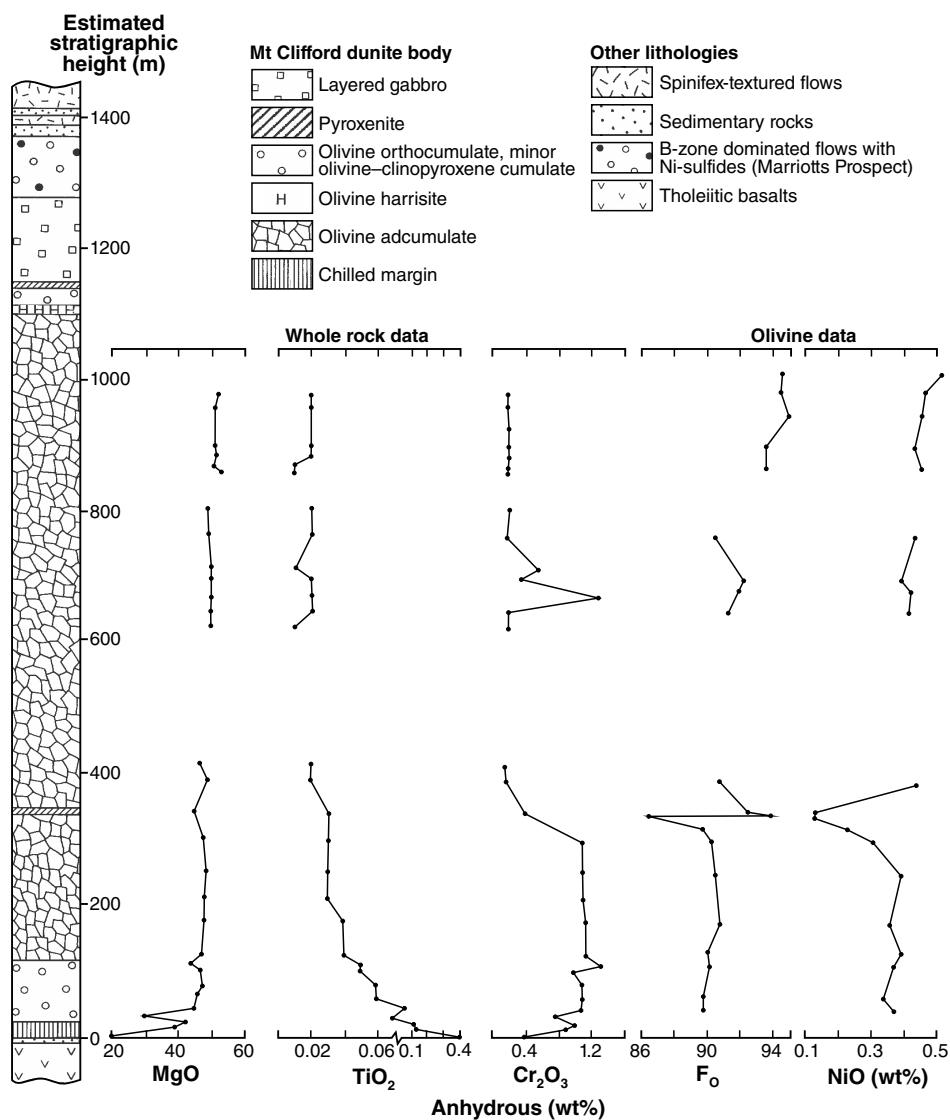


Figure 57. Lithological and geochemical profile through the Mount Clifford complex, after Hill et al. (2001)

The change in modal proportion of chromite is reflected in whole-rock Cr_2O_3 , which is relatively constant at about 1 wt% in the lower basal dunite and drops rapidly across the pyroxenite layer to a constant 0.2 wt% in the upper adcumulate pile (Donaldson et al., 1986). This phenomenon of cumulus chromite being rare, anhedral, and intergranular in adcumulates with olivine compositions greater than Fo_{92} , and in higher proportions in the form of anhedral to subhedral grains in adcumulates with olivines less than Fo_{92} , is a common feature of these ultramafic bodies (Barnes, 1998). The adcumulates are only sporadically exposed as silica cap in the upper few metres, where the field traverse begins.

Traverse from the Mount Clifford dunite to Marriotts nickel prospect

The traverse, starting at (MGA 303240E 6850660N) runs close to a north–south fence line and extends from the upper portion of the Mount Clifford adcumulate body into the overlying komatiite flows above the dunite–pyroxenite–gabbro complex. The contact zone between the adcumulate body and the base of the well-layered pyroxenites and gabbro is reasonably well exposed over the first 100 m of the traverse. Rubbly outcrop in this zone exposes a changeover about 30 m from coarse-grained olivine adcumulate to an inhomogeneous olivine orthocumulate with pockets closely approaching olivine harrisites (MGA 303233E 68050700N).

The orthocumulate–harrisite zone is overlain by a variety of bimodal porphyritic pyroxenite (MGA 303196E 6850764N), coarse clinopyroxenite (MGA 303204E 6850854N), and pyroxene-rich gabbros (MGA 303198E 6851000N). Continuing northwesterly, bearing toward the fence, the traverse continues through rubbly outcrop of layered gabbros. Fine-grained upper-chill zone of gabbro, with minor amounts of ‘string beef’ clinopyroxene spinifex, is exposed on the fenceline (MGA 303113 6851102) and on strike along the ridge. Spinifex textured samples contain 10–12% MgO. The presence of spinifex textures, conformable nature of the ultramafic–gabbro contact, and overall similarity to other localities visited on this excursion lead to the conclusion that the gabbro is an extrusive differentiated component formed within the same flow complex as the adcumulate body, probably by lava which backed up within a blocked flow pathway and fractionated in situ.

Moving to the east and continuing up section, the traverse continues through the Marriotts nickel prospect (MGA 303130E 6851115N). Spinifex-textured flows with thin B zones and one centimetre spherical sulfide globules are well exposed and sample material is abundant. The Marriotts prospect has an inhomogeneous, laterally restricted olivine orthocumulate directly overlying the chilled flow top on the gabbro, and is interpreted as a composite flow sequence (Donaldson et al., 1986). The rocks exhibit well-preserved pseudomorphs after closely packed polyhedral olivines in a fine-grained feathery matrix, and several thin zones with coarse-grained herringbone or branching plate-olivine pseudomorphs.

Nickel sulfides are concentrated in three narrow zones in the unusual form of scattered spherical or flattened spherical blebs up to one centimetre in diameter (Fig. 58) within olivine orthocumulates (Travis, 1975). These blebs reveal an interesting aspect of the physics of sulfide droplets: the larger droplets form strongly flattened oblate spheroids, whereas the smaller droplets (revealed by 3D X-ray tomography) are close to spherical. This reflects the changing balance of gravitational forces tending to ‘squash’ the settled droplets versus surface tension forces trying to keep them spherical; surface tension forces are relatively larger in the smaller droplets. Fresh samples contain unusual sulfur-deficient mineralogy, including Trevorite (Ni-magnetite), heazlewoodite, and native metal (Hudson and Travis, 1981). At the surface, the sulfide blebs have been replaced by limonite.

Marshall Pool area

The mafic and ultramafic rocks of the Marshall Pool area define the shallow north-plunging Hangover Bore syncline, 15 km north-northeast of the Marriotts prospect (Fig. 55). The core of the syncline is well exposed with a thick sequence of komatiites with very well preserved relict igneous textures and high-magnesium basalts. The thinner komatiite flows (2–5 m) exhibit a variety of spinifex textures, whereas the thicker flows are predominantly olivine orthocumulates. Discontinuous albite-rich cherty sediment horizons are interbedded with flows. Unlike the Mount Clifford area, there is no gabbro between the upper spinifex flows and the underlying olivine adcumulate body at Marshall Pool. The adcumulate does not outcrop: its extent has been outlined by many exploration percussion drillholes throughout the area and two diamond drillholes that were completed by WMC to intersect the eastern basal contact. The laterite developed over the dunite has been explored extensively as a potential lateritic nickel resource.

At its base on the eastern side of the Marshall Pool area, the olivine adcumulate is in contact with a thin, sheared unit of chloritic sedimentary rock. The adcumulate is estimated to be about 500 m thick, its upper limit being fixed by the presence of a thin cherty sedimentary horizon. Above the eastern basal contact, there is a marginal zone similar to that at Mount Clifford but with better preserved igneous textures. On the western side, a basal zone of spinifex-textured rocks can be identified in surface laterite cap and in percussion drill chips. The spatial and contact relationships between this horizon and the olivine adcumulate are not known. The marginal zone on the eastern limb is 50 m thick. The lower 20 m comprises a thin amphibole–chlorite chill zone grading to a horizon with former amphibole or pyroxene phenocrysts, which itself grades into an olivine orthocumulate with oikocrystic paragenetic and edenitic amphibole. These amphiboles were interpreted by Donaldson (1983) as primary igneous minerals. Twenty metres above the contact, oikocrysts of chromium-rich Mg-augite enclose serpentized olivines, and a gradual increase in modal olivine with height results in olivine adcumulate at 50 m.

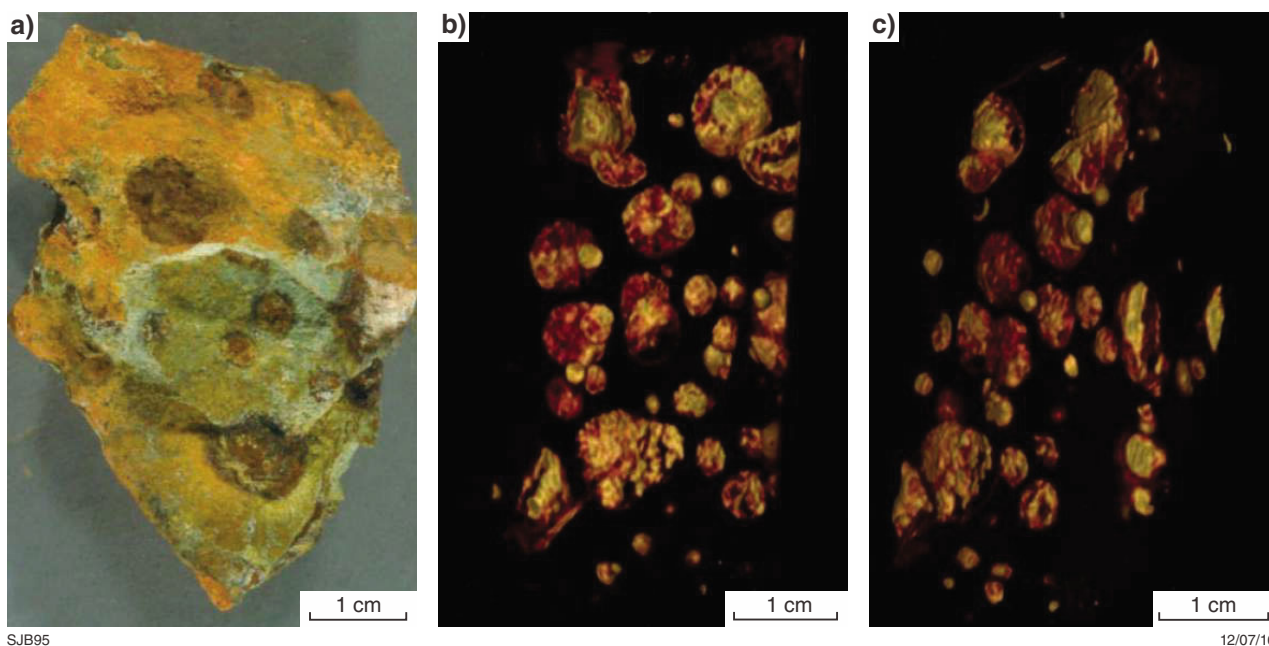


Figure 58. Globular sulfide blebs at the Marriotts Prospect: a) hand sample photograph; b) two perspectives of a 3D X-ray tomography image of the same sample. Flattening of oblate spheroids is more extensive in the larger globules. Modified from Robertson et al. (2016)

The Marshall Pool structure, also known as the Hangover Bore syncline (Fig. 55) is estimated to be at least 15 km long and the Mount Clifford sequence may be stratigraphically equivalent. The basal contact zone of each of the olivine-accumulate bodies and the immediate contact relationships are uncertain, but it is interpreted that the original substratum to the komatiite sequence was basalt. These features point to the olivine-accumulate body being originally in the form of an extensive sheet with similarities, including associated lithologies, to the larger Walter Williams Formation to the south. Such a sheet-like form is in contrast to the laterally restricted olivine-accumulate bodies confined to the ultramafic sequences between Agnew and Honeymoon Well, which have a felsic volcanic substrate.

Marshall Pool traverse

The traverse (east end at MGA 305840E 6862560N) is through rubbly subcrop of differentiated spinifex-textured flow lobes from the sequence immediately overlying the dunite complex. This is an excellent locality for samples of spinifex-textured rocks, where weathering reveals the 3D morphology of the olivine. The book-like morphology of parallel olivine plates in A3 zones of the flow lobes is particularly well represented here.

Melita Formation (MGA 352558E 6784296N)

Hallberg (1985), Witt (1994), Brown et al. (2002) and Barley et al. (2008) described two volcanic centres in the Melita area: the Jeedamyia and Melita volcanic complexes.

Mapping in this area has recently been revised and the Jeedamyia and Melita volcanic complexes have been assigned to the Melita Formation (Wyche et al., 2016). These rocks represent Gindalbie association of high-high field strength element (HFSE) bimodal calc-alkaline, intermediate-silicic volcanic rocks of Barley et al. (2008). Of the two, the Jeedamyia area is less well exposed, consisting of dacite and rhyolite pyroclastic rocks and related epiclastic rocks, felsic porphyry, and minor mafic extrusive and intrusive rocks. A SHRIMP U-Pb zircon age of c. 2683 Ma from the Melita area (Brown et al., 2002) is within error of the age of the c. 2681 Ma Jeedamyia area to the south (Nelson, 1997). Brown et al. (2002) considered the Melita volcanic complex to be a bimodal succession with coeval effusive submarine volcanism and voluminous (effusive, shallow intrusive and explosive) rhyolite volcanism in a shallow subaqueous setting.

On the eastern side of the fence south of the old Melita railway siding (MGA 352630E 6784570N), there is an east-dipping succession of fine to coarse fragmental rocks of the Melita Formation (Fig. 59). Here, Brown et al. (2002) have described a section which contains 'poorly sorted quartz-bearing volcanoclastic sandstones and fine breccias' which 'are generally massive to normally graded or diffusely bedded on a scale of cm-dm, with rarely preserved cross-bedding. Clasts are predominantly angular to subrounded fragments of porphyritic rhyolite, within a variably crystal-rich vitric (now recrystallized) matrix. Graded mm-cm-thick beds of fine-grained vitric to variably crystal-rich sandstone probably represent water-settled airfall tephra (Fig. 59). Accretionary lapilli have been observed in some of these units.

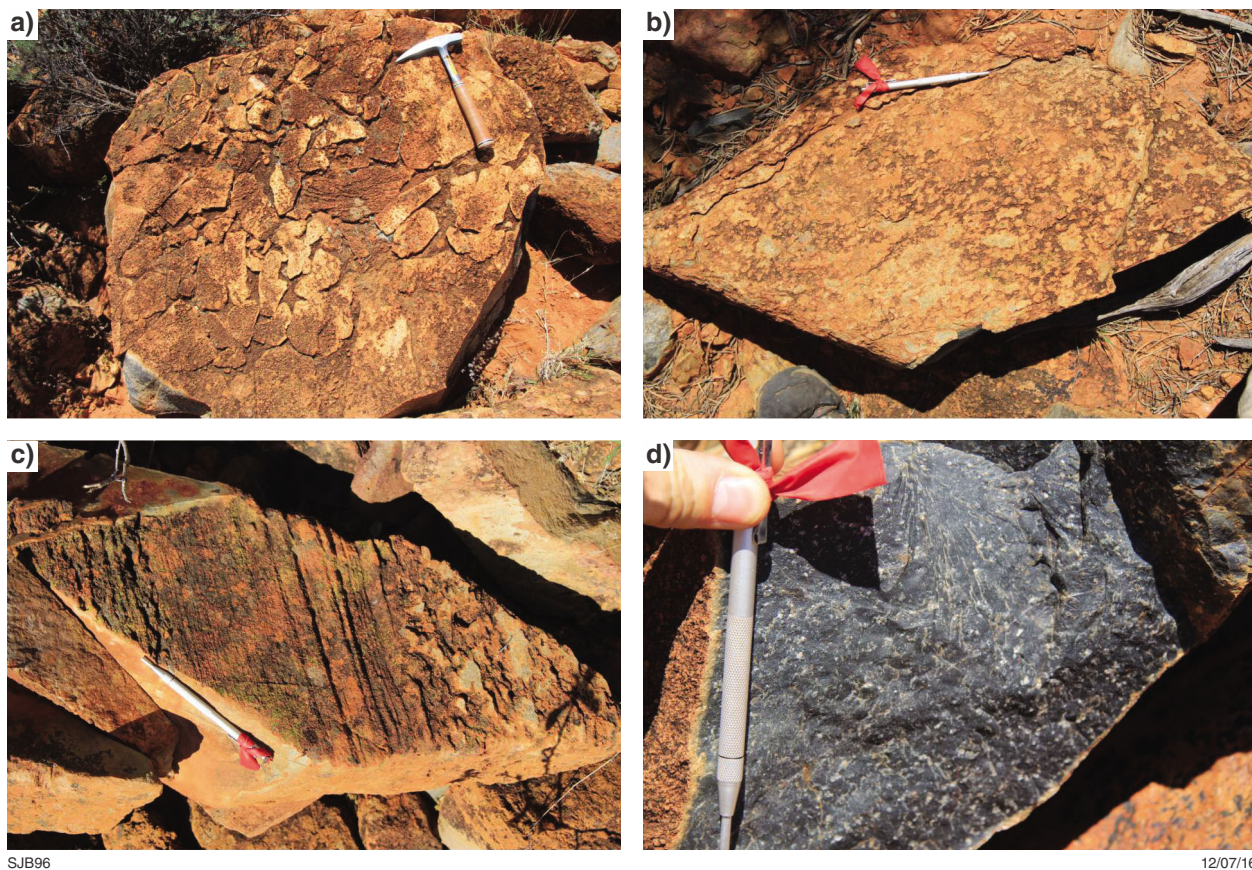


Figure 59. Volcanic, volcanoclastic and epiclastic rocks of the bimodal Melita Formation: a) chaotic, oligomictic breccia consisting of porphyritic rhyolite, bedded/laminated volcanogenic sandstones, and lesser fragmental rocks; b) monomictic fragmental breccia of rhyolite clasts, curvilinear and irregular edges suggests a possible quench fragmentation origin. Lack of jigsaw fit texture suggests reworking of primary hyaloclastite; c) well-bedded to laminated volcanogenic sandstone–siltstone, interbedded with more fragmental material (as shown in b); and d) glassy, micro- to cryptocrystalline porphyritic rhyolite lava (possibly endogenous)

Thick (>10 m) units of massive to bedded, volcanoclastic sandstone and breccia commonly grade upward from breccia, through massive crystal-rich sandstone, to planar-bedded sandstone. The breccias are matrix supported to locally clast supported and dominated by subrounded to angular clasts of porphyritic, commonly flow-banded rhyolite, and rare deformed pumice. They are locally intruded by dolerite.

In one area, the outcrop is dominated by clast-supported, fragmental rhyolitic rocks with elongate, tightly packed, angular to subrounded clasts up to 10 cm (Fig. 59). Just to the west, the rock is more feldspathic with common millimetre-scale euhedral to anhedral feldspar crystals.

Farther west (MGA 352538E 6784293N), there are some boulders with larger (commonly more than 30 cm), angular, close-packed fragments of feldspathic rhyolite with local jigsaw fit in a groundmass of the same material. The clasts are locally layered with some quartz phenocrysts. Also present are finer fragmental rocks, with subcentimetre-scale, angular fragments. The hill to the north contains layered felsic volcanic rocks with alternating fine- and coarse-grained beds.

King of the Hills Dolerite (MGA 324371E 6832069N)

The description of the King of the Hills Dolerite, which outcrops beside the Goldfields Highway about 31 km northwest of Leonora (Fig. 2), is modified after Wyche and Sapkota (2016). The dyke recently underwent SHRIMP U–Pb zircon dating, yielding age modes at c. 2595, 2628 and 2730 Ma (D Mole, unpublished data). Crosscutting relationships indicate the dolerite is Proterozoic so these groups of zircons are considered to be inherited, an interpretation that is supported by their rounded morphology. It probably belongs to the dominantly east–west-trending, c. 2410 Ma Widgiemooltha Supersuite (Wingate, 2007).

The King of the Hills Dolerite is evident on aeromagnetic images over a strike length of about 80 km between Sturt Meadows Homestead (MGA 301680E 6826130N) in the west and Charlie Bore (MGA 377820E 6838600N) in the east. It is a strongly contaminated dolerite that contains abundant xenoliths (Fig. 60). Peers (1972) and Ahmat (1984) have described samples from near

the excursion stop. Stewart (2004) has also described samples from the dolerite. The matrix is fine to medium grained or coarsely feldspar-phyric with a fine- to very fine-grained groundmass (Stewart, 2004). The dominant matrix minerals are quartz, plagioclase, clinopyroxene and chlorite pseudomorphs, possibly after orthopyroxene (Ahmat, 1984). Much of the quartz and feldspar may be xenocrystic. Minor components include opaque oxide minerals, uraltic amphibole, titanite and carbonate (Peers, 1972). According to Stewart (2004), the host rock is more felsic in the western part of the body, west of Linger and Die Well (MGA 335870E 6831530N), where it ranges in composition from diorite to monzogranite.

Xenoliths in the King of the Hills Dolerite are typically less than one metre across and composed dominantly of quartz with subordinate granite. Clasts vary in shape and size, are commonly rounded, and show common evidence of resorption into the intruding dyke (Thom and Barnes, 1977). They are typically quartz aggregates and granite but there are also many individual quartz and feldspar xenocryst grains. Thus, the contaminating material was most likely granitic (Ahmat, 1984).



Figure 60. Photographs of the King of the Hills Dolerite: a) the outcrop north of Leonora; b) the dolerite/diorite contains abundant xenoliths, most of which appear to be felsic, consisting of granoblastic granitic clasts, and quartz clasts/fragments, which commonly have irregular edges; c) a relatively uncontaminated section of the dolerite; and d) fresh surface showing dolerite and host xenoliths

References

- Ahmat, AL 1984, Mafic–ultramafic samples from basic intrusions in the Eastern Goldfields Province: Geological Survey of Western Australia Petrological Report 1369, 28p (unpublished).
- Ahmat, AL 1995, Geology of the Kanowna 1:100 000 sheet: Geological Survey of Western Australia, 1:100 000 Geological Series Explanatory Notes, 28p.
- Arndt, NT 1976, Melting relations of ultramafic lavas (komatiites) at one atmosphere and high pressure, in Carnegie Institution Washington Yearbook (75 edition): p. 555–561.
- Arndt, NT 1994, Archean komatiites, in Archean crustal evolution edited by KC Condie: Elsevier, Amsterdam, p. 11–44.
- Arndt, NT and Fleet, ME 1979, Stable and metastable pyroxene crystallisation in layered komatiite lava flows: American Mineralogist, v. 64, p. 846–856.
- Arndt, NT, Leshner, CM, Houlé, MG, Lewin, E and Lacaze, Y 2004, Intrusion and crystallization of a spinifex textured komatiite sill in Dundonald Township, Ontario: Journal of Petrology, v. 45, p. 2555–2571.
- Arndt, NT, Naldrett, AJ and Pyke, DR 1977, Komatiitic and iron-rich tholeiitic lavas of Munro Township, northeast Ontario: Journal of Petrology, v. 18, p. 319–369.
- Arndt, NT and Nisbet, EG 1982, What is a komatiite?, in Komatiites edited by NT Arndt and EG Nisbet: George Allen and Unwin, London, p. 19–28.
- Barley, ME, Brown, SJA and Krapež, B 2006, Felsic volcanism in the eastern Yilgarn Craton, Western Australia: evolution of a late Archean convergent margin: 16th annual V. M. Goldschmidt conference, Melbourne, Australia, Geochimica and Cosmochimica Acta 70, p. A35.
- Barley, ME, Brown, SJA, Krapež, B and Kositcin, N 2008, Physical volcanology and geochemistry of a Late Archean volcanic arc: Kurnalpi and Gindalbie Terranes, Eastern Goldfields Superterrane, Western Australia: Precambrian Research, v. 161, p. 53–76.
- Barnes, RG, Lewis, JD and Gee, RD 1974, Archean ultramafic lavas from Mount Clifford, in Annual report for the year 1973: Geological Survey of Western Australia, p. 59–70.
- Barnes, SJ 1998, Chromite in Komatiites, 1. Magmatic controls on crystallization and composition: Journal of Petrology, v. 39, p. 1689–1720.
- Barnes, SJ 2004, Komatiites and nickel sulfide ores of the Black Swan area, Yilgarn Craton, Western Australia. 4. Platinum group element distribution in the ores, and genetic implications: Mineralium Deposita, v. 39, p. 752–765.
- Barnes, SJ 2006a, Komatiite-hosted nickel sulfide deposits: Geology, geochemistry, and genesis, in Nickel deposits of the Yilgarn Craton: Geology, geochemistry, and geophysics applied to exploration edited by SJ Barnes: Society of Economic Geologists, Inc., Colorado, US, Special Publication Number 13, p. 51–97.
- Barnes, SJ 2006b, Komatiites: volcanology, metamorphism and geochemistry: Society of Economic Geologists, Special Publication 13, p. 13–49.
- Barnes, SJ, Cruden, AR, Arndt, NT and Saumum, BM 2016, The mineral system approach applied to magmatic Ni–Cu–PGE sulphide deposits: Ore Geology Reviews, v. 76, p. 296–316.
- Barnes, SJ and Fiorentini, ML 2012, Komatiite magmas and sulfide nickel deposits: a comparison of variably endowed Archean Terranes: Economic Geology, v. 107, p. 755–780.
- Barnes, SJ, Fiorentini, ML, Durning, P, Grguric, BA and Perring, CS 2011, The Perseverance and Mount Keith nickel deposits of the Agnew–Wiluna belt, Yilgarn Craton, Western Australia, in Magmatic Ni–Cu and PGE deposits: geology, geochemistry, and genesis edited by C Li and EM Ripley: Society of Economic Geologists, Inc., Reviews in Economic Geology 17, p. 51–88.
- Barnes, SJ, Heggie, GJ and Fiorentini, ML 2013, Spatial variation in platinum group element concentrations in ore-bearing komatiite at the Long-Victor deposit, Kambalda Dome, Western Australia: enlarging the footprint of nickel sulfide orebodies: Economic Geology, v. 108, p. 913–933.
- Barnes, SJ, Hill, RET and Evans, NJ 2004, Komatiites and nickel sulfide ores of the Black Swan area, Yilgarn Craton, Western Australia. 3. Komatiite geochemistry, and implications for ore forming processes: Mineralium Deposita, v. 39, p. 729–751.
- Barnes, SJ, Hill, RET and Gole, MJ 1988, The Perseverance ultramafic complex, Western Australia: product of a komatiite lava river: Journal of Petrology, v. 29, p. 305–331.
- Barnes, SJ and Hill, RET 1995, Poikilitic chromite in komatiitic cumulates: Mineralogy and Petrology, v. 54, p. 85–92.
- Barnes, SJ and Van Kranendonk, MJ 2014, Archean andesites in the east Yilgarn craton, Australia: Products of plume-crust interaction?: Lithosphere, v. 6, no. 2, p. 80–92.
- Barnes, SJ, Van Kranendonk, MJ and Sonntag, I 2012, Geochemistry and tectonic setting of basalts from the Eastern Goldfields Superterrane, Yilgarn Craton: Australian Journal of Earth Sciences, v. 59, no. 5, p. 707–735.
- Barnes, SJ, Wells, MA and Verrall, MR 2009, Effects of magmatic processes, serpentinization and talc–carbonate alteration on sulfide mineralogy and ore textures in the Black Swan disseminated sulfide deposit, Yilgarn Craton: Economic Geology, v. 104, p. 539–562.
- Begg, GC, Griffin, WL, Natapov, LM, O'Reilly, SY, Grand, CJ, Hronsky, JMA, Poudjom Djomani, Y, Swain, CJ, Deen, T and Bowden, P 2009, The lithospheric architecture of Africa: Seismic tomography, mantle petrology, and tectonic evolution: Geosphere, v. 5, p. 23–50.
- Beresford, S, Cas, R, Lahaye, Y and Jane, M 2002, Facies architecture of an Archean komatiite-hosted Ni-sulphide ore deposit, Victor, Kambalda, Western Australia: implications for komatiite lava emplacement: Journal of Volcanology and Geothermal Research, v. 118, p. 57–75.
- Beresford, S, Stone, WE, Cas, R, Lahaye, Y and Jane, M 2005, Volcanological controls on the localization of the komatiite-hosted Ni–Cu–(PGE) Coronet Deposit, Kambalda, Western Australia: Economic Geology, v. 100, p. 1457–1467.
- Blewett, RS, Czarnota, K and Henson, PA 2010, Structural-event framework for the eastern Yilgarn Craton, Western Australia, and its implications for orogenic gold: Precambrian Research, v. 183, p. 203–209.
- Boyd, FR, Gurney, JJ and Richardson, SH 1985, Evidence for a 150–200-km thick Archean lithosphere from diamond inclusion thermobarometry: Nature, v. 315, p. 387–389.
- Brown, SJA, Barley, ME, Krapež, B and Cas, RAF 2002, The Late Archean Melita Complex, Eastern Goldfields, Western Australia: shallow submarine bimodal volcanism in a rifted arc environment: Journal of Volcanology and Geothermal Research, v. 115, no. 3–4, p. 303–327.
- Campbell, IH 1978, Some problems with the cumulus theory: Lithos, v. 11, p. 311–323.
- Campbell, IH 1987, Distribution of orthocumulate textures in the Jimberlana Intrusion: Journal of Geology, v. 95, p. 35–54.
- Campbell, IH, Griffiths, RW and Hill, RI 1989, Melting in an Archean mantle plume: heads it's basalts, tails it's komatiites: Nature, v. 339, p. 697–699.
- Cassidy, KF, Champion, DC, Krapež, B, Barley, ME, Brown, SJA, Blewett, RS, Groenewald, PB and Tyler, IM 2006, A revised geological framework for the Yilgarn Craton, Western Australia: Geological Survey of Western Australia, Record 2006/8, 8p.

- Costa, A, Blake, S and Self, S 2006, Segregation Processes in Vesiculating Crystallizing Magmas: *Journal of Volcanology and Geothermal Research*, v. 153, no. 3-4, p. 287–300.
- Czarnota, K, Champion, DC, Cassidy, KF, Goscombe, B, Blewett, R, Henson, PA and Groenewald, PB 2010, Geodynamics of the eastern Yilgarn Craton: *Precambrian Research*, v. 183, p. 175–202.
- Davis, PC 1999, Classic komatiite localities and magmatic Fe-Ni-Cu-(PGE) sulphide deposits of the Abitibi Greenstone Belt, Ontario-Quebec (Volume 1): Laurentian University, Sudbury, Canada, 70p.
- Donaldson, CH 1974, Olivine morphology in the Tertiary harrisites of Rhum and in some Archean spinifex rocks: *Bulletin of the Geological Society of America*, v. 85, p. 1721–1726.
- Donaldson, CH 1976, An experimental investigation of olivine morphology: *Contributions to Mineralogy and Petrology*, v. 57, p. 187–213.
- Donaldson, CH 1982a, Spinifex-textured komatiites: a review of textures, mineral compositions and layering, in *Komatiites* edited by NT Arndt and EG Nisbet: George Allen and Unwin, London, p. 213–242.
- Donaldson, MJ 1982b, Mount Clifford – Marshall Pool area, in *Regional geology and nickel deposits of the Norseman–Wiluna belt* edited by DI Groves and CM Lesher: The University of Western Australia, Geology Department and Extension Service, Perth, Western Australia, Publication No. 7, p. C53–C67.
- Donaldson, MJ 1983, Progressive alteration of barren and weakly mineralized Archaean dunites from Western Australia: a petrological, mineralogical and geochemical study of some komatiitic dunites from the Eastern Goldfields: The University of Western Australia, Perth, Western Australia, PhD thesis (unpublished).
- Donaldson, MJ, Lesher, CM, Groves, DI and Gresham, JJ 1986, Comparison of Archaean dunites and komatiites associated with nickel mineralization in Western Australia: implications for dunite genesis: *Mineralium Deposita*, v. 21, p. 296–305.
- Dowling, SE, Barnes, SJ, Hill, RET and Hicks, J 2004, Komatiites and Nickel Sulfide Ores of the Black Swan area, Yilgarn Craton, Western Australia. 2. Geology and Genesis of the Orebodies: *Mineralium Deposita*, v. 39, p. 707–728.
- Duuring, P, Bleeker, W, Beresford, SW, Fiorentini, ML and Rosengren, NM 2012, Structural evolution of the Agnew–Wiluna greenstone belt, Eastern Yilgarn Craton and implications for komatiite-hosted Ni sulfide exploration: *Australian Journal of Earth Sciences*, v. 59, no. 5, p. 765–791.
- Ernst, RE 2007, Mafic-ultramafic large igneous provinces (LIPs): importance of the pre-Mesozoic record: *Episodes*, v. 30, no. 2, p. 108–114.
- Faure, F, Arndt, N and Libourel, G 2002, Crystallisation of plate spinifex texture at 1 atm. pressure in a thermal gradient: *Geochimica et Cosmochimica Acta*, v. 66 (Abstracts of the 12th annual V. M. Goldschmidt conference), p. 225.
- Fiorentini, ML, Beresford, SW, Barley, ME, Duuring, P, Bekker, A, Rosengren, NM, Cas, RAF and Hronsky, JMA 2012, District to Camp Controls on the Genesis of Komatiite-Hosted Nickel Sulfide Deposits, Agnew–Wiluna Greenstone Belt, Western Australia: Insights from the Multiple Sulfur Isotopes: *Economic Geology*, v. 107, no. 5, p. 781–796.
- Fowler, AD, Berger, B, Shore, M, Jones, MI and Ropchan, J 2002, Supercooled rocks: development and significance of varioles, spherulites, dendrites and spinifex in Archaean volcanic rocks, Abitibi greenstone belt, Canada: *Precambrian Research*, v. 115, p. 311–328.
- Godel, BM, Barnes, SJ, Gurer, D, Austin, P and Fiorentini, ML 2013, Chromite in komatiites: 3D morphologies with implications for crystallization mechanisms: *Contributions to Mineralogy and Petrology*, v. 165, p. 173–189.
- Gole, MJ and Hill, RET 1989, The Walter Williams Formation: the result of a regionally extensive single komatiite eruptive event, Yilgarn Block, Western Australia: *Bulletin of the Geological Survey of Finland*, v. 61, p. 24.
- Gole, MJ and Hill, RET 1990, The refinement of extrusive models for the genesis of nickel deposits: implications from case studies at Honeymoon Well and the Walter Williams Formation (Volume 68): Minerals and Energy Research Institute of Western Australia (MERIWA), 93p.
- Gole, MJ, Robertson, J and Barnes, SJ 2013, Extrusive origin and structural modification of the komatiitic Mount Keith ultramafic unit: *Economic Geology*, v. 108, p. 1731–1752.
- Green, DH 1975, Genesis of Archean peridotitic magmas and constraints on Archean geothermal gradients and tectonics: *Geology*, v. 3, p. 15–18.
- Gresham, JJ 1986, Depositional environments of volcanic peridotite-associated nickel sulfide deposits with special reference to the Kambalda Dome, in *Geology and Metallogeny of Copper Deposits* edited by GH Friedrick, AD Genkin, AJ Naldrett, JD Ridge, RH Sillitoe and FM Vokes: Springer-Verlag, Berlin, Germany, p. 63–90.
- Gresham, JJ and Loftus-Hills, GD 1981, The geology of the Kambalda nickel field, Western Australia: *Economic Geology*, v. 76, p. 1372–1416.
- Griffin, TJ, Hunter, WM, Keats, W, and Quick, DR 1983, Description of excursion localities, in *Eastern Goldfields geological field conference: abstracts and excursion guide*: Geological Society of Australia (WA Division), p. 28–50 (unpublished).
- Hallberg, JA 1972, Spilitic lavas at Mt Hunt, Western Australia: *Journal of the Royal Society of Western Australia*, v. 55, p. 45–56.
- Hallberg, JA 1985, Geology and mineral deposits of the Leonora-Laverton area, northeastern Yilgarn Block, Western Australia: *Geological Survey of Western Australia, Record 1983/8*, 140p.
- Hallberg, JA and Williams, DAC 1972, Archaean mafic and ultramafic rock associations in the Eastern Goldfields region, Western Australia: *Earth and Planetary Science Letters*, v. 15, p. 191–200.
- Hand, J 1998, The sedimentological and stratigraphic evolution of the Archaean Black Flag Beds, Kalgoorlie, Western Australia: implications for regional stratigraphy and basin setting within the Kalgoorlie Terrane: Monash University, Melbourne, Victoria, PhD thesis (unpublished), 251p.
- Hart, TR, Gibson, HL and Lesher, CM 2004, Trace element geochemistry and petrogenesis of felsic volcanic rocks associated with volcanogenic massive Cu–Zn–Pb sulfide deposits: *Economic Geology*, v. 99, no. 5, p. 1003–1013.
- Hayman, PC, Thébaud, N, Pawley, MJ, Barnes, SJ, Cas, RAF, Amelin, Y, Sapkota, J, Squire, RJ, Campbell, IH and Pegg, I 2015, Evolution of a ~2.7 Ga large igneous province: a volcanological, geochemical and geochronological study of the Agnew greenstone belt, and new regional correlations for the Kalgoorlie Terrane (Yilgarn Craton, Western Australia): *Precambrian Research*, v. 270, p. 334–368.
- Herzberg, C and O'Hara, MJ 1998, Phase equilibrium constraints on the origin of basalts, picrites, and komatiites: *Earth-Science Reviews*, v. 44, p. 39–79.
- Heggie, GJ, Fiorentini, ML, Barnes, SJ and Barley, ME 2012, Maggie Hays Ni deposit: Part 1. Stratigraphic control on the style of komatiite emplacement in the 2.9 Ga Lake Johnston greenstone belt, Yilgarn Craton, Western Australia: *Economic Geology*, v. 107, no. 5, p. 797–816, doi:10.2113/econgeo.107.5.797.
- Hill, RET 2001, Komatiite volcanology, volcanological setting and primary geochemical properties of komatiite-associated nickel deposits: *Geochemistry: Exploration, Environment, Analysis*, v. 1, p. 365–381.

- Hill, RET, Barnes, SJ and Dowling, SE 2001, Komatiites of the Norseman–Wiluna greenstone belt, Western Australia — a field guide: Geological Survey of Western Australia, Record 2001/10, 71p.
- Hill, RET, Barnes, SJ, Dowling, SE and Thordarson, T 2004, Komatiites and nickel sulfide ores of the Black Swan area, Yilgarn Craton, Western Australia. 1. Petrology and volcanology of host rocks: *Mineralium Deposita*, v. 39, p. 684–706.
- Hill, RET, Barnes, SJ, Gole, MJ and Dowling, SJ 1995, The volcanology of komatiites as deduced from field relationships in the Norseman–Wiluna greenstone belt, Western Australia: *Lithos*, v. 34, p. 159–188.
- Hollis, SP, Yeats, CJ, Wyche, S, Barnes, SJ, Ivanic, TJ, Belford, SM, Davidson, GJ, Roache, AJ and Wingate, MTD 2015, A review of volcanic-hosted massive sulfide (VHMS) mineralization in the Archaean Yilgarn Craton, Western Australia: tectonic, stratigraphic and geochemical associations: *Precambrian Research*, v. 260, p. 113–135.
- Houlé, MG, Gibson, HL, Leshner, CM, Davis, PC, Cas, RAF, Beresford, SW and Arndt, NT 2008, Komatiitic sills and multigenerational peperite at Dundonald Beach, Abitibi greenstone belt, Ontario: volcanic architecture and nickel sulfide distribution: *Economic Geology*, v. 103, no. 6, p. 1269–1284.
- Houlé, MG, Prefontaine, S, Fowler, AD and Gibson, HL 2009, Endogenous growth in channelized komatiite lava flows: evidence from spinifex-textured sills at Pyke Hill and Serpentine Mountain, western Abitibi greenstone belt, northeastern Ontario, Canada: *Bulletin of Volcanology*, v. 71, p. 881–901.
- Hudson, DR and Travis, GA 1981, A native nickel–heazlewoodite–ferroan trevorite assemblage from Mount Clifford, Western Australia: *Economic Geology*, v. 76, p. 1686–1697.
- Independence Group NL 2015, Mineral resources and ore reserves update: Report to Australian Securities Exchange, 28 October 2015, 64p.
- Irvine, TN 1982, Terminology for layered intrusions: *Journal of Petrology*, v. 23, p. 127–162.
- Keats, W 1987, Kalgoorlie–Boulder district outcrop geology (1:50 000 scale) in Regional geology of the Kalgoorlie–Boulder gold-mining district by W Keats: Geological Survey of Western Australia, Report 21, Plate 3.
- Kerr, RC and Tait, SR 1985, Convective exchange between pore fluid and an overlying reservoir of dense fluid: a postcumulus process in layered intrusions: *Earth and Planetary Science Letters*, v. 75, p. 147–156.
- Krapež, B and Hand, JL 2008, Late Archaean deep-marine volcanoclastic sedimentation in an arc-related basin: the Kalgoorlie Sequence of the Eastern Goldfields Superterrane, Yilgarn Craton, Western Australia: *Precambrian Research*, v. 161, p. 89–113.
- Latypov, R, Chistyakova, S, Page, A and Hornsey, R 2015, Field evidence for the in situ crystallization of the Merensky Reef: *Journal of Petrology*, v. 56, p. 2341–2372.
- Leshner, CM 1989, Komatiite-associated nickel sulfide deposits, in *Ore Deposition Associated with Magmas* (4th edition) edited by JA Whitney and AJ Naldrett: Society of Economic Geologists, El Paso, p. 44–101.
- Leshner, CM, Arndt, NT and Groves, DI 1984, Genesis of komatiite-associated nickel sulphide deposits at Kambalda, Western Australia: a distal volcanic model, in *Sulphide deposits in mafic and ultramafic rocks* edited by DL Buchanan and MJ Jones: The Institution of Mining and Metallurgy, London, p. 70–80.
- Leshner, CM and Keays, RR 2002, Komatiite-associated Ni–Cu–(PGE) deposits: geology, mineralogy, geochemistry and genesis, in *The geology, geochemistry, mineralogy and mineral beneficiation of the platinum-group elements* edited by LJ Cabri: Canadian Institute of Mining, Metallurgy and Petroleum, Special Volume 54, p. 579–617.
- Martin, H, Smithies, RH, Rapp, R, Moya, J-F and Champion, DC 2005, An overview of adakite, tonalite–trondhjemite–granodiorite (TTG), and sanukitoid: relationships and some implications for crustal evolution: *Lithos*, v. 79, p. 1–24.
- McBirney, AR and Noyes, RM 1979, Crystallization and layering of the Skaergaard Intrusion: *Journal of Petrology*, v. 20, no. 3, p. 487–554.
- McCall, GJH and Leishman, J 1971, Clues to the origin of Archaean eugeosynclinal peridotites and the nature of serpentinisation, in *Symposium on Archaean Rocks*: Geological Society of Australia, Sydney, NSW, Special Publication, Geological Society of Australia 3, p. 281–299.
- Mole, DR, Fiorentini, ML, Thebaud, N, Cassidy, KF, McCuaig, TC, Kirkland, CL, Romano, SS, Doublier, MP, Belousova, EA, Barnes, SJ and Miller, J 2014, Archaean komatiite volcanism controlled by the evolution of early continents: *Proceedings of the National Academy of Sciences of the United States of America*, v. 111, no. 28, p. 10083–10088.
- Naldrett, AJ and Turner, AR 1977, The geology and petrogenesis of a greenstone belt and related nickel sulfide mineralisation at Yakabindie, Western Australia: *Precambrian Research*, v. 3, p. 43–103.
- Nelson, DR 1997, Evolution of the Archaean granite–greenstone terranes of the Eastern Goldfields, Western Australia: SHRIMP U–Pb zircon constraints: *Precambrian Research*, v. 83, no. 1–3, p. 57–81.
- Nelson, DR 1998, Granite–greenstone crust formation on the Archaean Earth: a consequence of two superimposed processes: *Earth and Planetary Science Letters*, v. 158, no. 3–4, p. 109–119.
- Peers, R 1972, Petrography of 5 rocks from Leonora 1:250 000 Sheet: Geological Survey of Western Australia, 7p. (unpublished).
- Perring, CS, Barnes, SJ and Hill, RET 1995a, Physical volcanology and geochemical variation of Forresteria komatiites as a guide to their prospectivity for nickel sulphide mineralisation: *CSIRO Exploration Mining Report 125R*, 90p.
- Perring, CS, Barnes, SJ and Hill, RET 1995b, The physical volcanology of Archaean komatiite sequences from Forresteria, Southern Cross Province, Western Australia: *Lithos*, v. 34, no. 1–3, p. 189–207.
- Pyke, DR, Naldrett, AJ and Eckstrand, OR 1973, Archaean ultramafic flows in Munro Township, Ontario: *Geological Society of America Bulletin*, v. 84, no. 3, p. 955–978, doi:10.1130/0016-7606(1973)84<955:AUFIMT>2.0.CO;2.
- Robertson, JC, Barnes, SJ and Le Vaillant, M 2016, Dynamics of magmatic sulphide droplets during transport in silicate melts and implications for magmatic sulphide ore formation: *Journal of Petrology*, v. 56, p. 2445–2472.
- Rosengren, NM 2004, Architecture and emplacement origin of an Archaean komatiitic dunite and associated NiS mineralisation: Mount Keith, Agnew–Wiluna greenstone belt, Yilgarn Craton, Western Australia: Monash University, Melbourne, PhD thesis (unpublished).
- Rosengren, NM, Beresford, SW, Grguric, BA and Cas, RAF 2005, An intrusive origin for the komatiitic dunite-hosted Mount Keith disseminated nickel sulfide deposit, Western Australia: *Economic Geology*, v. 100, p. 149–156.
- Shore, M and Fowler, AD 1999, The origin of spinifex texture in komatiites: *Nature*, v. 397, p. 691–694.
- Sleep, NH 1997, Lateral flow and ponding of starting plume material: *Journal of geophysical research*, v. 102, no. B5, p. 10001–10012.
- Sleep, NH, Ebinger, CJ and Kendall, J-M 2002, Deflection of mantle plume material by cratonic keels, in *The Early Earth: Physical, Chemical and Biological Development* edited by CMR Fowler, CJ Ebinger and CJ Hawkesworth: The Geological Society, London, Geological Society Special Publication 199, p. 135–150.

- Sigmasson, O, Thordarson, T and Jakobsson, SP 2009, Segregations in Surtsey lavas (Iceland) reveal extreme magma differentiation during late stage flow emplacement: Special Publications of the International Association of Volcanology and Chemistry of the Earth's Interior, v. 2, p. 85–104.
- Smithies, RH 2000, The Archaean tonalite–trondhjemite–granodiorite (TTG) series is not an analogue of Cenozoic adakite: Earth and Planetary Science Letters, v. 182, p. 115–125.
- Squire, RJ, Allen, CM, Cas, RAF, Campbell, IH, Blewett, RS and Nemchin, AA 2010, Two cycles of voluminous pyroclastic volcanism and sedimentation related to episodic granite emplacement during the late Archaean: Eastern Yilgarn Craton, Western Australia: Precambrian Research, v. 183, no. 2, p. 251–274.
- Stauda, S, Le Vaillant, M and Barnes, SJ 2015, Spinel formation during thermomechanical erosion of footwall basalt beneath a sulfide melt pool at the komatiite-hosted Ni-Cu(-PGE) Moran deposit, Kambalda, Western Australia, in SEG 2015: World-Class Ore Deposits: Discovery to Recovery: Society of Economic Geologists; Hobart, Tasmania, 27 September 2015, 1p.
- Stauda, S, Sheppard, S, Parker, P and Paggi, J in prep., Long-Victor nickel sulfide complex, Kambalda, Western Australia, in Australian Ore Deposits: Australasian Institute of Mining and Metallurgy Monograph.
- Stone, WE and Archibald, NJ 2004, Structural controls on nickel sulfide ore shoots in Archaean komatiite, Kambalda, WA: the volcanic trough controversy revisited: Journal of Structural Geology, v. 26, p. 1173–1194.
- Stone, WE, Beresford, SW and Archibald, NJ 2005, Structural setting and shape analysis of nickel sulphide shoots at the Kambalda Dome, Western Australia: implications for deformation and remobilization: Economic Geology, v. 100, p. 1441–1455.
- Stone, WE and Masterman, EE 1998, Kambalda nickel deposits, in Geology of Australian and Papua New Guinean mineral deposits edited by DA Berkman and DH Mackenzie: Australasian Institute of Mining and Metallurgy, Melbourne, Monograph 22, p. 347–355.
- Swager, CP 1989, Structure of the Kalgoorlie greenstones — regional deformation history and implications for the structural setting of the Golden Mile deposits, in Professional papers: Geological Survey of Western Australia, Report 25, p. 59–84.
- Swager, CP 1990, Locality 12, Hannan Lake and Mount Hunt, in 3rd International Archaean Symposium Guidebook edited by SE Ho, JE Glover, JS Myers and JR Muhling: The University of Western Australia, Perth, Geology Department and University Extension 21, p. 252–253.
- Swager, CP 1994, Geology of the Menzies 1:100 000 sheet (and adjacent Ghost Rocks area): Geological Survey of Western Australia, 1:100 000 Geological Series Explanatory Notes, 31p.
- Swager, CP, Griffin, TJ, Witt, WK, Wyche, S, Ahmat, AL, Hunter, WM and McGoldrick, PJ 1995, Geology of the Archaean Kalgoorlie Terrane — an explanatory note (reprint of Record 1990/12): Geological Survey of Western Australia, Report 48, 26p.
- Thébaud, N, Barnes, S and Fiorentini, M 2012, Komatiites of the Wildara–Leonora Belt, Yilgarn Craton, WA: The missing link in the Kalgoorlie Terrane?: Precambrian Research, v. 196–197, p. 234–246.
- Thom, R and Barnes, RG (compilers) 1977, Leonora, Western Australia: Geological Survey of Western Australia, 1:250 000 Geological Series Explanatory Notes, 29p.
- Thompson, RN and Gibson, SA 1991, Subcontinental mantle plumes, hotspots and pre-existing thinspots: Journal of the Geological Society of London, v. 148, no. 6, p. 973–977.
- Thy, P 1995, Low pressure experimental constraints on the origin of komatiites: Journal of Petrology, v. 36, no. 6, p. 1529–1548.
- Travis, GA 1975, Mount Clifford nickel deposit, in Economic geology of Australia and Papua New Guinea, 1. Metals edited by CL Knight: Australasian Institute of Mining and Metallurgy, Monograph 5, p. 144–146.
- Travis, GA, Woodall, R and Bartram, GD 1971, The geology of the Kalgoorlie Goldfields, in Symposium on Archaean rocks edited by JE Glover: Geological Society of Australia; Symposium on Archaean rocks, Perth, 23 May 1970; Special Publication 3, p. 175–190.
- Trofimovs, J, Cas, RAF and Davis, BK 2004a, An Archaean submarine volcanic debris avalanche deposit, Yilgarn Craton, western Australia, with komatiite, basalt and dacite megablocks: the product of dome collapse: Journal of Volcanology and Geothermal Research, v. 138, p. 111–126.
- Trofimovs, J, Davis, BK and Cas, RAF 2004b, Contemporaneous ultramafic and felsic intrusive and extrusive magmatism in the Archaean Boorara Domain, Eastern Goldfields Superterrane, Western Australia, and its implications: Precambrian Research, v. 131, p. 283–304.
- Trofimovs, J, Davis, BK, Cas, RAF, Barley, ME and Tripp, GI 2006, Reconstructing the event stratigraphy from the complex structural — stratigraphic architecture of an Archaean volcanic–intrusive–sedimentary succession: the Boorara Domain, Eastern Goldfields Superterrane, Western Australia: Australian Journal of Earth Sciences, v. 53, p. 303–327.
- Trofimovs, J, Tait, MA, Cas, RAF, McArthur, A and Beresford, SW 2003, Can the role of thermal erosion in strongly deformed komatiite–Ni–Cu–(PGE) deposits be determined? Perseverance, Agnew–Wiluna Belt, Western Australia: Australian Journal of Earth Sciences, v. 50, p. 199–214.
- Turner, JS, Huppert, HE and Sparks, RSJ 1986, Komatiites II: experimental and theoretical investigations of post-emplacement cooling and crystallization: Journal of Petrology, v. 27, p. 397–437.
- Viljoen, MJ and Viljoen, RP (compilers) 1969, Evidence for the existence of a mobile extrusive peridotitic magma from the Komati Formation of the Onverwacht Group: Geological Society of South Africa, Johannesburg, Special Publication 2, p. 87–112.
- Wager, LR and Brown, GM 1968, Layered igneous rocks: Oliver and Boyd, Edinburgh, 588p.
- Wager, LR, Brown, GM and Wadsworth, WJ 1960, Types of igneous cumulates: Journal of Petrology, v. 1, p. 73–85.
- Williams, DAC 1971, Determination of primary mineralogy and textures in ultramafic rocks from Mt Monger, Western Australia, in Symposium on Archaean Rocks: Geological Society of Australia, Sydney, NSW, Special Publication 3, p. 259–267.
- Williams, DAC and Hallberg, JA 1973, Archaean layered intrusions of the Eastern Goldfields region, Western Australia: Contributions to Mineralogy and Petrology, v. 38, p. 45–70.
- Wilson, AH 1992, The geology of the Great Dyke, Zimbabwe: crystallization, layering and cumulate formation in the P1 pyroxenite of Cyclic Unit 1 of the Darwendale Subchamber: Journal of Petrology, v. 33, p. 611–663.
- Wingate, MTD 2007, Proterozoic mafic dykes in the Yilgarn Craton, in Proceedings of Geoconferences (WA) Inc. Kalgoorlie '07 Conference edited by FP Bierlein and CM Knox-Robinson: Geoscience Australia, Record 2007/14, p. 80–84.
- Witt, WK 1994, Geology of the Melita 1:100 000 sheet: Geological Survey of Western Australia, 1:100 000 Geological Series Explanatory Notes, 63p.
- Wyche, S 2007, Stratigraphy and structure of the Kalgoorlie Terrane at Hannan Lake and Mount Hunt — a field guide: Geological Survey of Western Australia, Record 2007/15, 11p.
- Wyche, N, Wyche, S and Sapkota, J 2016, Melita Formation: Geological Survey of Western Australia, viewed 4 July 2016, <www.dmp.wa.gov.au/ens>.
- Wyche, S and Sapkota, J 2016, King of the Hills Dolerite: Geological Survey of Western Australia, WA Geology Online, Explanatory Notes extract, viewed 4 July 2016, <www.dmp.wa.gov.au/ens>.

This Record is published in digital format (PDF) and is available as a free download from the DMP website at www.dmp.wa.gov.au/GSWApublications.

Further details of geological products produced by the Geological Survey of Western Australia can be obtained by contacting:

Information Centre
Department of Mines and Petroleum
100 Plain Street
EAST PERTH WESTERN AUSTRALIA 6004
Phone: +61 8 9222 3459 Fax: +61 8 9222 3444
www.dmp.wa.gov.au/GSWApublications

KOMATIITES AND ASSOCIATED ROCKS OF THE
KALGOORLIE-LEONORA REGION

